

FEM AND STATISTICS FOR BRIDGE CONDITION PREDICTION

FINITE ELEMENT MODELLING AND HIGH-LEVEL STATISTICAL
ANALYSIS FOR BRIDGE CONDITION PREDICTION AND MANAGEMENT

By

AHMED ABDELMAKSoud, B.Sc., M.Sc.

A Thesis Submitted to the School of Graduate Studies
in Partial Fulfilment of the Requirements for the Degree
Doctor of Philosophy

Doctor of Philosophy (2022) McMaster University, Hamilton, Ontario

(Civil Engineering)

TITLE: Finite Element Modelling and High-Level Statistical Analysis for Bridge
Condition Prediction and Management

AUTHOR: Ahmed Abdelmaksoud, B.Sc. (Cairo University), M.Sc. (Cairo University)

SUPERVISOR: Assistant Professor Georgios Balomenos, Ph.D., P.Eng.

CO- SUPERVISOR: Associate Professor Tracy Becker, Ph.D., P.Eng.

NUMBER OF PAGES: xviii, 188

Lay Abstract

Regular inspection and maintenance of bridges are vital to the integrity of transportation networks. The planning and scheduling of such activities have become known as bridge management. Given the limitations of budget and resources, there is a high demand for optimized bridge management. The fundamental goal of this thesis is to explore potential improvements for the current practices of bridge management. Towards this goal, this thesis proposes enhanced methodologies for a more accurate prediction of future bridge conditions and maintenance needs, a better understanding of the lifespan of various bridge components, and early detection of any vulnerabilities that may be detrimental to the functionality of bridges and the safety of bridge users.

Abstract

Efficient management strategies are essential to ensure bridge safety and functionality while accommodating budget limitations. For such purpose, bridge management systems (BMSs) developed policies to predict the global bridge conditions and any performance deficiencies in the individual components. However, the current policies have some shortcomings that may limit their efficiencies. To address these shortcomings, this thesis proposes several enhancements to three major BMS policies covering inspection and maintenance planning, bearing performance assessment, and seismic screening.

Inspection and maintenance are often planned using Markov Chains deterioration models derived from past inspection records. However, Markov Chains models employ impractical assumptions and neglect the subjectivity of inspections. Alternatively, parameterized fuzzy-logistic deterioration models are proposed to predict future conditions given easy-to-track parameters, such as age and last maintenance date. The proposed models can yield better maintenance predictions compared to Markov Chains and can reduce inspection costs by 30%.

Bearing performance assessment policies are limited to testing bearing material or its behaviour at design displacements. In practice, bearings experience fatigue with repeated displacement cycles even if at low magnitudes, leading to bearing degradation and long-term increase in demands. Thus, a parameterized loading protocol is proposed to guide laboratory testing in assessing the fatigue life. The protocol is derived from the bearing demands attributes observed from a 3D nonlinear analysis in OpenSees for various bridge configurations and loading conditions.

Seismic screening policies were developed to identify the most vulnerable

bridges, giving them the highest priorities. The current policies are qualitative, relying on identifying vulnerable details, rather than quantifying the actual performance. Furthermore, the vulnerability estimates are not updated with deterioration. Thus, new risk-based screening procedures are proposed via fragility analysis of the critical components, bearings and columns, while considering their deterioration. Given the components' fragilities, a seismic vulnerability index is computed to rank the bridge's priority.

Acknowledgement

First and foremost, I would like to thank Dr. Balomenos and Dr. Becker for their support, mentoring, and supervision for the past four years. I feel lucky to have been a student of such inspiring researchers. One day, I aspire to be a researcher of their caliber.

I also would like to express my sincere appreciation to Mr. Hao Zhang, Mr. Kris Mermigas, Mr. Jim Au, and Mr. Walter Kenedi from the Ministry of Transportation of Ontario (MTO) for providing their valuable expert opinion and documents on the current management policies in MTO which helped to guide my research directions.

I am also grateful for the support from the Ontario Graduate Scholarship provided by the Government of Ontario, and the start-up funding provided by the Faculty of Engineering at McMaster.

Last but not least, I want to express my sincere gratitude to my family who supported me all the way during my study. To my father, mother, and sisters, thank you for your continuous help, encouragement, and support which helped me throughout my whole life until this moment.

Preface

The following Ph.D. thesis comprises four main chapters (chapters 2 to 5) that form separate manuscripts for publication in peer-reviewed journals. An introduction section (chapter 1) is provided to put this research into context. Complete references for all chapters that have been published or are in preparation can be found below. Chapter 2 has been published in the *Journal of Bridge Engineering, ASCE*, chapter 3 has been published in the *Journal of Risk and Uncertainty in Engineering Systems, Part A: Civil Engineering, ASCE-ASME*, chapter 4 has been published in the *Journal of Engineering Structures, Elsevier*, and chapter 5 is currently in preparation.

As the first author for all manuscripts, I have designed the methodology, compiled literature review and data, conducted the analysis, and wrote all the manuscripts under the supervision of Dr. Balomenos and Dr. Becker. Portions of the modelling and writing in chapter 4 were done by Minesh K. Patel; hence, he was included as a co-author on this manuscript.

Abdelmaksoud, Ahmed M, Georgios P Balomenos, and Tracy C Becker. 2021. "Parameterized Logistic Models for Bridge Inspection and Maintenance Scheduling." *Journal of Bridge Engineering* 26 (10): 4021072. DOI: 10.1061/(ASCE)BE.1943-5592.0001774.

Abdelmaksoud, Ahmed M, Georgios P Balomenos, and Tracy C Becker. 2022. "Fuzzy-Logistic Models for Incorporating Epistemic Uncertainty in Bridge Management Decisions." *Journal of Risk and Uncertainty in Engineering Systems, Part A: Civil Engineering* 8 (3): 04022025. DOI: 10.1061/AJRUA6.0001247

Abdelmaksoud, Ahmed M., Minesh K. Patel, Tracy C. Becker, and Georgios P. Balomenos. "Parameterized models for prediction of lifetime bearing demands." *Engineering Structures* 252 (2022): 113649.

Abdelmaksoud, Ahmed M., Tracy C. Becker, and Georgios P. Balomenos. "Fuzzy-Probabilistic Seismic Vulnerability Index for Deteriorating Multi-span Continuous Concrete Girders Bridges." (In preparation)

Table of Contents

Lay Abstract	iii
Abstract	iv
Acknowledgement	vi
Preface	vii
Table of Contents	ix
List of Figures	xiii
List of Tables	xvii
1. Introduction	1
1.1. Bridge Management Systems.....	1
1.2. Literature Review	2
1.2.1. Time-Dependent Deterioration of Global Bridge Condition	2
1.2.2. Performance Deterioration of Bridge Bearings	7
1.2.3. Seismic Vulnerability of Deteriorating Bridges	8
1.3. Objectives and Methodology	9
1.4. Outline of Thesis	12
1.5. References	13
2. Parameterized Logistic Models for Bridge Inspection and Maintenance Scheduling	24
2.1. Abstract	24
2.2. Introduction	25
2.3. Inspection Data.....	28
2.3.1. Data Description	28
2.3.2. Data Pre-processing	31
2.4. Methodology	31
2.4.1. Logistic Regression.....	31
2.4.2. LASSO Regularization	34
2.4.3. Markov Chains.....	34
2.4.4. Confusion Matrix	36
2.5. Maintenance Decision Models	37
2.5.1. Group Level LASSO-Logistic Model.....	37
2.5.2. Individual Level LASSO-Logistic Model	40
2.5.3. Markov Chains Model	41

2.6.	Inspection Decision Models	44
2.7.	Framework for Inspection and Maintenance Scheduling.....	45
2.8.	Optimum Thresholds using LCC Analysis	49
2.8.1.	LCC for MLS	49
2.8.2.	LCC for ILS	52
2.8.3.	Creating Inspection and Maintenance Scheduling using Optimum Thresholds.....	53
2.9.	Conclusions	54
2.10.	Data Availability Statement.....	55
2.11.	Acknowledgments	55
2.12.	References	55
3.	Fuzzy-Logistic Models for Incorporating Epistemic Uncertainty in Bridge Management Decisions	62
3.1.	Abstract	62
3.2.	Introduction	63
3.3.	Inspection Data.....	65
3.3.1.	Bridge Condition Index (BCI)	65
3.3.2.	Influencing Parameters for BCI.....	66
3.3.3.	Sources of Epistemic Uncertainty.....	67
3.3.4.	Data Pre-Processing	68
3.4.	Methodology	68
3.4.1.	Logistic Regression.....	68
3.4.2.	LASSO Regularization	69
3.4.3.	Fuzzy Set Theory	69
3.4.4.	Formulation of Fuzzy-Logistic Models	74
3.5.	Fuzzy-Logistic Models.....	76
3.5.1.	Maintenance Limit State (MLS)	76
3.5.2.	Inspection Limit State (ILS)	77
3.6.	Case Study.....	78
3.7.	Life Cycle Cost (LCC) Analysis	83
3.7.1.	Maintenance Limit State (MLS)	84
3.7.2.	Inspection Limit State (ILS)	88
3.8.	Development of Maintenance and Inspection Strategies	90
3.8.1.	Potential Extensions for Network Level Strategies	90

3.8.2.	Updating Maintenance and Inspection Strategies.....	91
3.9.	Conclusions	92
3.10.	Data Availability Statement.....	93
3.11.	Acknowledgments	93
3.12.	References	94
4.	Parameterized Models for Prediction of Lifetime Bearing Demands.....	102
4.1.	Abstract	102
4.2.	Introduction	103
4.3.	Bridge Design and Modelling	105
4.3.1.	Bridge Design Parameters.....	105
4.3.2.	Bridge Modelling Elements	108
4.3.3.	Bridge Aging.....	109
4.4.	Bridge Loading.....	111
4.4.1.	Temperature Loading.....	112
4.4.2.	Traffic Loading	115
4.4.3.	Seismic Loading.....	117
4.5.	Bearing Demands	118
4.5.1.	Temperature Demands	119
4.5.2.	Traffic Demands	124
4.5.3.	Seismic Demands.....	129
4.6.	Case Study.....	132
4.7.	Conclusions	138
4.8.	Acknowledgments	140
4.9.	References	140
5.	Fuzzy-Probabilistic Seismic Vulnerability Index for Deteriorating Multi-span Continuous Concrete Girders Bridges.....	146
5.1.	Abstract	146
5.2.	Introduction	147
5.3.	Methodology	151
5.3.1.	Condition Indices for Critical Bridge Components	152
5.3.2.	Seismic Performance Assessment.....	158
5.3.3.	Formulation of the Seismic Vulnerability Index (SVI)	162
5.4.	Case Study Bridge and OpenSees Model.....	164

5.5.	Application of Proposed Framework for MSC Concrete Girders Bridges .	166
5.5.1.	Condition Indices for Bearings (BeCI) and Columns (CCI)	166
5.5.2.	Prediction Models for the Confidence Level (CL _o).....	167
5.5.3.	Proposed Seismic Screening Procedures	170
5.6.	Conclusions	171
5.7.	Data Availability Statement	172
5.8.	Acknowledgements	173
5.9.	References	173
6.	Summary, Conclusions, and Future Work.....	184
6.1.	Summary and Conclusions.....	184
6.1.1.	Risk-based Management in Presence of Time-Dependent Deterioration 184	
6.1.2.	Loading Protocol for Life-span Assessment of Bridge Bearings	185
6.1.3.	Risk-based Seismic Screening for Deteriorating Bridges.....	186
6.2.	Future Work	187

List of Figures

Fig. 2.1 MTO data showing BCI-age relationship	31
Fig. 2.2 A bridge with a BCI approaching 70: Deck soffit with wet longitudinal cracks and delamination.....	33
Fig. 2.3 Deviance vs. λ (group-level LASSO-Logistic model without material classification).....	38
Fig. 2.4 (a) Recall, and (b) FRR vs. $P_{\text{threshold}}$ for group-level model with and without material classification.....	40
Fig. 2.5 (a) Recall, and (b) FRR vs. $P_{\text{threshold}}$ comparing the individual-level and group-level models.....	41
Fig. 2.6 (a) Recall, and (b) FRR vs. $P_{\text{threshold}}$ comparing Markov Chains vs. LASSO-Logistic models.....	43
Fig. 2.7 Bridge condition map of Ontario, Canada for the year 2021: (a) $P_{\text{MLS-threshold}} = 0.1$, (b) $P_{\text{MLS-threshold}} = 0.4$	45
Fig. 2.8 MLS profile for the example bridge.....	47
Fig. 2.9 ILS profile for the example bridge.....	48
Fig. 2.10 Inspection and maintenance schedule ($P_{\text{MLS-threshold}} = 0.2$ and $P_{\text{ILS-threshold}} = 0.08$).....	48
Fig. 2.11 (a) LCC_{MLS} vs. $P_{\text{MLS-threshold}}$, and (b) maintenance and replacement timings for the optimum $P_{\text{MLS-threshold}}$	51
Fig. 2.12 LCC_{ILS} vs. $P_{\text{ILS-threshold}}$	53
Fig. 2.13 Inspection and maintenance schedule for the example bridge.....	53
Fig. 3.1 Membership function of the BCI.....	70
Fig. 3.2 Estimation of $BCI_{\mu=0,\text{max}}$ and $BCI_{\mu=0,\text{min}}$	71

Fig. 3.3 Membership function for the meteorological parameters	72
Fig. 3.4 (a) Meteorological stations clusters and (b) Meteorological map of Ontario, Canada.....	73
Fig. 3.5 COV of DOSF versus d	74
Fig. 3.6 Deviance versus λ	76
Fig. 3.7 Membership functions for (a) DOSF and (b) DOGS	79
Fig. 3.8 P_{MLS} profile for $P_{MLS\text{-threshold}} = 0.35$ with (a) $\mu_{MLS} = 1$ and (b) $\mu_{MLS} = 0$	80
Fig. 3.9 P_{ILS} profile for $P_{ILS\text{-threshold}} = 0.15$ with (a) $\mu_{ILS} = 1$ and (b) $\mu_{ILS} = 0.5$ (maintenance timings based on $\mu_{MLS} = 1$ and $P_{MLS\text{-threshold}} = 0.35$)	82
Fig. 3.10 LCC_{MLS} given $\mu_{MLS}=1$ versus $P_{MLS\text{-threshold}}$	86
Fig. 3.11 Planned versus unplanned MLS profile	88
Fig. 3.12 (a) Total cost for maintenance strategies in Table 3.6 and (b) optimum maintenance strategy for the case study bridge ($\mu_{MLS} = 0.1$ and $P_{MLS\text{-threshold}} = 0.35$).....	88
Fig. 3.13 (a) Total cost for inspection strategies in Table 3.7 and (b) optimum inspection strategy for the case study bridge ($\mu_{ILS} = 0.7$ and $P_{ILS\text{-threshold}} = 0.09$).....	89
Fig. 3.14 Optimum maintenance and inspection strategy for the case study bridge ..	90
Fig. 3.15 Flowchart for the proposed fuzzy-probabilistic framework.....	91
Fig. 4.1 Nonlinear OpenSees model	106
Fig. 4.2 Bridge deck and span variation models.....	107
Fig. 4.3 (a) Air temperature data from the “JEAN LESAGE INTL A” station in Quebec and (b) random annual air temperature and bridge temperature profiles for a concrete bridge.	113
Fig. 4.4 Average differential temperature profile for (a) concrete girder bridges and (b) concrete slab on steel girder bridges	114

Fig. 4.5 (a) Bearing displacement profiles and (b) normalized bearing displacement profiles at a given time instant.	116
Fig. 4.6 Total longitudinal displacement history of bearings	120
Fig. 4.7 Normalized RMSE vs. number of simulations for the temperature loading	120
Fig. 4.8 (a) Genome tree representation of the CDD _T model and (b) Pareto optimal plot	121
Fig. 4.9 Temperature differential component of CDD _T for bridges with (a) concrete girders and (b) steel girders.....	122
Fig. 4.10 (a) Bearing displacement history relative to the mean bearing position (mm), (b) bearing displacement history relative to the mean bearing position (normalized by the $A_{ref T}$), and (c) distribution of the normalized temperature cycle amplitudes	124
Fig. 4.11 (a) Loading line of a single axle of a CL-625 truck in alignment with a bearing and (b) longitudinal displacement history of the bearing directly below the loading line (no-braking).	124
Fig. 4.12 Longitudinal displacement with and without braking on a three span bridge	125
Fig. 4.13 CDD _{ho} vs. depth-to-span ratio for (a) concrete and (b) steel girders configurations	127
Fig. 4.14 Displacement percentage p for (a) concrete and (b) steel girders configurations	128
Fig. 4.15 Distribution of traffic cycle amplitudes.....	129
Fig. 4.16 $\ln(D_{L max})$ vs. $S_a(0.2)$ for multi- and single-span bridge configurations (Eastern EQ).....	131

Fig. 4.17 Traffic loading scenarios considered in the case study bridge	135
Fig. 4.18 Representative loading protocol due to the annual temperature and traffic loading.....	137
Fig. 4.19 Winter segment of the annual loading protocol due to temperature and traffic loading.....	137
Fig. 4.20 Seismic cycles added to the winter segment of the loading protocol.....	138
Fig. 5.1 Proposed framework for seismic vulnerability assessment of deteriorating bridges.....	152
Fig. 5.2 Membership functions for (a) reinforcement corrosion in columns, (b) stiffness losses in elastomeric bearings, and (c) stiffness losses in high rocker bearings.....	156
Fig. 5.3 Safety margin between demand and capacity for a confidence level (CL %)	158
Fig. 5.4 Column drift δ_{col} (%) vs. number of earthquake records N_{EQ}	161
Fig. 5.5 (a) Aggregation of bridge components' CL_o membership functions and (b) overall CL_o membership function with threshold value ($CL_{o-threshold}$) = 90%	164
Fig. 5.6 (a) Elevation of Chemin des Dalles Bridge and (b) Elevation of OpenSees model.....	166
Fig. 5.7 Column drift δ_{col} (%) vs. CCI for sample simulations at $Sa(T_1) = 0.75$ g ...	167
Fig. 5.8 Membership functions of CL_o for the Chemin des Dalles Bridge's columns and elastomeric bearings.....	170

List of Tables

Table 2.1 Sample of BCI records dating back to 2004	29
Table 2.2 Sample calculations for Markov Chains model	42
Table 2.3 Regression and exponent coefficients for the group-level inspection decision model.....	44
Table 2.4 Regression and exponent coefficients for the individual-level inspection decision model	44
Table 3.1. Extreme values of MP for each meteorological cluster	73
Table 3.2. Regression and exponent coefficients for MLS fuzzy-logistic models	77
Table 3.3. Regression and exponent coefficients for ILS fuzzy-logistic models for Δt of 2 years.....	78
Table 3.4. Regression and exponent coefficients for ILS fuzzy-logistic models for Δt of 4 years.....	78
Table 3.5. Regression and exponent coefficients for ILS fuzzy-logistic models for Δt of 6 years.....	78
Table 3.6. Optimum $P_{\text{MLS-threshold}}$ for various μ_{MLS} degrees	86
Table 3.7. Optimum $P_{\text{ILS-threshold}}$ for various μ_{ILS} degrees	89
Table 4.1. Distribution of bridge design parameters	108
Table 4.2. Bridge temperature ranges taken from [30]	112
Table 4.3. Meteorological data for the “JEAN LESAGE INTL A” station in Quebec	113
Table 4.4. $D_{\text{L max multi}}$ model coefficients for multi-span bridges	130
Table 4.5. $D_{\text{L max single}}$ model coefficients for single-span bridges.....	130
Table 4.6. Expected cycle count for amplitudes larger than 50% of $D_{\text{L max}}$	132

Table 4.7. Design parameters for the case study bridge.....	133
Table 4.8. Displacement percentages for traffic loading scenarios of the case study bridge	135
Table 4.9. Expected cycle count for the case study bridge	135
Table 5.1. Investigated properties for the parametric study	160
Table 5.2. Fragility definitions for critical bridge components.....	162
Table 5.3. Regression coefficients for the prediction models of CL_o	168

1. Introduction

1.1. Bridge Management Systems

Bridges are crucial components of any national transportation network. Bridge failures or malfunctions can lead to severe consequences beyond the cost of repair, extending to traffic delays, construction of temporary alternative routes, safety hazards, and disruptions to modern societies' social and financial well-being (Pregolato 2019; Moehle and Eberhard 2003). Throughout their service life, bridges are subject to multiple hazards that can lead to their failure or malfunction, which in turn affects the performance of the whole transportation network. These hazards can be either time-dependent, such as reinforcement corrosion (Biondini et al. 2014), fatigue (Kim et al. 2013), and scour (Stein et al. 1999), or extreme events, such as seismic events (Priestley et al. 1996; Padgett et al. 2010), hurricanes (Stearns and Padgett 2012), and floods (Pregolato 2019).

Ensuring bridge safety against both types of hazards and mitigating the consequences of failure or malfunction require proper inspection and maintenance to track the global bridge condition and address any performance deficiencies in the individual bridge components (Mirzaei et al. 2014; Filiatrault et al. 1994). Planning and scheduling such activities became known as bridge management (Hurt and Schrock 2016) and is typically handled by software-based digital bridge management systems (BMSs) (Mirzaei, Adey, Klatter, et al. 2014). Given the limited budget and resources, there is a demand for more optimized BMSs that can maximize the benefits of the available budgets to face time-dependent deterioration and extreme events (Hurt and Schrock 2016). Towards this goal, this thesis reviews some of the current practices of BMSs in tracking the global bridge condition and identifying performance deficiencies

in individual components. The thesis then discusses potential points of improvement.

1.2. Literature Review

1.2.1. Time-Dependent Deterioration of Global Bridge Condition

When it comes to managing bridge inspection and maintenance in the presence of time-dependent deterioration, the core of BMSs are the deterioration models, maintenance models, and optimization models. Deterioration models approximate and predict future bridge conditions based on past trends of condition data obtained from inspections. Maintenance models care about assessing the improvement in bridge condition with future applied maintenance interventions. Optimization models involve life-cycle cost analysis to determine the most effective bridge management strategies from cost and safety perspectives. There are several types of such models; however, they are all generally used to track the overall condition of bridges. Deterioration and maintenance models can be formulated based on numerical or statistical analysis or a mixture of both and can be either deterministic or probabilistic (Srikanth and Arockiasamy 2020).

1.2.1.1. Numerical Models

In numerical analysis, deterioration is typically modelled as a time-variant reduction in the load carrying capacity of bridge components. For example, Biondini et al. (2014) and Alipour et al. (2013) modelled the corrosion of concrete bridge components by reducing the reinforcement area as well as the unconfined strength of the concrete cover to account for spalling and cracking. Numerical models can also be used to assess specialized retrofit measures. For example, Almomani et al. (2020) conducted a 3D numerical analysis to evaluate the use of carbon fiber-reinforced polymer (CFRP) laminates as a retrofit measure for a deteriorating concrete bent cap subject to reinforcement corrosion and concrete spalling. While numerical models provide the

most accurate representation of bridge deterioration and the impact of repairs, they require extensive modelling parameters, including structural configuration, environmental conditions, and loading parameters (Jia and Gardoni 2018). Predicting the bridge condition solely using numerical analysis is suitable for project-level problems but time consuming when managing large bridge populations.

1.2.1.2. Deterministic Models

BMSs typically prefer statistical-based models rather than numerical-based models for large scale management decisions. The simplest form of statistical-based models is deterministic regression analysis formulated by applying regression analysis on bridge inspection data. A variety of regression techniques exist, such as multiple linear regression (Weisberg 2005), dynamic linear regression (Zhang et al. 2020), and nonlinear regression (Rhinehart 2016), which can be used to establish an empirical relationship between the bridge condition and one or more independent parameters. A variety of studies showed that the average bridge deterioration with age could be approximated using a third-degree polynomial model, and some studies established such models for a variety of bridge classes with different design and loading parameters (Bolukbasi et al. 2004; Jiang and Sinha 1989; Tolliver and Lu 2012; Kallen and Van Noortwijk 2006). Abdelmaksoud et al. (2019) proposed a simplified linear model that predicts the bridge condition given its age, repair history, and location, allowing for planning maintenance activities. While being simple, deterministic models can underestimate the bridge maintenance needs as these models neglect the inherent uncertainties from (1) the randomness in material properties, loading, and deterioration process, (2) the qualitative and subjective nature of visual bridge inspections, and (3)

occasional lack of information on the bridge environment (Brown and Yao 1983).

1.2.1.3. Probabilistic Models

To account for the uncertainty in bridge conditions, many BMSs opt to derive their deterioration models via probabilistic analysis of inspection data (Mirzaei et al. 2014). Probabilistic deterioration models come with various degrees of complexity and accuracy. Among those, reliability analysis is argued to be one of the most rational probabilistic methods for bridge management (Frangopol et al. 2001; Estes and Frangopol 2003; Lark and Flaig 2005).

Reliability models have a mechanistic nature as they are typically formulated based on mathematical expressions of the initiation and propagation of deterioration mechanisms (e.g., reinforcement corrosion). As such, reliability analysis provides a quantitative assessment of the bridge condition that can be directly related to physical deterioration measurements (e.g., percentage loss of reinforcement area) as well as other quantitative parameters such as material properties, stress conditions, structural behavior, etc. (Morcouc and Lounis 2007; Srikanth and Arockiasamy 2020). For example, Estes and Frangopol (1999) proposed a reliability deterioration model by modelling bridges as a system of series-parallel failure modes. Ghodoosi et al. (2014) proposed a methodology for predicting the reliability of simply supported concrete bridges designed according to the Canadian Highway Bridge Design Code (CHBDC) (CSA 2019). Mechanistic models were also preferred when investigating the adverse impacts of reinforcement corrosion on bridge performance (Morcouc et al. 2010; Roelfstra et al. 2004). Frangopol (1998) combined reliability index models for maintenance actions with reliability deterioration models to optimize maintenance

strategies. To accurately capture the bridge condition improvement provided by maintenance, the proposed maintenance models constituted eight random variables such as the immediate performance improvement, post-maintenance deterioration rate, and duration of maintenance effects. Other reliability index maintenance models were proposed by Grussing et al. (2006), Ghodoosi et al. (2018), and Van Noortwijk and Frangopol (2004). Generally, reliability models provide the most accurate representation and prediction of future bridge conditions in the presence of uncertainties, allowing for highly optimized risk-based planning of maintenance actions. Unfortunately, this comes at the cost of extensive data and modelling requirements (Estes and Frangopol 2003), making mechanistic models inefficient for BMSs managing large bridge populations (Srikanth and Arockiasamy 2020).

A more popular probabilistic tool with BMSs is the Markov Chains method (Mirzaei et al. 2014). This method discretizes the bridge or bridge component condition into a finite set of condition states (e.g., poor, fair, etc.), then evaluates the probability of being in one of these states by accumulating the state transition probabilities throughout the service life (Bocchini et al. 2013; Cesare et al. 1992). The transition probabilities are often assessed based on the Percentage Prediction Method (Jiang and Sinha 1989), regression-based optimization (Butt et al. 1987), or expert opinion (Betti 2010). The popularity of the Markov Chains method with BMSs stems from its simplicity and compatibility with existing qualitative/discrete bridge condition rating systems (Srikanth and Arockiasamy 2020). However, the Markov Chains method employs several impractical assumptions that might limit its accuracy (Madanat et al. 1997; George Morcouc 2006; Zambon et al. 2017). Examples of such assumptions

include (1) future bridge condition is independent of past condition, (2) state transition probabilities are constant throughout the bridge's service life, and (3) constant bridge populations (Zambon et al. 2017).

While probabilistic models can address the uncertainties arising from the randomness in bridge deterioration, they fail to capture other sources of uncertainty, such as the subjectivity of inspection data or lack of knowledge. This can considerably underestimate the bridge condition (Der Kiureghian and Ditlevsen 2009).

1.2.1.4. Fuzzy-Probabilistic Models

In an effort to incorporate all types of uncertainties (i.e., randomness or subjectiveness), several deterioration models were proposed using a hybrid of probabilistic analysis and fuzzy set theory (Zadeh 1965). The fuzzy set theory is a classical tool for incorporating subjectiveness into deterioration models (Tee et al. 1988). Numerous studies on this front focused on combining the fuzzy set theory with reliability analysis (Möller et al. 2006; Wu 2004). The classical reliability method models random variables using probability density functions (PDFs), whereas the fuzzy set theory models subjective information, such as visual inspection ratings or deterioration measurements, using membership functions. To make both methods work in concert, some studies proposed methodologies for converting membership functions into equivalent PDFs (Ma et al. 2015; Wang et al. 2015). Marano et al. (2008) and Wang et al. (2013) used a similar approach to develop fuzzy time-dependent reliability models for corroded reinforced concrete beams. Most of these proposed approaches are mechanistic in nature and require extensive deterioration data collection from bridge inspections. The majority of these proposed approaches are mechanistic, given the reliability component. Hence,

such approaches are not compatible with BMSs managing large bridge portfolios.

1.2.2. Performance Deterioration of Bridge Bearings

In addition to tracking the global bridge condition via inspections, it is imperative to look out for performance deficiencies resulting from the deterioration of individual components such as bridge bearings. Bridge bearings are a vital element for load transfer and deformation accommodation of bridge superstructure; hence, they directly impact bridge safety and functionality. That being said, the current design codes (AASHTO 2017; CSA 2019) and bearing testing procedures provide only minimal information on bearing performance lifespan under in-practice loading conditions (Noade and Becker 2019). Currently, bearing performance assessment is dependent on visual inspections and engineering judgment, hence, inducing considerable uncertainty in bridge safety and functionality.

In practice, bearings experience a mixture of numerous cycles with small displacement magnitudes and a few cycles with large displacement magnitudes. The former results from daily loads, such as temperature and traffic, whereas extreme events, such as earthquakes, cause the latter. Rating the bearing performance and life-span require accounting for such magnitude variant loading pattern. Nevertheless, the standard bearing tests do not incorporate such a loading pattern. Also, most experimental and analytical studies that investigated the life-span of bearings under cyclic compression and shear loading did not account for such loading pattern (Roeder et al. 1990; Mars and Fatemi 2002; Muhr 2006; Suryatal et al. 2015).

To address this issue, Noade and Becker (2019) recently proposed an amplitude-variant loading protocol for elastomeric bearings based on elastic analysis of the

Chemin des Dalles Bridge, located in Trois-Rivières, Province of Quebec, Canada, under temperature, traffic, and seismic loading. The protocol was derived based on the observed attributes of the displacement demands (i.e., cycle amplitudes and cycle counts) in the analysis. However, the proposed protocol is restricted to the investigated bridge configuration and must be generalized to include other bridge designs. Furthermore, the potential nonlinearity in the columns and deck during seismic and traffic loads is not investigated.

1.2.3. Seismic Vulnerability of Deteriorating Bridges

Seismic performance evaluation of bridges is critical to ensure the post-earthquake integrity of transportation networks and mitigate any potential severe traffic, social, and financial disruptions (Moehle and Eberhard 2003). Given budget and resource limitations, BMSs are required to prioritize the potentially critical bridges for detailed seismic evaluations. Towards this purpose, many BMSs developed seismic screening policies to identify the most seismically vulnerable bridges (Filiatrault et al. 1994; Bagnariol and Au 2000; Tesfamariam and Modirzadeh 2009). Each bridge is assigned a seismic vulnerability index (SVI) based on an expert-opinion scoring system based on the seismic hazard conditions, structural configuration, soil properties, and importance. The higher the SVI, the higher the priority for a detailed seismic investigation.

The policies are typically qualitative and rely only on recognizing the presence of vulnerable seismic details (e.g., rocker bearing). This can induce significant uncertainty. Furthermore, bridge deterioration is ignored despite its undeniable contribution to bridge vulnerability during seismic events (Bazzucchi et al. 2018). To

mitigate such consequences, a risk-based method for seismic screening of bridges while considering their deterioration level is essential.

Very few studies attempted to indirectly account for deterioration by incorporating the bridge age in the SVI computations (Kenedi and Bagnariol 2007; Tesfamariam and Modirzadeh 2009; Bonthron et al. 2021), and some even incorporated the time since last maintenance as a measure of the bridge repair history (Kenedi and Bagnariol 2007). Nevertheless, such indicators (i.e., age and time since last maintenance) may not inform the actual bridge-specific deterioration and working conditions. Some quantitative and risk-based approaches for seismic screening were proposed using simplified expressions for predicting the seismic response of critical bridge components (e.g., column drift and bearing replacement) and comparing these responses to a capacity or damage limit (Dicleli and Bruneau 1996; Dukes et al. 2018; Bonthron et al. 2021). However, even such approaches ignored modelling the bridge deterioration.

1.3. Objectives and Methodology

Based on the discussions in the literature review, four main objectives were identified to optimize the current practices of BMSs further:

- Providing an alternative probabilistic technique for the Markov Chain method that does not require impractical assumptions.
- Proposing a BMS-compatible framework for incorporating the uncertainty arising from the subjectiveness of visual inspections into bridge management decisions.
- Deriving a bearing loading protocol representative of in-practice loading to rate and test sample bearings and to determine their expected lifespan.

- Providing a quantitative risk-based framework for seismic screening of deteriorating bridges.

The proposed alternative probabilistic method is the logistic regression. This method has the advantage of not needing impractical assumptions, as in the case of Markov Chains, or high data requirements, as in the case of reliability analysis. Previous studies have shown that logistic regression is a powerful probabilistic tool for risk-based management of infrastructure under extreme events. For example, Balomenos and Padgett (2018) used logistic models to predict the failure risks of ports during hurricanes. A similar study was conducted for bridges by Balomenos et al. (2020). Another example is the use of logistic models for post-hazard evaluation of infrastructure accessibility (Bernier et al. 2019; Balomenos et al. 2019). Here, logistic regression was used to derive deterioration models to plan bridge maintenance and inspection in the presence of time-dependent deterioration. A logistic model is used to predict the probability of exceeding a limit state (P_{LS}), beyond which a maintenance or inspection action is triggered, given a set of input parameters as

$$P_{LS} = \frac{\exp[\beta_o + \sum_{j=1}^n \beta_j x_j^{\gamma_j}]}{1 + \exp[\beta_o + \sum_{j=1}^n \beta_j x_j^{\gamma_j}]} \quad (1)$$

where n is the number of input parameters, β_o is the model intercept, and β_j and γ_j are the regression and exponent coefficients, x_j is an input parameter available from inspection data, such as age and maintenance history. The definition of the limit states for maintenance and inspection is based on the guidelines of the Ministry of Transportation of Ontario (MTO 2015). The performance of the logistic models is

compared to a Markov Chain model developed using the procedures in Cesare et al. (1992).

After validating the effectiveness of logistic regression as a probabilistic tool for capturing the randomness in bridge deterioration, it is combined with the fuzzy set theory (Zadeh 1965) to account for the subjectiveness in inspection data. As the condition assessment from visual inspections is subjective, then the inspection measurements (e.g., inspector's ratings) are uncertain, and the actual bridge condition may be shifted. Using the fuzzy set theory, a subjective reading (e.g., inspector's ratings) is modelled using membership functions depicting a range of possible values with different degrees of confidence (μ) rather than a discrete value. These functions are incorporated into Eq. (1), resulting in a range of possible logistic models bound by a worst- and a best-case scenario model for a given confidence level μ . Conservatively, only the worst-case scenario models are of interest. Finally, a life cycle cost analysis is conducted to determine the optimum confidence level (μ) and probability threshold ($P_{LS\text{-threshold}}$) of the logistic deterioration models to ensure safe and economic management decisions.

To derive a bearing loading protocol representative of in-practice loading, the framework proposed by Noade and Becker (2019) is generalized to account for a range of bridge superstructure types (e.g., deck on concrete girder and deck on steel girder systems), geometric parameters (e.g., number of spans, stiffness of pier and deck, etc.), bearing properties (e.g., horizontal stiffness), and possible nonlinearities in the deck and piers due to traffic and seismic loads, respectively. Using the Monte Carlo simulation with Latin hypercube sampling (McKay et al. 2000), random bridge

configurations and loading conditions (e.g., temperature profiles, earthquake records, and traffic loading scenarios) are generated and modelled in OpenSees (McKenna et al. 2010). Then, the bearing demand attributes (i.e., cycle amplitudes and cycle counts) are evaluated, and prediction models are formulated for these attributes as a function of the configuration and loading parameters. A general loading protocol is derived for testing and rating sample bearings based on these models.

Finally, a quantitative risk-based framework for seismic screening of deteriorating is proposed using a hybrid of fragility analysis and fuzzy set theory. The bridge fragility is estimated using multiple stripe analysis (MSA) (Baker 2015) in OpenSees while considering several deterioration mechanisms, such as reinforcement corrosion, bearing fatigue, and bearing corrosion. To facilitate capturing the trends in bridge fragility with deterioration, new BMS-compatible condition indices are proposed for the most critical bridge components during seismic events (i.e., columns and bearings). The proposed indices can be easily evaluated from typical visual inspections and are calibrated using fuzzy logic principles to inform the seismic response of the deteriorating bridge component. Based on the fuzzy-fragility analysis, parameterized models are formulated to predict the seismic damage risks given the condition indices and other relevant properties, such as seismic intensity, type of bearing, foundation stiffness, etc. Then, a risk-based seismic vulnerability index (SVI) is derived to aid in setting bridge priority for detailed seismic investigation.

1.4. Outline of Thesis

Chapter 1

Introduces a brief overview of bridge management systems and current management

practices. Then, it identifies possible improvements for modelling bridge deterioration to allow for better management decisions. Based on this discussion, thesis objectives and methodologies are defined.

Chapter 2

Discusses the use of logistic regression for modelling time-dependent deterioration as an alternative to the Markov Chain method adopted in many North American BMSs.

Chapter 3

Establishes a BMS compatible framework for incorporating subjectiveness of inspection data into management decisions using a hybrid of logistic regression and fuzzy set theory.

Chapter 4

Proposes a framework for deriving a parameterized loading protocol to test and rate sample bridge bearings to estimate their lifespan.

Chapter 5

Develops a risk-based seismic screening procedure for deteriorating bridges using a hybrid of fragility analysis and fuzzy set theory.

Chapter 6

Summarizes the finding of the thesis and suggests future research to improve bridge management practices further.

1.5. References

AASHTO. 2017. *LRFD Bridge Design Specification*. Washington, DC.

Abdelmaksoud, A.M., T.C. Becker, and G.P. Balomenos. 2019. “Statistical Analysis of Bridge Management System Inspection Data.” In *International Association for*

Bridge and Structural Engineering (IABSE) 20th Congress – The Evolving Metropolis, 898–902. New York City, United States.

Alipour, Azadeh, Behrouz Shafei, and Masanobu S Shinozuka. 2013. “Capacity Loss Evaluation of Reinforced Concrete Bridges Located in Extreme Chloride-Laden Environments.” *Structure and Infrastructure Engineering* 9 (1): 8–27.

Almomani, Yazan, Nur Yazdani, and Eyosias Beneberu. 2020. “Numerical Modeling of Deteriorated Concrete Bridge Bent Caps with Externally Bonded CFRP Retrofit.” *Innovative Infrastructure Solutions* 5 (2): 1–10.

Bagnariol, Dino, and Jim Au. 2000. “Seismic Assessment of Provincial Bridges: Phase 1 – Preliminary Screening.” Bridge Office, Engineering Standards Branch, Ministry of Transportation of Ontario (MTO).

Baker, Jack W. 2015. “Efficient Analytical Fragility Function Fitting Using Dynamic Structural Analysis.” *Earthquake Spectra* 31 (1): 579–99.

Balomenos, Georgios P, Yujie Hu, Jamie E Padgett, and Kyle Shelton. 2019. “Impact of Coastal Hazards on Residents’ Spatial Accessibility to Health Services.” *Journal of Infrastructure Systems* 25 (4): 4019028.

Balomenos, Georgios P, Sabarethinam Kameshwar, and Jamie E Padgett. 2020. “Parameterized Fragility Models for Multi-Bridge Classes Subjected to Hurricane Loads.” *Engineering Structures* 208: 110213.

Balomenos, Georgios P, and Jamie E Padgett. 2018. “Fragility Analysis of Pile-Supported Wharves and Piers Exposed to Storm Surge and Waves.” *Journal of Waterway, Port, Coastal, and Ocean Engineering* 144 (2): 4017046.

Bazzucchi, Fabio, Luciana Restuccia, and Giuseppe Andrea Ferro. 2018.

“Considerations over the Italian Road Bridge Infrastructure Safety after the Polcevera Viaduct Collapse: Past Errors and Future Perspectives.” *Frattura e Integrita Strutturale* 12.

Bernier, Carl, Ioannis Gidaris, Georgios P Balomenos, and Jamie E Padgett. 2019.

“Assessing the Accessibility of Petrochemical Facilities during Storm Surge Events.” *Reliability Engineering & System Safety* 188: 155–67.

Betti, R. 2010. “Aging Infrastructure: Issues.” *Research, and Technology. Buildings and Infrastructure Protection Series. Infrastructure Protection and Disaster Management Division, Science & Technology Directorate, US Department of Homeland Security.*

Biondini, Fabio, Elena Camnasio, and Alessandro Palermo. 2014. “Lifetime Seismic Performance of Concrete Bridges Exposed to Corrosion.” *Structure and Infrastructure Engineering* 10 (7): 880–900.

Bocchini, Paolo, Duygu Saydam, and Dan M Frangopol. 2013. “Efficient, Accurate, and Simple Markov Chain Model for the Life-Cycle Analysis of Bridge Groups.” *Structural Safety* 40: 51–64.

Bolukbasi, Melik, Jamshid Mohammadi, and David Arditi. 2004. “Estimating the Future Condition of Highway Bridge Components Using National Bridge Inventory Data.” *Practice Periodical on Structural Design and Construction* 9 (1): 16–25.

Bonthron, Leslie, Corey Beck, Alana Lund, Farida Mahmud, Xin Zhang, Rebeca Orellana Montano, Shirley J Dyke, Julio Ramirez, Yenan Cao, and George P Mavroeidis. 2021. “Empowering the Indiana Bridge Inventory Database Toward

- Rapid Seismic Vulnerability Assessment.” Joint Transportation Research Program Publication No. FHWA/IN/JTRP-2021/03. West Lafayette, IN: Purdue University.
- Brown, Colin B, and James T P Yao. 1983. “Fuzzy Sets and Structural Engineering.” *Journal of Structural Engineering* 109 (5): 1211–25.
- Butt, Abbas A, Mohamed Y Shahin, Kieran J Feighan, and Samuel H Carpenter. 1987. *Pavement Performance Prediction Model Using the Markov Process*.
- Cesare, Mark A, Carlos Santamarina, Carl Turkstra, and Erik H Vanmarcke. 1992. “Modeling Bridge Deterioration with Markov Chains.” *Journal of Transportation Engineering* 118 (6): 820–33.
- CSA, (Canadian Standards Association). 2019. *Canadian Highway Bridge Design Code. CSA S6-19*. Toronto, Canada.
- Dicleli, Murat, and Michel Bruneau. 1996. “Quantitative Approach to Rapid Seismic Evaluation of Slab-on-Girder Steel Highway Bridges.” *Journal of Structural Engineering* 122 (10): 1160–68.
- Dukes, Jazalyn, Sujith Mangalathu, Jamie E Padgett, and Reginald DesRoches. 2018. “Development of a Bridge-Specific Fragility Methodology to Improve the Seismic Resilience of Bridges.” *Earthquake and Structures* 15 (3): 253–61.
- Estes, Allen C, and Dan M Frangopol. 1999. “Repair Optimization of Highway Bridges Using System Reliability Approach.” *Journal of Structural Engineering* 125 (7): 766–75.
- Estes, Allen C, and Dan M Frangopol. 2003. “Updating Bridge Reliability Based on Bridge Management Systems Visual Inspection Results.” *Journal of Bridge*

Engineering 8 (6): 374–82.

Filiatrault, André, Stéphane Tremblay, and René Tinawi. 1994. “A Rapid Seismic Screening Procedure for Existing Bridges in Canada.” *Canadian Journal of Civil Engineering* 21 (4): 626–42.

Frangopol, D M. 1998. “A Probabilistic Model Based on Eight Random Variables for Preventive Maintenance of Bridges.” In *Progress Meeting “Optimum Maintenance Strategies for Different Bridge Types,”* Highways Agency, London, November.

Frangopol, Dan M, Jung S Kong, and Emhaidy S Gharaibeh. 2001. “Reliability-Based Life-Cycle Management of Highway Bridges.” *Journal of Computing in Civil Engineering* 15 (1): 27–34.

Ghodoosi, Farzad, Soliman Abu-Samra, Mehran Zeynalian, and Tarek Zayed. 2018. “Maintenance Cost Optimization for Bridge Structures Using System Reliability Analysis and Genetic Algorithms.” *Journal of Construction Engineering and Management* 144 (2): 4017116.

Ghodoosi, Farzad, Ashutosh Bagchi, Tarek Zayed, and Adel R Zaki. 2014. “Reliability-Based Condition Assessment of a Deteriorated Concrete Bridge.” *Structural Monitoring and Maintenance* 1 (4): 357–69.

Grussing, Michael N, Donald R Uzarski, and Lance R Marrano. 2006. “Condition and Reliability Prediction Models Using the Weibull Probability Distribution.” In *Applications of Advanced Technology in Transportation*, 19–24.

Hedegaard, Brock D, Catherine E W French, and Carol K Shield. 2013. “Investigation of Thermal Gradient Effects in the I-35W St. Anthony Falls Bridge.” *Journal of*

- Bridge Engineering* 18 (9): 890–900.
- Hurt, M, and S Schrock. 2016. “Chapter 1-Introduction.” *Highway Bridge Maintenance Planning and Scheduling*, 1–30.
- Jia, Gaofeng, and Paolo Gardoni. 2018. “State-Dependent Stochastic Models: A General Stochastic Framework for Modeling Deteriorating Engineering Systems Considering Multiple Deterioration Processes and Their Interactions.” *Structural Safety* 72: 99–110.
- Jiang, Yi, and Kumares C Sinha. 1989. “Bridge Service Life Prediction Model Using the Markov Chain.” *Transportation Research Record* 1223: 24–30.
- Kallen, M J, and J M Van Noortwijk. 2006. “Statistical Inference for Markov Deterioration Models of Bridge Conditions in the Netherlands.” In *Proceedings of the Third International Conference on Bridge Maintenance, Safety and Management (IABMAS)*, 16–19. Citeseer.
- Kenedi, Walter, and Dino Bagnariol. 2007. “Seismic Index in the Bridge Management System (BMS).” Bridge Office, Ministry of Transportation of Ontario (MTO), 301 St. Paul Street St. Catharines, ON.
- Kennedy, John B, and Mohamed H Soliman. 1987. “Temperature Distribution in Composite Bridges.” *Journal of Structural Engineering* 113 (3): 475–82.
- Kim, Sunyong, Dan M Frangopol, and Mohamed Soliman. 2013. “Generalized Probabilistic Framework for Optimum Inspection and Maintenance Planning.” *Journal of Structural Engineering* 139 (3): 435–47.
- Kiureghian, Armen Der, and Ove Ditlevsen. 2009. “Aleatory or Epistemic? Does It Matter?” *Structural Safety* 31 (2): 105–12.

- Lark, Robert J, and Katja D Flaig. 2005. “The Use of Reliability Analysis to Aid Bridge Management.” *Structural Engineer* 83 (5): 27–31.
- Ma, Yafei, Lei Wang, Jianren Zhang, Yibing Xiang, Tishun Peng, and Yongming Liu. 2015. “Hybrid Uncertainty Quantification for Probabilistic Corrosion Damage Prediction for Aging RC Bridges.” *Journal of Materials in Civil Engineering* 27 (4): 4014152.
- Madanat, Samer M, Matthew G Karlaftis, and Patrick S McCarthy. 1997. “Probabilistic Infrastructure Deterioration Models with Panel Data.” *Journal of Infrastructure Systems* 3 (1): 4–9.
- Marano, Giuseppe Carlo, Giuseppe Quaranta, and Mauro Mezzina. 2008. “Fuzzy Time-Dependent Reliability Analysis of RC Beams Subject to Pitting Corrosion.” *Journal of Materials in Civil Engineering* 20 (9): 578–87.
- Mars, W V, and A Fatemi. 2002. “A Literature Survey on Fatigue Analysis Approaches for Rubber.” *International Journal of Fatigue* 24 (9): 949–61.
- McKay, Michael D, Richard J Beckman, and William J Conover. 2000. “A Comparison of Three Methods for Selecting Values of Input Variables in the Analysis of Output from a Computer Code.” *Technometrics* 42 (1): 55–61.
- McKenna, Frank, Michael H Scott, and Gregory L Fenves. 2010. “Nonlinear Finite-Element Analysis Software Architecture Using Object Composition.” *Journal of Computing in Civil Engineering* 24 (1): 95–107.
- Mirzaei, Zanyar, Bryan T Adey, Leo Klatter, and Paul D Thompson. 2014. “Overview of Existing Bridge Management Systems.” *Bridge Management Committee, IABMAS*.

- Mirzaei, Zanyar, Bryan T Adey, Paul Thompson, and Leo Klatter. 2014. “Overview of Existing Bridge Management Systems-Report by the IABMAS Bridge Management Committee (2014).” In *7th International Conference on Bridge Maintenance, Safety and Management (IABMAS 2014)*.
- Moehle, Jack P, and Marc O Eberhard. 2003. “Earthquake Damage to Bridges.” In *Bridge Engineering*, 52–84. CRC Press.
- Möller, Bernd, Michael Beer, Wolfgang Graf, and Jan-Uwe Sickert. 2006. “Time-Dependent Reliability of Textile-Strengthened RC Structures under Consideration of Fuzzy Randomness.” *Computers & Structures* 84 (8–9): 585–603.
- Morcous, G, and Z Lounis. 2007. “Probabilistic and Mechanistic Deterioration Models for Bridge Management.” In *Computing in Civil Engineering (2007)*, 364–73.
- Morcous, George. 2006. “Performance Prediction of Bridge Deck Systems Using Markov Chains.” *Journal of Performance of Constructed Facilities* 20 (2): 146–55.
- Morcous, George, Z Lounis, and Yong Cho. 2010. “An Integrated System for Bridge Management Using Probabilistic and Mechanistic Deterioration Models: Application to Bridge Decks.” *KSCE Journal of Civil Engineering* 14 (4): 527–37.
- MTO (Ministry of Transportation Ontario). 2015. “Bridge Repairs.” 2015. <http://www.mto.gov.on.ca/english/highway-bridges/ontario-bridges.shtml> (Accessed October 2018).
- Muhr, A H. 2006. “Fracture of Rubber-Steel Laminated Bearings.” In *Elastomers and Components*, 209–26. Elsevier.

- Noade, Bryanna M, and Tracy C Becker. 2019. “Probabilistic Framework for Lifetime Bridge-Bearing Demands.” *Journal of Bridge Engineering* 24 (7): 4019065.
- Noortwijk, Jan M van, and Dan M Frangopol. 2004. “Two Probabilistic Life-Cycle Maintenance Models for Deteriorating Civil Infrastructures.” *Probabilistic Engineering Mechanics* 19 (4): 345–59.
- Padgett, Jamie E, Kristina Dennemann, and Jayadipta Ghosh. 2010. “Risk-Based Seismic Life-Cycle Cost–Benefit (LCC-B) Analysis for Bridge Retrofit Assessment.” *Structural Safety* 32 (3): 165–73.
- Pregolato, Maria. 2019. “Bridge Safety Is Not for Granted—A Novel Approach to Bridge Management.” *Engineering Structures* 196: 109193.
- Priestley, M J Nigel, Frieder Seible, and Gian Michele Calvi. 1996. *Seismic Design and Retrofit of Bridges*. John Wiley & Sons.
- Rhinehart, R Russell. 2016. *Nonlinear Regression Modeling for Engineering Applications: Modeling, Model Validation, and Enabling Design of Experiments*. John Wiley & Sons.
- Roeder, Charles W, John F Stanton, and Andrew W Taylor. 1990. “Fatigue of Steel-Reinforced Elastomeric Bearings.” *Journal of Structural Engineering* 116 (2): 407–26.
- Roelfstra, Guido, Rade Hajdin, Bryan Adey, and Eugen Brühwiler. 2004. “Condition Evolution in Bridge Management Systems and Corrosion-Induced Deterioration.” *Journal of Bridge Engineering* 9 (3): 268–77.
- Srikanth, Ishwarya, and Madasamy Arockiasamy. 2020. “Deterioration Models for Prediction of Remaining Useful Life of Timber and Concrete Bridges: A Review.”

Journal of Traffic and Transportation Engineering (English Edition) 7 (2): 152–73.

Stearns, Matthew, and Jamie E Padgett. 2012. “Impact of 2008 Hurricane Ike on Bridge Infrastructure in the Houston/Galveston Region.” *Journal of Performance of Constructed Facilities* 26 (4): 441–52.

Stein, Stuart M, G Kenneth Young, Roy E Trent, and David R Pearson. 1999. “Prioritizing Scour Vulnerable Bridges Using Risk.” *Journal of Infrastructure Systems* 5 (3): 95–101.

Suryatal, Baban, Haribhau Phakatkar, Kasilingam Rajkumar, and Ponniah Thavamani. 2015. “Fatigue Life Estimation of an Elastomeric Pad by ϵ -N Curve and FEA.” *Journal of Surface Engineered Materials and Advanced Technology* 5 (02): 85.

Tee, A B, M D Bowman, and K C Sinha. 1988. “A Fuzzy Mathematical Approach for Bridge Condition Evaluation.” *Civil Engineering Systems* 5 (1): 17–24.

Tesfamariam, S, and S M Modirzadeh. 2009. “Risk-Based Rapid Visual Screening of Bridges.” In *TCLEE 2009: Lifeline Earthquake Engineering in a Multihazard Environment*, 1–12.

Tolliver, Denver, and Pan Lu. 2012. “Analysis of Bridge Deterioration Rates: A Case Study of the Northern Plains Region.” In *Journal of the Transportation Research Forum*. Vol. 50.

Wang, Lei, Yafei Ma, Jianren Zhang, and Yongming Liu. 2013. “Probabilistic Analysis of Corrosion of Reinforcement in RC Bridges Considering Fuzziness and Randomness.” *Journal of Structural Engineering* 139 (9): 1529–40.

Wang, Lei, Yafei Ma, Jianren Zhang, Xuhui Zhang, and Yongming Liu. 2015.

“Uncertainty Quantification and Structural Reliability Estimation Considering Inspection Data Scarcity.” *ASCE-ASME Journal of Risk and Uncertainty in Engineering Systems, Part A: Civil Engineering* 1 (2): 4015004.

Weisberg, Sanford. 2005. *Applied Linear Regression*. Vol. 528. John Wiley & Sons.

Wu, Hsien-Chung. 2004. “Bayesian System Reliability Assessment under Fuzzy Environments.” *Reliability Engineering & System Safety* 83 (3): 277–86.

Zadeh, Lotfi A. 1965. “Fuzzy Sets.” *Information and Control* 8 (3): 338–53.

Zambon, Ivan, Anja Vidovic, Alfred Strauss, Jose Matos, and Joao Amado. 2017. “Comparison of Stochastic Prediction Models Based on Visual Inspections of Bridge Decks.” *Journal of Civil Engineering and Management* 23 (5): 553–61.

Zhang, Yi-Ming, Hao Wang, Hua-Ping Wan, Jian-Xiao Mao, and Yi-Chao Xu. 2020. “Anomaly Detection of Structural Health Monitoring Data Using the Maximum Likelihood Estimation-Based Bayesian Dynamic Linear Model.” *Structural Health Monitoring*, 1475921720977020.

2. Parameterized Logistic Models for Bridge Inspection and Maintenance Scheduling

Reprinted with permission from Journal of Bridge Engineering, ASCE

Abdelmaksoud, Ahmed M, Georgios P Balomenos, and Tracy C Becker. 2021. “Parameterized Logistic Models for Bridge Inspection and Maintenance Scheduling.” *Journal of Bridge Engineering* 26 (10): 4021072. DOI: 10.1061/(ASCE)BE.1943-5592.0001774.

2.1. Abstract

Proper inspection and maintenance schedules are integral to bridge functionality and safety; however, they also pose challenges in light of budget and resource limitations. As such, bridge management systems (BMSs) are always concerned with finding the best deterioration and maintenance models to optimize scheduling. The current work proposes parameterized logistic models that can capture bridge deterioration and the effect of maintenance interventions. Given a handful of easy-to-track bridge parameters, such as age, time since last major maintenance, and location, the proposed models predict the probability of a bridge (or group of bridges) to need repair throughout its service life. Combined with the appropriate probability threshold, obtained from life-cycle cost analysis, this allows for the optimization of inspection frequency and helps in maintenance planning. The results indicate that the proposed models predict the bridge condition more accurately compared to the Markov Chains models adopted by many North American BMSs. Finally, the application of the parameterized logistic models is demonstrated through a case study.

Author keywords: Bridge management, Inspection, Maintenance, Logistic Models, Bridge Condition Index, Life-cycle costs.

2.2. Introduction

Bridge deterioration can lead to severe consequences beyond the cost of repair, extending to traffic delays, construction of temporary alternative routes, and safety hazards (Biezma and Schanack 2007; Bazzucchi et al. 2018; Moehle and Eberhard 2003). Proper inspection and maintenance strategies can mitigate such consequences, but in light of budget constraints, the scheduling of interventions must be carefully planned. As such, reliable models for deterioration and the effects of maintenance on bridge performance are essential for bridge management systems (BMSs) to help optimize inspection and maintenance practices (Mirzaei et al. 2012).

A typical approach to modelling deterioration is through numerical analysis where the deterioration is modelled as a time variant reduction in the load-carrying resistance of bridge elements. For example, Biondini et al. (2014) and Alipour et al. (2013) modelled corrosion of RC bridge elements by reducing the reinforcement bar diameter and reducing the unconfined strength of the concrete cover to account for cover spalling and cracking. Although this approach provides detailed information about future bridge performance, it requires complex structural, environmental (e.g. humidity and chloride availability), and loading parameters especially when considering concurrent deterioration mechanisms and uncertainty in modelling variables (Jia and Gardoni 2018). Furthermore, updating complex numerical models individually for each bridge poses a problem when managing a large portfolio of bridges.

Another approach for bridge performance prediction is through deterministic or probabilistic statistical analysis of inspection data without the use of numerical bridge

models. A common deterministic analysis technique is the ordinary least squares (OLS) regression which is known for its simplicity and ability to make full use of available historical condition data to predict future condition trends. For example, Jiang and Sinha (1989) and Bolukbasi et al. (2004) analysed the inspection data from the National Bridge Inventory (NBI) and proposed OLS regression models to predict the condition rating of bridge elements given the bridge age. These models can estimate the average bridge condition. However, due to inherent uncertainties (e.g. randomness in material properties, loading, and deterioration process), it is most likely that the actual bridge condition will vary from the deterministic estimate. Thus, deterministic-based methods involve a considerable risk of underestimating the bridge inspection and maintenance needs. To account for such risk, it is essential to incorporate uncertainties in the decision making process via probabilistic analysis (Ford et al. 2011). Hence, probabilistic techniques, such as Markov Chains and reliability analysis, have been proposed to predict future bridge condition.

Markov Chains models have been popular with many BMSs in North America such as PONTIS (Golabi and Shepard 1997), BRIDGIT (Hawk and Small 1998), and OBMS (Thompson et al. 1999). This method has been used to predict the probability that the condition of an individual bridge, or a group of bridges, would change from one state to another (e.g. good to fair condition or fair to poor condition) by accumulating the state transition probabilities over time (Bocchini et al. 2013). However, Markov Chains has some impractical or unrealistic assumptions such as the independence of future condition from past condition, constant inspection periods for all investigated bridges, stationary transition probabilities, and constant bridge

population (Zambon et al. 2017; Morcoux 2006). Zambon et al. (2017) evaluated the impact of these assumptions by analyzing inspection data from a state owned Portuguese infrastructure database and concluded that these assumptions may lead to underestimating the actual bridge maintenance needs. Morcoux (2006) conducted a similar study using field data obtained from the Ministère des Transports du Québec in Canada and found that variation of inspection intervals from one bridge to another may cause a noticeable error in estimating bridge lifetime. Also, Morcoux (2006) concluded that ignoring the condition history is erroneous for individual bridges and elements.

Another probabilistic technique is reliability analysis. Frangopol (1998) combined reliability index profiles for maintenance actions with reliability deterioration model to obtain the final reliability profile. The proposed maintenance profiles, however, require a substantial amount of information that may not be readily available or known, such as the instantaneous performance improvement, post maintenance deterioration rate, and duration of maintenance effects. Researchers attempted to address this issue by assuming that the maintenance restores a constant percentage of the bridge condition (Grussing et al. 2006; Ghodoosi et al. 2018). Although that reliability-based approaches do not require the assumptions necessary for Markov Chains, they are computationally expensive and require extensive data collection from bridge inspections making them inefficient when managing a large portfolio of bridges (Srikanth and Arockiasamy 2020).

The current work proposes a new probabilistic framework for scheduling bridge inspection and maintenance based on logistic regression analysis. The proposed framework has the advantage of incorporating uncertainty without the assumptions

imposed by Markov Chains. Additionally, the proposed framework models deterioration and maintenance effects with easily accessible parameters unlike reliability-based approaches. The current study demonstrates the application of the framework using the condition data of bridges owned by the Ministry of Transportation of Ontario (MTO) in Canada. However, this framework can be applied to develop similar models for other bridge management databases.

Based on a parametric study, two sets of logistic models are proposed to predict the probability of reaching a critical condition given a limited amount of information from inspection data. The first set can be used to estimate the appropriate timing of maintenance interventions, and the second set can be used for optimizing inspection intervals. Each set consists of two models that support decisions on the bridge group level and the individual bridge level. The performance of the proposed probabilistic models is compared to that of Markov Chains which is popular among many North American BMSs. Then, the application of the framework is demonstrated through a case study bridge. Finally, life-cycle cost (LCC) analysis is conducted to optimize inspection and maintenance decisions from a safety and cost perspective.

2.3. Inspection Data

2.3.1. Data Description

The data used in this study is publicly available from MTO in Canada (Government of Ontario 2018). The MTO conducts biennial routine inspections of roughly 3000 bridges; each bridge is assigned a Bridge Condition Index (BCI) that reflects the general bridge condition. These inspections involve element-by-element visual assessments of material defects, performance deficiencies, and maintenance needs (MTO, 2008). Based on the condition of the elements, the inspector determines the current value of

the bridge. The BCI of a bridge is computed as the ratio between the current value of the bridge and the replacement cost (MTO, 2015).

The BCI is then used by the MTO for maintenance planning (MTO, 2015). A BCI score ranging from 70 to 100 indicates satisfactory performance with no maintenance needed in the subsequent five years. Bridges with a BCI between 60 and 70 may need repairs within the next five years. Finally, if the BCI is less than 60, repairs should be performed within one year. The Ontario database holds BCI records that date back to 18 years for some bridges; a sample of these records is shown in Table 2.1. For many bridges, the BCI is recorded in regular two-year intervals; however, some bridges may have shorter or longer intervals between inspections.

Table 2.1 Sample of BCI records dating back to 2004

Bridge ID	BCI recording year													
	2017	2016	2015	2014	2013	2012	2011	2010	2009	2008	2007	2006	2005	2004
43 - 5/	-	82.6	-	80.8	-	80.8	-	73.2	-	73.4	72.9	-	73.7	-
49 - 2/	-	75.5	-	75.8	-	76.3	-	54.9	-	54.8	55.2	-	-	51.4
10 - 150/2	-	82.6	-	83.8	-	83.9	-	-	-	-	-	-	-	-
37 - 59/2	69.9	-	69	-	70.9	-	71.6	-	-	-	-	-	-	-
37 - 59/1	72.7	-	72.9	-	73	-	72.6	-	-	-	-	-	-	-
11 - 44/	-	72.5	-	62.9	-	62.9	-	64.3	-	65.2	-	66	-	66.3
10 - 160/1	-	80.4	-	80.7	-	82.4	-	-	-	-	-	71.6	-	71.7
38S- 56/	83.7	-	87.3	-	93.6	-	98.5	-	100	-	-	-	-	-

In addition to the BCI, other parameters are recorded in the inspection data that could potentially influence the BCI value such as the bridge age, maintenance history, location, and construction material. It is reasonable to assume that the BCI decreases with age due to degradation caused by loading, environmental, and climatic conditions

(Stewart et al. 2011). Meanwhile, maintenance improves the BCI and is represented in the current study by two parameters: time to last major (T_{major}) and time to last minor (T_{minor}) maintenance. Retrofit of the bridge deck and extensive rehabilitation or replacement of other elements are examples of a major maintenance, while maintenance to any element rather than the deck, such as bearings, expansion joints, or barrier walls can be classified as minor maintenance as defined by the Ontario Structure Inspection Manual (MTO, 2008). For bridges with only major maintenance, T_{minor} is assumed to be equal to T_{major} ; for bridges with only minor maintenance, T_{major} is measured from the construction date; for bridges with no maintenance, T_{minor} and T_{major} are both measured from the construction date.

The bridge location, represented by its latitude and longitude coordinates, is a possible indicator for the surrounding environmental conditions. For example, northern Ontario regions often experience lower temperatures and larger snow depths. Consequently, northern bridges can be exposed to higher concentrations of de-icing chemicals, a main contributor to material deterioration (Shi et al. 2009), suggesting that the northern bridges may be more susceptible to rapid reduction of BCI. Another investigated parameter is the bridge material. Previous studies have shown that the impact of bridge material on the deterioration varies depending on the bridge population sample being analyzed and the analysis method (Veshosky et al. 1994; Tabatabai et al. 2016). The current study investigates how the deterioration of MTO owned bridges is influenced by two typical bridge materials: concrete and steel which comprise 71% and 28% of the MTO's bridge population, respectively

This study uses parameters that are available in the MTO database. Other

parameters, such as the presence of water, traffic volume, loads, design specifications, etc., may affect the bridge condition but are not recorded in the MTO database. Other bridge agencies can use the proposed framework to investigate the parameters available in their database.

2.3.2. *Data Pre-processing*

Prior to analysis, outliers (shown in Fig. 2.1) are excluded. Bridges in which the BCI dropped below 85 in less than 5 years are considered outliers. Such early drastic drop in the BCI may be attributed to accidents, extreme events, or even inaccurate data entry. It is expected that bridges would be inspected directly after these events as the proposed prediction models do not account for accidents or extreme events. After removal of outliers and bridges with missing information, a total of 2759 bridges remained in the analysis. The data from the most recent inspection records (from either 2016 or 2017 as seen in Table 2.1) is used to assess the models' prediction accuracy, whereas, the remaining data from all other dates (2015 and before) is used for training the models.

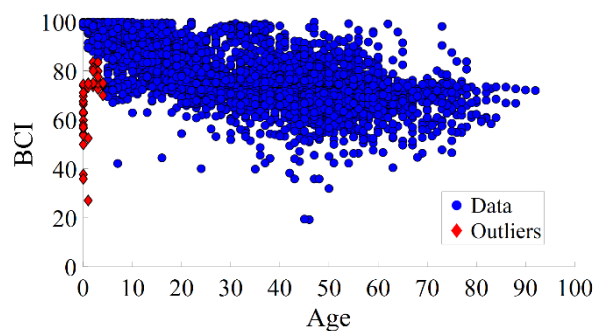


Fig. 2.1 MTO data showing BCI-age relationship

2.4. Methodology

2.4.1. *Logistic Regression*

Towards aiding bridge owners in determining whether a bridge is approaching a limit

state, such as repair or no-repair (R/NR), logistic regression (Verhulst 1845) is adopted as it can relate the occurrence probability of an outcome to the predictor variables as shown in Eq. (1)

$$p = \frac{\exp[\beta_o + \sum_{j=1}^n \beta_j x_j^{\gamma_j}]}{1 + \exp[\beta_o + \sum_{j=1}^n \beta_j x_j^{\gamma_j}]} \quad (1)$$

where p is the probability of exceeding a limit state (e.g. repair), n is the number of independent parameters, β_o is the model intercept, and β_j and γ_j are the regression and exponent coefficients for the independent parameter x_j , respectively. Previous studies applied logistic regression to predict the failure risks associated with extreme events. For example, logistic models were developed to predict the uplift failure risks of ports (Balomenos and Padgett 2018) and bridges (Balomenos et al. 2020) exposed to hurricanes. These models in turn, were easily integrated to a framework for assessing the post-hazard accessibility of petrochemical facilities (Bernier et al. 2019) and healthcare facilities (Balomenos et al. 2019). Here, logistic regression is adopted in this study to develop predictive models for bridge inspection and maintenance needs.

This study uses nonlinear logistic regression to predict the probability of a group of bridges or of an individual bridge reaching a critical state, in support of maintenance and inspection decisions. The group level models can be useful for a budget estimation on a network level. The individual level models account for the actual working conditions, such as traffic demands and local environment, for a specific bridge by including an updating factor related to the BCI deterioration rate of that bridge. As such, these models can be used to construct bridge-specific inspection and maintenance schedules, allowing for better budget and resource distribution.

To formulate the decision models, the maintenance limit state (MLS) and the inspection limit state (ILS) are defined based on MTO guidelines (MTO, 2015). For safety, the bridge is assumed to be in a critical condition when the BCI reaches 70, at which time the bridge may start showing signs of noticeable deterioration as shown in Fig. 2.2. Thus, the MLS is defined as the BCI falling below 70 at a given time. For scheduling inspections, the interval between inspections (Δt) should be selected based on the likelihood of the bridge reaching a critical condition within the interval. As such, the ILS is defined as the BCI falling below 70 within a chosen inspection interval (Δt). The study uses Δt values of 2, 4, and 6 years. An upper bound of 6 years is chosen based on a survey of common inspection intervals in BMSs outside North America (Everett et al. 2008). Based on these definitions, the BCI values within the training data are replaced with a binary state, repair needed or no repair needed (R/NR). Logistic regression is then conducted to predict the probability of exceeding the MLS or ILS.



Fig. 2.2 A bridge with a BCI approaching 70: Deck soffit with wet longitudinal cracks and delamination

2.4.2. *LASSO Regularization*

To develop accurate and interpretable prediction models, logistic regression is integrated with the least absolute shrinkage and selection operator (LASSO) regularization (Tibshirani 1996). The LASSO regularization modifies the objective function of logistic regression so as to constrain the summation of the absolute regression coefficients via the regularization tuning parameter (λ) as

$$\min \left[\frac{1}{N} \text{Deviance}(\beta_o, \beta_j, \gamma_j) + \lambda \sum_{j=1}^n |\beta_j| \right] \quad (2)$$

where N is the number of data points, and the deviance is a goodness-of-fit statistic which is inversely proportional to the likelihood function (Nelder and Wedderburn 1972).

The regularization tuning parameter (λ) penalizes regression coefficients, leading to the removal of less significant parameters, minimizing overfitting, and simplifying the model input. The larger the λ , the more the regression coefficients are penalized, hence forcing more parameters to be excluded from the model. Too low a value of λ will lead to insignificant variables remaining in the model, while too high a value of λ may exclude important parameters. Thus, a range of values of λ is first investigated, and an appropriate value is chosen based on 10-fold cross validation (Tibshirani 1996; McLachlan et al. 2005).

2.4.3. *Markov Chains*

Unlike logistic regression, Markov chains predict the probability of future condition states by accumulating the probability of transitioning from one state to another over time (Barlow and Proschan 1996; Cesare et al. 1992) as follows

$$\mathbf{q}_t = \mathbf{q}_o \mathbf{P}^t \quad (3)$$

where \mathbf{q}_t and \mathbf{q}_o are the future and initial condition vectors respectively, \mathbf{P} is the transition matrix which describes the probability of transitioning from one condition state to another within a year, and t is the time from the known initial condition in years. If two bridge condition states are used (e.g. state 1 = repair unnecessary, and state 2 = repair necessary), Eq. (3) is expressed as

$$[P_{1,t} \quad P_{2,t}] = [P_{1,0} \quad P_{2,0}] \times \begin{bmatrix} P_{11} & P_{12} \\ P_{21} & P_{22} \end{bmatrix}^t \quad (4)$$

where $P_{i,t}$ is probability of being in condition state i at time t , and P_{ij} is the probability of transitioning from state i to j . The transition matrix can also be simplified based on two facts: 1) summation of each row should be equal to one as each row represents a set of events from which one must occur (Walpole and Myers 2012), and 2) $P_{ij} = 0$ when i is greater than j as the bridge condition will not improve without maintenance. The simplified matrix is expressed as

$$\mathbf{P} = \begin{bmatrix} P_{11} & 1-P_{11} \\ 0 & 1 \end{bmatrix} \quad (5)$$

To evaluate the transition matrix \mathbf{P} , the BCI values within the training data are replaced with a binary state of the bridge based on the limit state definitions. Then, the available bridge-state data points are classified into groups based on the time to initial condition t . For each time group with known t , the actual relative frequency of each bridge condition state ($f_{i,t}$) is computed, and the Markov Chains prediction for each condition state is expressed as $(\mathbf{q}_o \mathbf{P}^t)_i$ where $i = 1,2$. The transition matrix can then be evaluated by minimizing the summation of the weighted squared errors for all condition states and all time groups (Butt et al. 1987; Cesare et al. 1992)

$$\min \sum_{t=1}^{t=m} [w_t \sum_{i=1}^{i=2} [f_{i,t} - (\mathbf{q}_o \mathbf{P}^t)_i]^2] \quad \text{subject to } 0 \leq P_{11} \leq 1 \quad (6)$$

where w_t is a weighting factor equal to the number of data points per time group, and m is the number of time groups. This optimization problem requires a series of consecutive bridge condition records without any major maintenance interventions (Cesare et al. 1992; Morcous 2006). Hence, if a bridge has a maintenance history, the initial condition for that bridge is set to be right after the last major maintenance, and thus, only the subsequent condition records are used. Otherwise, the initial condition for a bridge is set at its construction date, and thus, all of the condition records for that bridge are used.

In the current study, the initial condition vector \mathbf{q}_o and the transition probability P_{11} are established separately for each initial maintenance condition. At the construction date, a bridge is in its top condition and has zero probability of needing repair, thus \mathbf{q}_o is taken as [1 0]. Whereas the bridge condition after the last major maintenance depends on the effectiveness of repairs. Based on the available MTO data, about 95% of bridges that received major repairs had their condition improved from state 2 to 1. Thus, after receiving a major maintenance, \mathbf{q}_o is to be taken as [0.95 0.05] representing a 95% and 5% probability of being in state 1 or 2, respectively. It is also reasonable to assume that P_{11} is lower after maintenance than that on the construction date, as repair will not fully restore the bridge to its as-good-as-new condition.

2.4.4. Confusion Matrix

To assess the predication accuracy of the logistic and Markov Chains models, the confusion matrix (Kohavi and Provost 1998) is adopted. In the case of a binary event

(e.g. repair or no-repair), the confusion matrix is expressed as a two by two matrix (Balomenos and Padgett 2018). From this matrix, several metrics can be derived to assess the models' prediction accuracy such as the recall, which is the ratio of the correct repair predictions to the total number of bridges requiring repairs, and the false repair rate (FRR), which is the ratio of false repair predictions to the total number of bridges not in need of repairs (Murphy 2012).

To formulate the matrix, the probability of exceeding a limit state is computed for all bridges at the time of their last recorded inspection (2016 or 2017). Then, these probabilities are compared to a threshold value, and each bridge is classified. The estimated states are then compared to the actual states recorded at the last recorded inspection to formulate the confusion matrix, and the metrics are then computed to assess the variation in models' prediction accuracy with the threshold.

2.5. Maintenance Decision Models

2.5.1. Group Level LASSO-Logistic Model

MATLAB (2018) is used for the analysis required to estimate the probability of exceeding the MLS on bridge group level (P_{MLS-GL}). The impact of the bridge construction material on the predictive capability of the developed models is also investigated, and thus, the LASSO-Logistic analysis is conducted for two cases. For the first case, a single LASSO-Logistic model is developed without considering the construction material of the bridge, and for the second case the training and validation data are classified into two groups, concrete and steel bridges, and a separate LASSO-Logistic model is trained for each material.

First, the study evaluates the optimum LASSO-Logistic model without bridge material classification. Typically, estimating the optimum exponent coefficients γ_j

requires testing a lot of permutations for the parameters (age, T_{major} , T_{minor} , latitude, and longitude). Hence, a two-step iterative procedure is used to reduce the number of tested γ_j permutations. In the first step, each parameter is separately related to the probability of exceeding the MLS using non-regularized logistic regression while varying its γ_j from 0.1 to 5 with a 0.1 step. Based on this, initial estimates of γ_j are obtained as 0.2, 0.8, 0.7, 1.1, and 1.5 for the age, T_{major} , T_{minor} , latitude, and longitude, respectively. In the second step, γ_j is varied within a ± 0.2 range around the initial estimates with a 0.1 step, and all γ_j permutations are tested using LASSO-Logistic regression.

For each investigated γ_j permutation, the regression analysis is conducted for a range of λ , resulting in new regression coefficients β_j . For each set of β_j the deviance is calculated and plotted against its corresponding λ resulting in a deviance- λ plot for each γ_j permutation, with an example shown in Fig. 2.3. The reduction in λ leads to an initial rapid reduction in the deviance which then plateaus. Seeking a relatively simple model with a high accuracy, the percentage of reduction in deviance with each λ is monitored until it reaches 0.1%. Then, the corresponding λ is compared across permutations to select the simplest possible model while minimizing the deviance. The optimum λ is found to be 0.0041 as shown in Fig. 2.3.

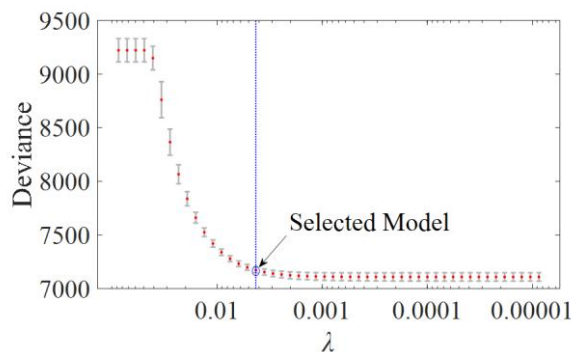


Fig. 2.3 Deviance vs. λ (group-level LASSO-Logistic model without material classification)

The proposed MLS model without consideration of construction material is

$$P_{MLS-GL} = \frac{\exp[-48.09 + 20.207 \cdot \text{age}^{0.1} + 0.255 \cdot T_{major}^{0.6} + 0.351 \cdot \text{latitude}]}{1 + \exp[-48.09 + 20.207 \cdot \text{age}^{0.1} + 0.255 \cdot T_{major}^{0.6} + 0.351 \cdot \text{latitude}]} \quad (7)$$

The LASSO regularization finds that age, T_{major} , and latitude are statistically significant, while the longitude, and T_{minor} are less significant and thus excluded from the final model. These findings are also in-line with the initial speculations that age of the bridge is a primary factor that affects BCI and that bridges in the northern Ontario tend to have a lower BCI compared to the ones in the southern Ontario because of the more intense climate conditions in the north. The exclusion of T_{minor} implies that the bridge functionality is mainly controlled by major maintenance.

The application of the LASSO-logistic model for budget projections requires choosing a threshold value for the bridge rehabilitation probability ($P_{threshold}$) beyond which the bridge is classified as needing repair. The confusion matrix is used to assess the impact of the $P_{threshold}$ value on the model performance. The variation of the Recall and false repair rate (FRR) with $P_{threshold}$ is plotted as shown in Fig. 2.4. Adopting a low $P_{threshold}$ value results in detecting most, if not all, of the bridges in need of repairs but at the cost of having more false repair alarms. For example, when $P_{threshold} = 0.1$, Recall = 97.9%, and FRR = 50.1%. On the other hand, a large $P_{threshold}$ value detects much less of the bridges needing repair despite the lower false repair alarms. For example, when $P_{threshold} = 0.7$, Recall = 12.7%, and FRR = 1.2%. Thus, from a safety perspective, the results indicate that a lower $P_{threshold}$ value is more beneficial for bridge authorities even in the presence of a relatively high FRR. However, the FRR can be further reduced given more bridge-specific information as shown in the next section.

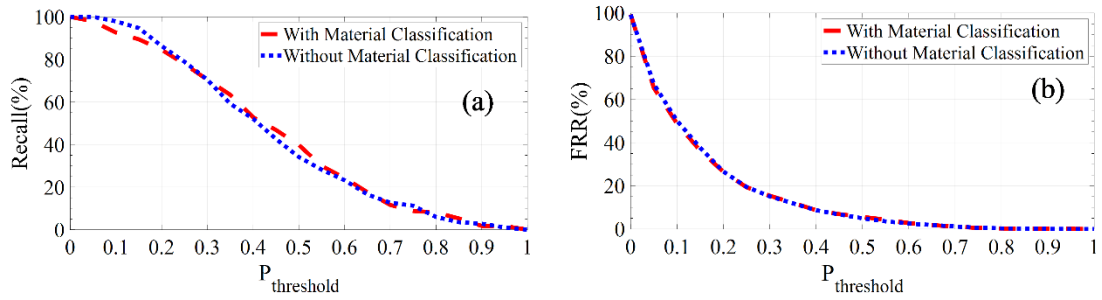


Fig. 2.4 (a) Recall, and (b) FRR vs. $P_{\text{threshold}}$ for group-level model with and without material classification

The above procedures are also conducted for the case that bridges are classified based on the construction material, and the prediction performance metrics are plotted as shown in Fig. 2.4. For the MTO dataset, material classification adds little benefit to the prediction accuracy. Based on this result, material classification is neglected in the rest of the analysis. However, bridge material should be reinvestigated if a different bridge dataset is used (Veshosky et al. 1994).

2.5.2. Individual Level LASSO-Logistic Model

To assess the probability of exceeding the MLS (i.e. the probability of the BCI falling below 70) on the individual bridge level ($P_{\text{MLS-IL}}$), an updating factor is incorporated into the model. The proposed factor is the annual degradation rate (ADR) of the BCI. The ADR can account for influences that are not accounted for in the inspection data (e.g. traffic volume). The ADR is computed at the time of each inspection i based on the recorded BCI values in inspection i and $i-1$

$$\text{ADR}_i = \frac{\text{BCI}_i - \text{BCI}_{i-1}}{t_i - t_{i-1}} \quad (8)$$

The individual bridge level model is then constructed as a function of the ADR and the other bridge parameters following the same approach for constructing the group-level model. The proposed individual bridge level model is found with λ equal

to 0.0045 and is found as

$$P_{MLS-IL} = \frac{\exp[-51.27 + 22.4*age^{0.1} + 0.17*T_{major}^{0.7} + 0.33*latitude + 1.25*ADR^{0.3}]}{1 + \exp[-51.27 + 22.4*age^{0.1} + 0.17*T_{major}^{0.7} + 0.33*latitude + 1.25*ADR^{0.3}]} \quad (9)$$

The model's performance is evaluated similarly to the group-level model. In general, the updating factor (i.e. ADR) significantly reduces the false predictions compared to the group-level model as shown in Fig. 2.5. For example, Fig. 2.5 (a) indicates that there is almost no change in Recall between the individual-level and group-level no matter the selected $P_{threshold}$. However, Fig. 2.5 (b) shows a noticeable reduction in the FRR of the individual-level model for $P_{threshold} < 0.4$, (e.g. for $P_{threshold} = 0.1$, FRR decreases from 50.1% at the group-level to 39% at the individual-level).

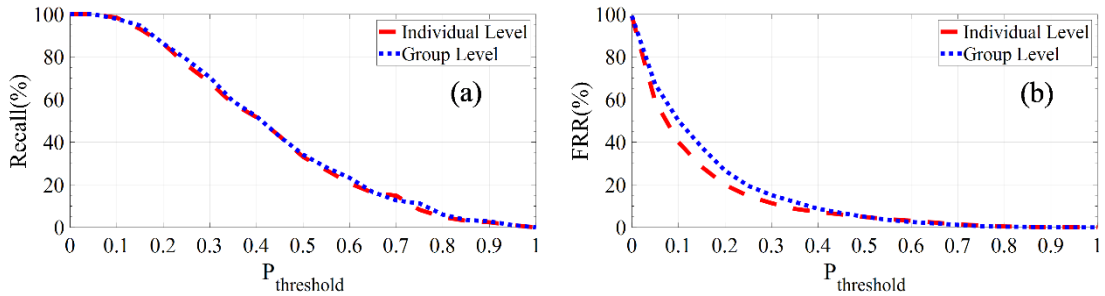


Fig. 2.5 (a) Recall, and (b) FRR vs. $P_{threshold}$ comparing the individual-level and group-level models

2.5.3. Markov Chains Model

The transition matrices in the absence of (P_{no-m}) or following maintenance (P_{post-m}) are evaluated using the steps shown in Table 2.2. For example, consider having two sets of bridge-state data points belonging to bridges with and without maintenance history, each set is subdivided into three subgroups with time to initial condition t of 10, 30, and 50 years. Note that in this study, t has the same definition as T_{major} . First, each subgroup is assigned a weight (w_i) equal to the number of data points. Secondly, the relative

frequency vector (f) of bridge states is found as the percentage of bridges in each condition state. Next, the appropriate initial condition vector (q_o) is selected. Then, the Markov Chain predictions and the weighted prediction errors are computed as a function of the unknown P_{no-m} and P_{post-m} . Finally, the optimization problem in Eq. (6) is solved twice to evaluate P_{no-m} and P_{post-m} .

Table 2.2 Sample calculations for Markov Chains model

Groups	Without maintenance history			With maintenance history		
	$T_{major} = 10$ yrs	$T_{major} = 30$ yrs	$T_{major} = 50$ yrs	$T_{major} = 10$ yrs	$T_{major} = 30$ yrs	$T_{major} = 50$ yrs
Data Points ^a	C	NC	C	C	C	C
	NC	C	C	NC	C	C
	NC	NC	NC	C	NC	
	NC			NC		
w_t	4	3	3	4	3	2
f	[0.75 0.25]	[0.67 0.33]	[0.33 0.67]	[0.5 0.5]	[0.33 0.67]	[0 1]
q_o	[1 0]	[1 0]	[1 0]	[0.95 0.05]	[0.95 0.05]	[0.95 0.05]
Predictions	$q_o P_{no-m}^{10}$	$q_o P_{no-m}^{20}$	$q_o P_{no-m}^{30}$	$q_o P_{post-m}^{10}$	$q_o P_{post-m}^{20}$	$q_o P_{post-m}^{30}$
Error	$\sum_{\text{al groups}} w \times [\sum_{\text{all states}} (f - q_o P_{no-m}^{T_{major}})^2]$			$\sum_{\text{all groups}} w \times [\sum_{\text{all states}} (f - q_o P_{post-m}^{T_{major}})^2]$		

^aC and NC denote critical and not-critical respectively

For the examined MTO data, the transition matrices are found to be

$$P_{no-m} = \begin{bmatrix} 0.994 & 0.006 \\ 0 & 1 \end{bmatrix}, P_{post-m} = \begin{bmatrix} 0.987 & 0.013 \\ 0 & 1 \end{bmatrix}$$

The results agree with initial speculations that maintenance may not fully restore the bridge to its as-good-as-new condition, and hence, $P_{1,1}$ is reduced from 0.994 to 0.987. Despite the apparent small difference, its accumulation with time can be significant. For example, a newly constructed bridge with $P_{1,1}$ of 0.994 would take about 37 years to reach a 20% repair probability, while a newly maintained bridge, with

$P_{1,1}$ of 0.987, would take 17 years to reach the same probability. This indicates that distinguishing the transition matrices may provide better prediction accuracy.

The performance of Markov Chains is assessed using the confusion matrix to facilitate comparison with the proposed LASSO-Logistic models. Using the appropriate initial condition vectors and transition matrices, the probability of reaching a critical state ($P_{2,t}$) at the time of latest inspection is found using Eq. (4) for each bridge. Then, using the same procedures as with the LASSO-Logistic models, the performance metrics are plotted as shown in Fig. 2.6. For the examined MTO data, the performance of the proposed LASSO-Logistic models are better compared to the Markov Chains. Fig. 2.6 (a) indicates that for smaller $P_{threshold}$ (< 0.2), the LASSO-Logistic models are slightly better in terms of Recall (average difference of 3.1%), and Fig. 2.6 (b) indicates that LASSO-Logistic models have much lower FRR (average difference of 10.5% and 15.4% for the group- and individual-level models, respectively). However, Fig. 2.6 (a) indicates that for $P_{threshold} > 0.2$, the LASSO-Logistic models perform much better in terms of Recall (average difference of 20%), but, Fig. 2.6 (b) indicates that they have slightly higher FRR compared to the Markov Chains (average difference of 2.7% and 2% for group- and individual-level models, respectively).

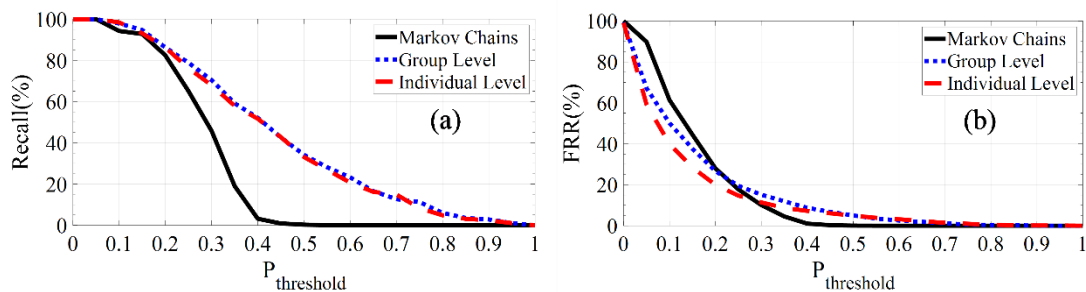


Fig. 2.6 (a) Recall, and (b) FRR vs. $P_{threshold}$ comparing Markov Chains vs. LASSO-Logistic models

2.6. Inspection Decision Models

The inspection decision models are constructed similarly to the maintenance decision models except for the limit state definition. LASSO-Logistic regression is used to relate the age, T_{major} , and T_{minor} at the start of an inspection interval, together with the location and ADR parameters, to the probability of exceeding the ILS within the chosen inspection interval on the group- and individual-levels (P_{ILS-GL} and P_{ILS-IL} , respectively).

The proposed group-level model is

$$P_{ILS-GL} = \frac{\exp [\beta_0 + \beta_1 * \text{age}^{\gamma_1} + \beta_2 * T_{major}^{\gamma_2} + \beta_3 * \text{latitude}^{\gamma_3}]}{1 + \exp [\beta_0 + \beta_1 * \text{age}^{\gamma_1} + \beta_2 * T_{major}^{\gamma_2} + \beta_3 * \text{latitude}^{\gamma_3}]} \quad (10)$$

The individual-level model is formulated as

$$P_{ILS-IL} = \frac{\exp [\beta_0 + \beta_1 * \text{age}^{\gamma_1} + \beta_2 * T_{major}^{\gamma_2} + \beta_3 * \text{latitude}^{\gamma_3} + \beta_4 * \text{ADR}^{\gamma_4}]}{1 + \exp [\beta_0 + \beta_1 * \text{age}^{\gamma_1} + \beta_2 * T_{major}^{\gamma_2} + \beta_3 * \text{latitude}^{\gamma_3} + \beta_4 * \text{ADR}^{\gamma_4}]} \quad (11)$$

where the values of the regression and exponent coefficients corresponding to inspection intervals (Δt) of 2, 4, and 6 years are as shown in Table 2.3 and Table 2.4 for the group- and individual-level models, respectively.

Table 2.3 Regression and exponent coefficients for the group-level inspection decision model

Δt	β_0	β_1	γ_1	β_2	γ_2	β_3	γ_3
6 yrs	-21.367	3.062	0.3	0.725	0.4	0.161	1
4 yrs	-36.011	15.844	0.1	0.355	0.5	0.197	1
2 yrs	-32.012	12.910	0.1	0.446	0.4	0.195	1

Table 2.4 Regression and exponent coefficients for the individual-level inspection decision model

Δt	β_0	β_1	γ_1	β_2	γ_2	β_3	γ_3	β_4	γ_4
6 yrs	-43.183	22.392	0.1	0.314	0.6	1.102	0.6	0.133	1
4 yrs	-40.038	19.325	0.1	0.176	0.7	1.707	0.4	0.152	1
2 yrs	-48.654	18.294	0.1	0.251	0.6	10.117	0.1	0.182	1

2.7. Framework for Inspection and Maintenance Scheduling

The proposed LASSO-Logistic models have many applications that can aid bridge management authorities. On a bridge network level, authorities can use the group-level MLS model, shown in Eq. (7), to develop bridge condition maps showing the repair likelihood of each bridge across a region or province. This facilitates the monitoring of maintenance requirements of a bridge network at any given year, allowing for better budget and resource planning.

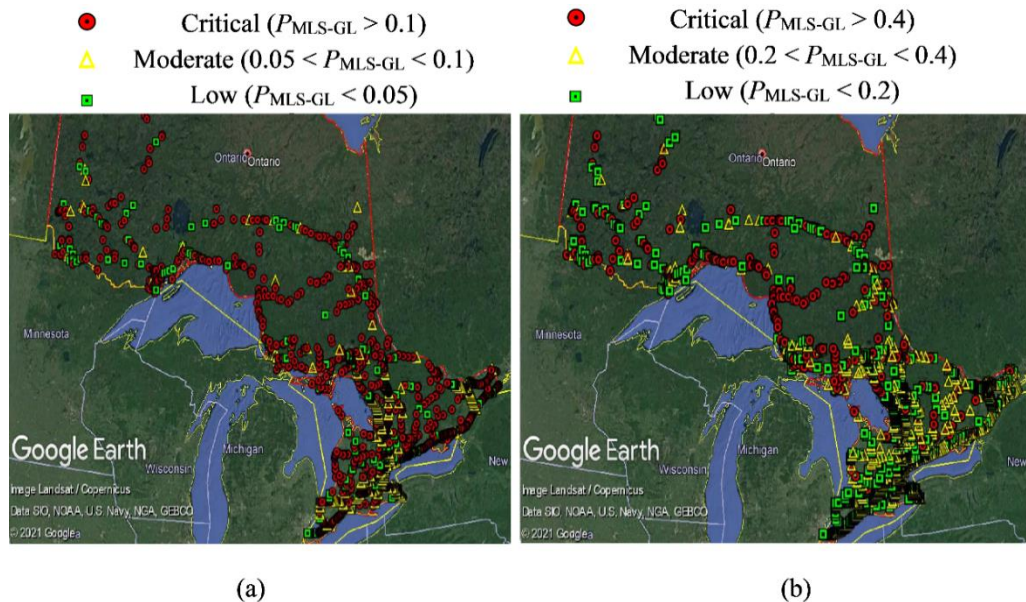


Fig. 2.7 Bridge condition map of Ontario, Canada for the year 2021: (a) P_{MLS} -threshold = 0.1, (b) P_{MLS} -threshold = 0.4

As an example, Fig. 2.7 shows the bridge condition map for Ontario, Canada for 2021, identifying bridge repair requirements for the range from 2021 to 2026. First, the MLS exceedance probabilities are computed using Eq. (7). Then, assuming a P_{MLS} -threshold of 0.1 (more discussion about the optimum P_{MLS} -threshold is presented in the LCC section), the bridges can be grouped into critical ($P_{MLS-GL} > 0.1$) and non-critical ($P_{MLS-GL} < 0.1$). For planning purposes, authorities can also further subdivide the non-critical bridges into two or more classes, such as moderate-risk (e.g. $0.05 < P_{MLS-GL} < 0.1$) and

low-risk (e.g. $P_{MLS-GL} < 0.05$) classes as shown in Fig. 2.7(a). The condition map has the advantage of easily adjusting the $P_{MLS-threshold}$. For example, adjusting the $P_{MLS-threshold}$ to 0.4 (Fig. 2.7(b)) pushes more bridges into non-critical condition.

Bridge management authorities can also use the group-level MLS and ILS models (Eq. (7) and Eq. (10), respectively) to plot initial MLS and ILS profiles for an individual bridge which can be later modified, once the ADR of the bridge is identified from future inspections. As an example, the profiles are plotted for a bridge located in the Niagara Falls, Ontario, Canada which was constructed in 2017 at latitude 43.03 N, and has yet to receive any maintenance. A $P_{MLS-threshold}$ of 0.2 is used for demonstration. The group-level MLS profile (Fig. 2.8) is constructed using the following steps, with the age, T_{major} , and P_{MLS-GL} values shown between parentheses:

1. Start point at construction date in 2017 (**Point 1**: age = T_{major} = P_{MLS-GL} = 0).
2. Age and T_{major} are increased incrementally until P_{MLS-GL} approaches $P_{MLS-threshold}$ at 2057 (**Point 2**: age = T_{major} = 40 years, and P_{MLS-GL} = 0.193). The bridge is expected to reach a critical condition that requires major maintenance between 2057 and 2062.
3. Assume that maintenance is applied five years after reaching $P_{MLS-threshold}$. Then, extend the MLS profile until 2062 (extended to **Point 3**: age = T_{major} = 45 years, and P_{MLS-GL} = 0.286).
4. In 2062, major maintenance is applied, resetting T_{major} to zero. This leads to an instantaneous drop in P_{MLS-GL} (**Point 4**: age = 45 years, T_{major} = 0, and P_{MLS-GL} = 0.032).
5. Repeat step 2 to step 4 to get the timing of all required interventions.

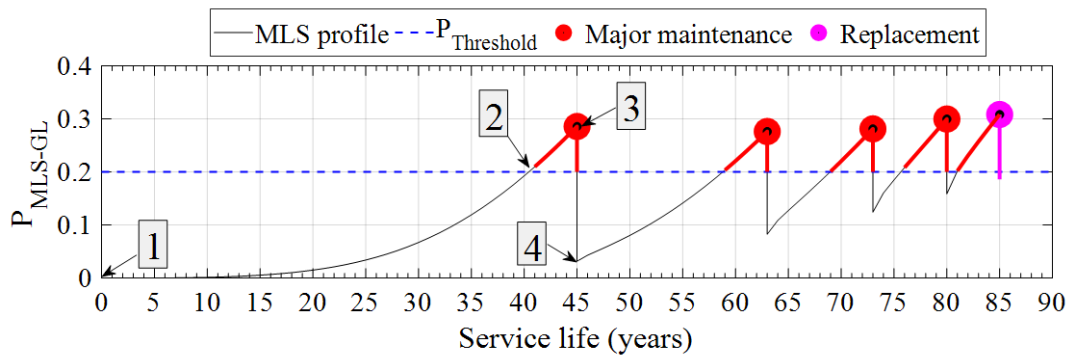


Fig. 2.8 MLS profile for the example bridge

Based on the above steps, an initial maintenance schedule is established (Fig. 2.10). It is evident that maintenance effectiveness is significantly reduced with each subsequent maintenance, and the bridge should be replaced after the fourth major maintenance if the same $P_{MLS-threshold}$ is to be maintained. The examined bridge is expected to remain in service for about 85 years for the specified safety level of $P_{MLS-threshold} = 0.2$.

Next, the ILS profile (Fig. 2.9) is plotted using the group-level ILS model in Eq. (10) and the coefficient values in Table 2.3, with $P_{ILS-threshold}$ of 0.08 as an example:

6. Repeat step 1 to 5 three times to plot an individual ILS profile for each inspection interval ($\Delta t = 2, 4, \text{ and } 6$ years).
7. Plot the max envelope ILS profile (Fig. 2.9). Start by tracking the profile of $\Delta t = 6$ years until the threshold of 0.08 is reached. Drop down and start tracking the profile of $\Delta t = 4$ years until the threshold is reached. Drop down and start tracking the profile of $\Delta t = 2$ years until the first major maintenance. Drop down and start tracking the profile of $\Delta t = 6$ years again. Repeat previous steps until the end of the service life.

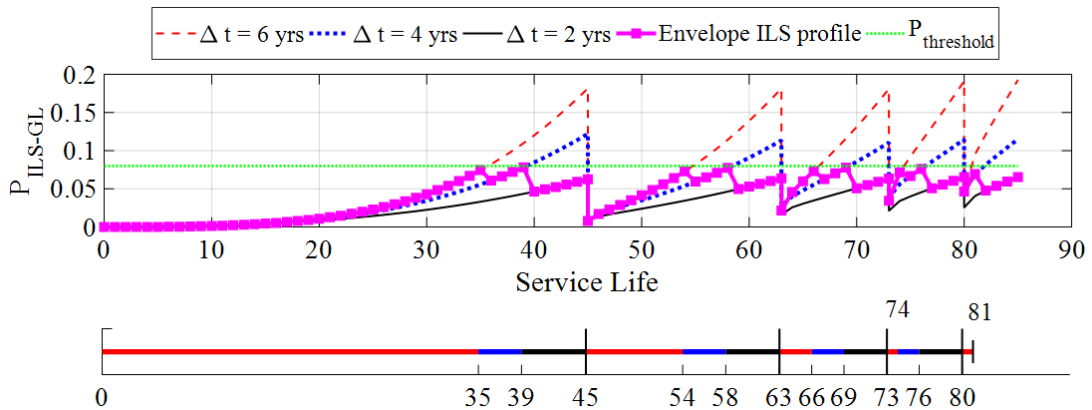


Fig. 2.9 ILS profile for the example bridge

The theoretical limits separating different inspection intervals are found from the envelope ILS profile, (Fig. 2.9). For a $P_{ILS-threshold}$ of 0.08, a 6 year inspection interval is satisfactory for 35 years when the $P_{ILS-threshold}$ is reached. Afterwards, 4 year intervals and 2 year intervals can be used from 35 to 39 years and 39 to 45 years, respectively. Based on these limits, a preliminary inspection schedule can be established as shown in Fig. 2.10 for a $P_{MLS-threshold}$ of 0.2 and a $P_{ILS-threshold}$ of 0.08.

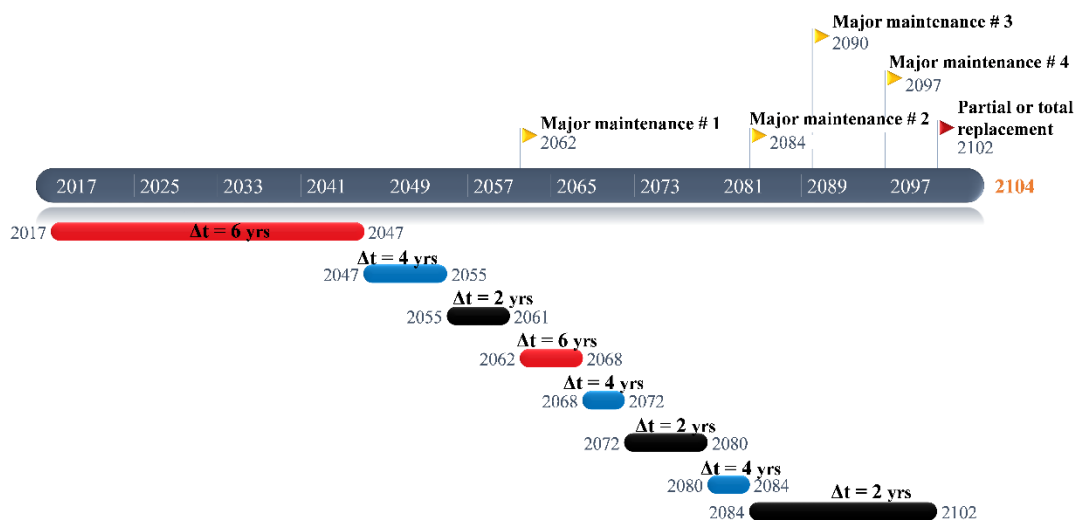


Fig. 2.10 Inspection and maintenance schedule ($P_{MLS-threshold} = 0.2$ and $P_{ILS-threshold} = 0.08$)

2.8. Optimum Thresholds using LCC Analysis

The selected $P_{threshold}$ value controls the planned budgets and initial schedules for inspection and maintenance work. A high $P_{threshold}$ increases the cost of service failure, whereas a low $P_{threshold}$ value may result in higher bridge operational costs. Life-cycle cost (LCC) analysis can be used to determine the optimal $P_{threshold}$ values. The same example bridge is selected as a study case, and the LCC required to keep it operational for 75 years is evaluated for various $P_{threshold}$ for MLS and ILS. In this example, the LCC is based on the group-level inspection and maintenance needs; however, bridge specific LCC can be found upon availability of actual condition data. To account for inflation, any future expenditure, incurred for the s^{th} time at a time instance t_s , is converted to its present value (Yanev 1994) using a discount rate r of 5% (MTO, 2013).

2.8.1. LCC for MLS

For MLS, the LCC includes construction, operation, and failure costs and can be calculated as

$$LCC_{MLS} = C_C + [C_{MM} + C_{MM-U} + C_{BR} + C_{BR-U}] + [C_{F-MLS} + C_{F-MLS-U}] \quad (12)$$

where C_C is the construction cost, and C_{MM} , C_{BR} , and C_{F-MLS} are the costs of major maintenance, bridge replacement, and service failure due to MLS exceedance, respectively. The associated user delay costs, due to traffic congestions and detouring, are C_{MM-U} , C_{BR-U} and $C_{F-MLS-U}$, respectively. To facilitate comparison between various thresholds, the following assumptions are made: (1) the bridge is replaced at the end of the target 75 years regardless of the threshold value and (2) if a bridge needs to be replaced prior to the target 75 years, then the costs incurred between the construction

of the replacement bridge and the end of the target 75 years are included in the LCC.

The example bridge is of precast concrete girder system, deck length of 22.8 m, and deck width of 14.05 m. For this bridge type, the base year costs of construction, major maintenance, and bridge replacement are estimated as 2.1, 0.6, and 2.4 million CAD\$, respectively, based on the typical cost ranges in Ontario, Canada (MTO, 2016).

C_{MM} and C_{BR} are then estimated as

$$C_{MM \text{ or } C_{BR}} = \sum_1^S (C_{MM-base} \text{ or } C_{BR-base}) \frac{1}{(1+r)^{ts}} \quad (13)$$

Maintenance or replacement activities are always accompanied by user delay costs (C_{MM-U} and C_{BR-U}) which are estimated using the method proposed by Chang and Shinozuka (1996) as

$$C_{MM-U} \text{ or } C_{BR-U} = \sum_1^S t_m b_m u \frac{1}{(1+r)^{ts}} \quad (14)$$

where t_m is the activity duration in years, b_m is the percentage of closed lanes during the activity, and u is the unit user cost. Major maintenance is assumed to take one week with closure of half of bridge lanes ($t_m = 1/52$, $b_m = 0.5$), whereas the replacement of a precast concrete bridge is assumed to take three months (Fowler, 2006; FHWA, 2017) with full bridge closure ($t_m = 3/12$, $b_m = 1$). The user unit cost u is estimated as

$$u = \text{Hourly delay cost} \times \text{average delay per user} \times \text{annual traffic or truck volume} \quad (15)$$

where the hourly delay cost is taken as 15 and 75 CAD\$ for vehicles and trucks, respectively (Armstrong et al. 2008). The delay per user is assumed to be one hour (Chang and Shinozuka 1996). Finally, the annual traffic and truck volumes are estimated based on an annual average daily traffic and truck traffic of 29000 vehicles

and 4640 trucks, respectively (MTO, 2019).

The service failure cost C_{F-MLS} is defined as that incurred to repair the bridge after reaching a critical condition and is found as

$$C_{F-MLS} = \sum_{t_{sl}=1}^{t_{sl}=75} P_{MLS}(t_{sl}) C_{F-MLS-base} \frac{1}{(1+r)^{t_{sl}}} \quad (16)$$

where the base year failure cost $C_{F-MLS-base}$ is taken the same as $C_{MM-base}$. The expected C_{F-MLS} is then computed by accumulating the probabilistic failure cost ($P_{MLS}(t_{sl}) \times C_{F-MLS-base}$) every year (t_{sl}) in the service life (Ghosh and Padgett 2011). The MLS exceedance probability is calculated using the group-level model in Eq. (7). The user cost $C_{F-MLS-U}$ is computed similarly to C_{MM-U} while multiplying by $P_{MLS}(t_{sl})$ from Eq.(7).

Using Eq. (12) to Eq. (16), the variation in LCC_{MLS} versus $P_{MLS-threshold}$ is plotted as shown in Fig. 2.11(a). As expected, low $P_{MLS-threshold}$ will result in higher operational costs (i.e. maintenance and replacement) and lower failure costs. Whereas the opposite is true for high $P_{MLS-threshold}$. The optimum $P_{MLS-threshold}$ for the example bridge is 0.16 corresponding to a minimum LCC_{MLS} of roughly 6 million CAD\$. The maintenance plan corresponding to the optimum $P_{MLS-threshold}$ include three major interventions at the bridge age of 42, 59, and 69 years as shown in Fig. 2.11(b).

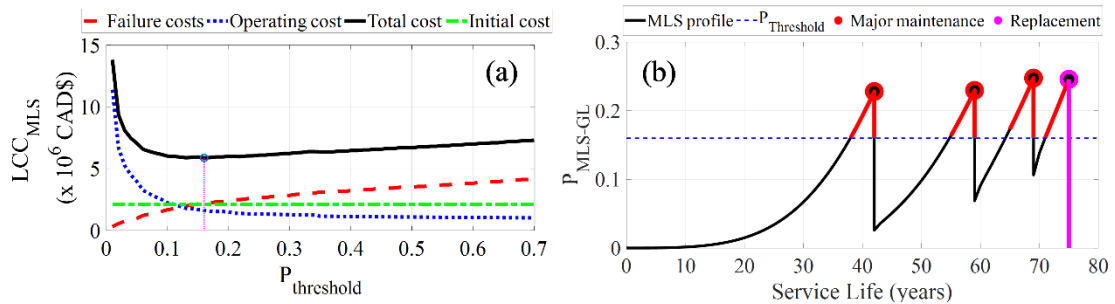


Fig. 2.11 (a) LCC_{MLS} vs. $P_{MLS-threshold}$, and (b) maintenance and replacement timings for the optimum $P_{MLS-threshold}$

2.8.2. LCC for ILS

For ILS, the LCC is estimated based on the inspection needs associated with the maintenance plan shown in Fig. 2.11(b). MTO conducts two types of inspections, ordinary and enhanced. The first is typically for bridges in good condition, and involves visual examination of bridge elements. The second is done at least once every six years for poorly conditioned bridges (typically over 30 years old) and involves close-up element examination which often requires lane closures and specialized equipment to access the whole bridge (MTO, 2008). It is assumed that enhanced inspections are conducted in the five years prior to the expected repair intervention (Fig. 2.11(b)), whereas the rest of inspections are ordinary. As such, the LCC for the ILS is found as

$$LCC_{ILS} = C_{IN-O} + C_{IN-E} + C_{IN-E-U} + [C_{F-ILS} + C_{F-ILS-U}] \quad (17)$$

where the costs of ordinary and enhanced inspections (C_{IN-O} and C_{IN-E}) are computed with assumed base costs of 0.5% and 1.5% of construction cost, respectively. C_{IN-E-U} is computed similar to Eq. (14) and (15), assuming that enhanced inspections take one day ($t_m = 1/365$) with half bridge closure ($b_m = 0.5$) and 2 hours of traffic delay. The ILS failure cost C_{F-ILS} resembles that of MLS, however, $P_{MLS}(t_{sl})$ is replaced by $P_{ILS}(t_{sl})$ which is obtained from the group-level ILS model in Eq. (10) and Table 2.3. It is assumed that if two year inspection intervals are not enough to keep $P_{ILS}(t_{sl})$ below $P_{ILS-threshold}$, then the bridge would be inspected on annual basis.

The relationship between LCC_{ILS} and $P_{ILS-threshold}$ (Fig. 2.12) follows the same pattern observed for the MLS. The optimum $P_{ILS-threshold}$ for the example bridge is 0.053 corresponding to a minimum LCC_{ILS} of roughly 1.55 million CAD\$.

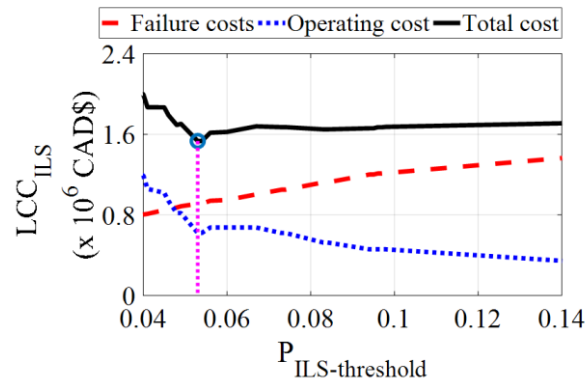


Fig. 2.12 LCC_{ILS} vs. $P_{ILS\text{-threshold}}$

2.8.3. Creating Inspection and Maintenance Scheduling using Optimum Thresholds

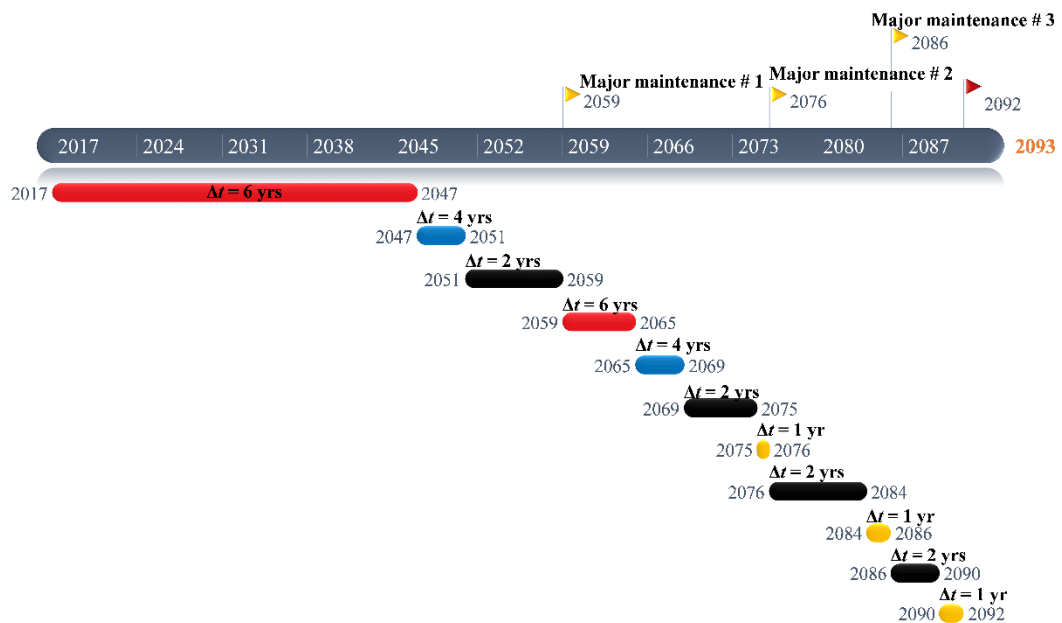


Fig. 2.13 Inspection and maintenance schedule for the example bridge

The conducted LCC analysis shows that the optimal thresholds for P_{MLS} and P_{ILS} on a group-level are 0.16 and 0.053, respectively. Using these values, the optimal scheduling for inspection and maintenance is constructed for the example bridge (Fig. 2.13). Based on this group-level schedule, the example bridge is expected to need three major maintenances during its 75-year life-cycle. Furthermore, it is expected that 26 inspections (including 9 enhanced inspections) would be sufficient to efficiently track

the bridge condition. This represents about 70% of the minimum inspection requirements imposed by the current biennial inspection practice which shows that there is a sufficient room for improving the current inspection practice better allocation of resources. Such improvement is enhanced with the bridge-specific versions of the proposed schedule.

2.9. Conclusions

This study proposes a framework for scheduling bridge inspection and maintenance based on parameterized logistic models. First, the maintenance and inspection limit states (MLS and ILS, respectively) are defined. For each limit state, a set of logistic models is constructed to support decisions on the level of bridge groups and individual bridges. Analysis of the MTO data showed that bridge condition is mainly controlled by age, time since the last major maintenance T_{major} , and location, whereas the bridge material and minor maintenance may not affect deterioration significantly. Based on the significant parameters, the proposed logistic models can track the probability of a bridge (or a group of bridges) requiring inspection or maintenance. The proposed models, combined with the appropriate probability threshold for each defined limit state, can anticipate the appropriate maintenance timing and optimize the frequency of inspections from an economic perspective without exceeding the selected probability threshold.

The proposed logistic models allow for easy tracking of the bridge condition with better accuracy compared to the Markov Chains method adopted by many North American BMSs. This could potentially aid BMSs to devise better management strategies and optimize the allocation of budget and resources. This study proposes the

use of LCC analysis to choose the optimum probability thresholds for MLS and ILS which vary for each bridge depending on its local environment and the economic consequences of disrupting the bridge service (e.g. consequences of traffic delays). Lower threshold values may be required for bridges with harsher climate conditions or supporting heavier traffic volumes. The LCC analysis results for the example bridge showed that the number of bridge inspections can be reduced by 30% over the lifespan without exceeding the selected threshold for the ILS ($P_{ILS-threshold}$). While the results may vary for other bridges, this highlights that there is room for optimizing current bridge management practices.

2.10. Data Availability Statement

All data, models, or code that support the findings of this study are available from the corresponding author upon reasonable request.

2.11. Acknowledgments

The authors gratefully acknowledge the support from the Ontario Early Researcher Award and start-up fund provided by the Faculty of Engineering at McMaster University. Any opinions, findings, and conclusions or recommendations expressed in this material are those of the authors and do not necessarily reflect the views of the sponsor. The authors also thankfully acknowledge Mr. Hao Zhang, P.Eng. (City of Toronto), for his constructive feedback on bridge inspection and maintenance practices in the Province of Ontario, Canada.

2.12. References

Alipour, A., B. Shafei, and M. S. Shinozuka. 2013. “Capacity loss evaluation of reinforced concrete bridges located in extreme chloride-laden environments.”

Struct. Infrastruct. Eng. 9 (1): 8–27. <https://doi.org/10.1080/15732479.2010.525243>.

Armstrong, J., J. Loftus, J. Weir, and W. Roy. 2008. “The highway element investment review (HEIR) guidelines: Making the right decisions in Ontario.” In Annual Conf. the Transportation Association of Canada: Transportation—A Key to a Sustainable Future. Ottawa: Transportation Association of Canada.

Balomenos, G. P., Y. Hu, J. E. Padgett, and K. Shelton. 2019. “Impact of coastal hazards on residents’ spatial accessibility to health services.” J. Infrastruct. Syst. 25 (4): 04019028. [https://doi.org/10.1061/\(ASCE\)IS.1943-555X.0000509](https://doi.org/10.1061/(ASCE)IS.1943-555X.0000509).

Balomenos, G. P., S. Kameshwar, and J. E. Padgett. 2020. “Parameterized fragility models for multi-bridge classes subjected to hurricane loads.” Eng. Struct. 208: 110213. <https://doi.org/10.1016/j.engstruct.2020.110213>.

Balomenos, G. P., and J. E. Padgett. 2018. “Fragility analysis of pile-supported wharves and piers exposed to storm surge and waves.” J. Waterway Port, Coastal, Ocean Eng. 144 (2): 04017046. [https://doi.org/10.1061/\(ASCE\)WW.1943-5460.0000436](https://doi.org/10.1061/(ASCE)WW.1943-5460.0000436).

Barlow, R. E., and F. Proschan. 1996. Mathematical theory of reliability. Philadelphia: SIAM.

Bazzucchi, F., L. Restuccia, and G. A. Ferro. 2018. “Considerations over the Italian road bridge infrastructure safety after the Polcevera viaduct collapse: Past errors and future perspectives.” Frattura Integr. Strutt. 46: 400–421. <https://doi.org/10.3221/IGF-ESIS.46.37>.

Bernier, C., I. Gidaris, G. P. Balomenos, and J. E. Padgett. 2019. “Assessing the accessibility of petrochemical facilities during storm surge events.” Reliab. Eng.

- Syst. Saf. 188: 155–167. <https://doi.org/10.1016/j.ress.2019.03.021>.
- Biezma, M. V., and F. Schanack. 2007. “Collapse of steel bridges.” *J. Perform. Constr. Facil* 21 (5): 398–405. [https://doi.org/10.1061/\(ASCE\)0887-3828\(2007\)21:5\(398\)](https://doi.org/10.1061/(ASCE)0887-3828(2007)21:5(398)).
- Biondini, F., E. Camnasio, and A. Palermo. 2014. “Lifetime seismic performance of concrete bridges exposed to corrosion.” *Struct. Infrastruct. Eng.* 10 (7): 880–900. <https://doi.org/10.1080/15732479.2012.761248>.
- Bocchini, P., D. Saydam, and D. M. Frangopol. 2013. “Efficient, accurate, and simple Markov chain model for the life-cycle analysis of bridge groups.” *Struct. Saf.* 40: 51–64. <https://doi.org/10.1016/j.strusafe.2012.09.004>.
- Bolukbasi, M., J. Mohammadi, and D. Arditi. 2004. “Estimating the future condition of highway bridge components using national bridge inventory data.” *Pract. Period. Struct. Des. Constr.* 9 (1): 16–25. [https://doi.org/10.1061/\(ASCE\)1084-0680\(2004\)9:1\(16\)](https://doi.org/10.1061/(ASCE)1084-0680(2004)9:1(16)).
- Butt, A. A., M. Y. Shahin, K. J. Feighan, and S. H. Carpenter. 1987. “Pavement performance prediction model using the Markov process.” *Transp. Res. Rec.* 1123: 12–19.
- Cesare, M. A., C. Santamarina, C. Turkstra, and E. H. Vanmarcke. 1992. “Modeling bridge deterioration with Markov chains.” *J. Transp. Eng.* 118 (6): 820–833. [https://doi.org/10.1061/\(ASCE\)0733-947X\(1992\)118:6\(820\)](https://doi.org/10.1061/(ASCE)0733-947X(1992)118:6(820)).
- Chang, S. E., and M. Shinozuka. 1996. “Life-cycle cost analysis with natural hazard risk.” *J. Infrastruct. Syst.* 2 (3): 118–126. [https://doi.org/10.1061/\(ASCE\)1076-0342\(1996\)2:3\(118\)](https://doi.org/10.1061/(ASCE)1076-0342(1996)2:3(118)).
- Everett, T. D., P. Weykamp, H. A. Capers, Jr., W. R. Cox, T. S. Drda, L. Hummel, P.

Jensen, D. A. Juntunen, T. Kimball, and G. A. Washer. 2008. Bridge evaluation quality assurance in Europe. Washington, DC: Federal Highway Administration (FHWA).

FHWA (Federal Highway Administration). 2017. Prefabricated bridge elements and systems cost study: Accelerated bridge construction success stories. Washington, DC: FHWA.

Ford, K. M., M. Arman, S. Labi, K. C. Sinha, A. Shirole, P. Thompson, and Z. Li. 2011. Methodology for estimating life expectancies of highway assets. Washington, DC: National Cooperative Highway Research Program.

Fowler, J. R. 2006. “Accelerated bridge construction.” In Annual Conf. of the Transportation Association of Canada: Bridges for the 21st Century. Ottawa: Transportation Association of Canada (TAC).

Ghodoosi, F., S. Abu-Samra, M. Zeynalian, and T. Zayed. 2018. “Maintenance cost optimization for bridge structures using system reliability analysis and genetic algorithms.” *J. Constr. Eng. Manage.* 144 (2): 04017116. [https://doi.org/10.1061/\(ASCE\)CO.1943-7862.0001435](https://doi.org/10.1061/(ASCE)CO.1943-7862.0001435).

Ghosh, J., and J. E. Padgett. 2011. “Probabilistic seismic loss assessment of aging bridges using a component-level cost estimation approach.” *Earthquake Eng. Struct. Dyn.* 40 (15): 1743–1761. <https://doi.org/10.1002/eqe.1114>.

Golabi, K., and R. Shepard. 1997. “Pontis: A system for maintenance optimization and improvement of US bridge networks.” *Interfaces* 27 (1): 71–88. <https://doi.org/10.1287/inte.27.1.71>.

Government of Ontario. 2018. “Bridge condition dataset.” Accessed October 1, 2018.

<https://data.ontario.ca/dataset/bridge-conditions>.

- Grussing, M. N., D. R. Uzarski, and L. R. Marrano. 2006. “Condition and reliability prediction models using the weibull probability distribution.” In Applications of Advanced Technology in Transportation, 19–24. Reston, VA: ASCE.
- Hawk, H., and E. P. Small. 1998. “The BRIDGIT bridge management system.” Struct. Eng. Int. 8 (4): 309–314. <https://doi.org/10.2749/101686698780488712>.
- Jia, G., and P. Gardoni. 2018. “State-dependent stochastic models: A general stochastic framework for modeling deteriorating engineering systems considering multiple deterioration processes and their interactions.” Struct. Saf. 72: 99–110. <https://doi.org/10.1016/j.strusafe.2018.01.001>.
- Jiang, Y., and K. C. Sinha. 1989. “Bridge service life prediction model using the Markov chain.” Transp. Res. Rec. 1223: 24–30. Kohavi, R., and F. Provost. 1998. “Glossary of terms.” J. Mach. Learn. 30: 271–274. <https://doi.org/10.1023/A:1017181826899>.
- MATLAB. 2018. Statistics toolbox release 2018a. Natick, MA: MathWorks.
- McLachlan, G. J., K.-A. Do, and C. Ambroise. 2005. Vol. 422 of Analyzing microarray gene expression data. Hoboken, NJ: Wiley.
- Mirzaei, Z., B. T. Adey, L. Klatter, and P. D. Thompson. 2014. “Overview of existing bridge management systems.” In Bridge Management Committee. Australia: International Association for Bridge Maintenance and Safety (IABMAS).
- Moehle, J. P., and M. O. Eberhard. 2003. “Earthquake damage to bridges.” In Bridge engineering, edited by W.-F. Chen and L. Duan, 52–84. Boca Raton, FL: CRC Press.
- Morcous, G. 2006. “Performance prediction of bridge deck systems using Markov

chains.” *J. Perform. Constr. Facil* 20 (2): 146–155. [https://doi.org/10.1061/\(ASCE\)0887-3828\(2006\)20:2\(146\)](https://doi.org/10.1061/(ASCE)0887-3828(2006)20:2(146)).

MTO (Ministry of Transportation). 2008. Ontario structure inspection manual (OSIM). St. Catharines, ON: MTO.

MTO (Ministry of Transportation). 2013. Pavement design and rehabilitation manual. St. Catharines, ON: MTO.

MTO (Ministry of Transportation). 2015. Bridge repairs. St. Catharines, ON: MTO.

MTO (Ministry of Transportation). 2016. Parametric estimating guide (PEG). St. Catharines, ON: MTO.

MTO (Ministry of Transportation). 2019. MTO ICorridor: Historical provincial highways traffic volumes. St. Catharines, ON: MTO.

Murphy, K. P. 2012. *Machine learning: A probabilistic perspective*. Cambridge, MA: MIT press.

Nelder, J. A., and R. W. M. Wedderburn. 1972. “Generalized linear models.” *J. R. Stat. Soc. Ser. A* 135 (3): 370–384. <https://doi.org/10.2307/2344614>.

Shi, X., M. Akin, T. Pan, L. Fay, Y. Liu, and Z. Yang. 2009. “Deicer impacts on pavement materials: Introduction and recent developments.” *Open Civ. Eng. J.* 3 (1): 16–27. <https://doi.org/10.2174/1874149500903010016>.

Srikanth, I., and M. Arockiasamy. 2020. “Deterioration models for prediction of remaining useful life of timber and concrete bridges: A review.” *J. Traffic Transp. Eng.* 7 (2): 152–173. <https://doi.org/10.1016/j.jtte.2019.09.005>.

Stewart, M. G., X. Wang, and M. N. Nguyen. 2011. “Climate change impact and risks of concrete infrastructure deterioration.” *Eng. Struct.* 33 (4): 1326–1337.

<https://doi.org/10.1016/j.engstruct.2011.01.010>.

Tabatabai, H., C.-W. Lee, and M. A. Tabatabai. 2016. Survival analyses for bridge decks in Northern United States. Civil and Environmental Engineering Faculty Article, Paper 7. Milwaukee: Univ. of Wisconsin.

Thompson, P. D., T. Merlo, B. Kerr, A. Cheetham, and R. Ellis. 1999. “The new Ontario bridge management system.” In Vol. 153 of Proc., 8th Int. Bridge Management Conf., 1–15. Washington, DC: Transportation Research Board.

Tibshirani, R. 1996. “Regression shrinkage and selection via the Lasso.” J. R. Stat. Soc. Ser. B 58 (1): 267–288. <https://doi.org/10.1111/j.2517-6161.1996.tb02080.x>.

Verhulst, P. F. 1845. “La Loi d’accroissement de La population.” Nouv. Mem. Acad. R. Sci. Bruxelles 18: 14–54.

Veshosky, D., C. R. Beidleman, G. W. Buetow, and M. Demir. 1994. “Comparative analysis of bridge superstructure deterioration.” J. Struct. Eng. 120 (7): 2123–2136. [https://doi.org/10.1061/\(ASCE\)0733-9445\(1994\)120:7\(2123\)](https://doi.org/10.1061/(ASCE)0733-9445(1994)120:7(2123)).

Walpole, R. E., and R. H. Myers. 2012. Probability & statistics for engineers & scientists. London: Pearson.

Yanev, B. 1994. “User costs in a bridge management system.” Transp. Res. Circ. 423: 130–138.

Zambon, I., A. Vidovic, A. Strauss, J. Matos, and J. Amado. 2017. “Comparison of stochastic prediction models based on visual inspections of bridge decks.” J. Civ. Eng. Manage. 23 (5): 553–561. <https://doi.org/10.3846/13923730.2017.1323795>.

3. Fuzzy-Logistic Models for Incorporating Epistemic Uncertainty in Bridge Management Decisions

Reprinted with permission from Journal of Risk and Uncertainty in Engineering Systems, Part A: Civil Engineering, ASCE-ASME

Abdelmaksoud, Ahmed M, Georgios P Balomenos, and Tracy C Becker. 2022. “Fuzzy-Logistic Models for Incorporating Epistemic Uncertainty in Bridge Management Decisions.” *Journal of Risk and Uncertainty in Engineering Systems, Part A: Civil Engineering* 8 (3): 04022025. DOI: 10.1061/AJRUA6.0001247

3.1. Abstract

Many bridge management systems (BMSs) plan future maintenance and inspection based on deterioration models derived from probabilistic analysis of field inspection data. Such analysis considers the aleatoric but not the epistemic uncertainty arising from subjective or imprecise data. This raises questions regarding the efficiency and safety of maintenance and inspection decisions. Several methodologies have been proposed to address both uncertainties, however, they tend to be taxing in terms of inspection data requirements. Thus, this work proposes a new BMS-compatible methodology to derive deterioration models using logistic regression to capture aleatoric uncertainty and fuzzy set theory to capture epistemic uncertainty. To formulate the models, subjective or imprecise data, such as bridge condition rating, is modelled using membership functions, rather than discrete values, and then integrated into logistic regression analysis. This results in logistic models with fuzzy coefficients. The proposed fuzzy-logistic models can be used to predict a range of possible future bridge conditions, rather than a discrete condition. Hence, leading to a range of possible management strategies which can be then optimized using life cycle cost analysis. The

application of the proposed framework is demonstrated through a case study.

Keywords: Bridge management; Maintenance; Fuzzy set theory; Membership functions; Logistic regression; Life cycle costs.

3.2. Introduction

Bridge agencies always aim for safe and economic bridge management while accounting for budget and resource limitations. Towards that goal, bridge management systems (BMSs) use predictions of future bridge condition to optimize the timing of maintenance and inspections (Frangopol et al. 2004). This involves deterioration models which are typically derived from statistical analysis of past bridge condition data acquired from field inspections. Such data has inherent uncertainties which can be classified as either aleatory or epistemic (Brown and Yao 1983). The first arises from the randomness in the natural deterioration, whereas the second arises from the potential lack of precise knowledge on the on-site bridge working conditions (e.g. on-site meteorological conditions, exposure to de-icing chemicals, etc.) and from the subjective nature of the inspection process which depends on the inspectors' expertise and judgment. Both types of uncertainties should be considered to avoid underestimating the bridge maintenance and inspection needs (Der Kiureghian and Ditlevsen 2009). However, many BMSs, such as PONTIS (Golabi and Shepard 1997), BRIDGIT (Hawk and Small 1998), and OBMS (Thompson et al. 1999), derive their models using probabilistic analysis which accounts only for the aleatoric uncertainty.

Gaining sufficient knowledge to eliminate the epistemic uncertainty can be challenging. Alternatively, the fuzzy set theory (Zadeh 1965) has been shown to be a

useful tool for modelling subjective and imprecise information regarding the bridge condition such as inspector-assigned condition ratings and field measurements of deterioration defects (Tee et al. 1988b, 1988a; Sasmal et al. 2006; Tarighat and Miyamoto 2009; Li and Burgueño 2010; Omar et al. 2017). As such, several studies have proposed merging fuzzy set theory with probabilistic analysis to derive fuzzy-probabilistic deterioration models. For example, Wang et al. (2013) adopted the fuzzy random theory (Kwakernaak 1978; Puri and Ralescu 1986) to propose a deterioration model for concrete bridges with corroded reinforcement. The proposed methodology considered the aleatory and epistemic uncertainties in the variables of the corrosion models. Ma et al. (2015) and Wang et al. (2015) proposed methodologies for transforming fuzzy variables into equivalent random variables with probability density functions (PDFs). The equivalent PDFs can be then used with traditional reliability techniques such as Monte Carlo (MC) and first- or second-order reliability method (FORM or SORM, respectively). Yuan et al. (2020) modelled deterioration using a probabilistic gamma model and added a fuzzy updating factor which is derived from field measurements of the deterioration in load-carrying resistance.

The fuzzy-probabilistic deterioration models in the available literature are mechanistic. Such models are formulated based on mathematical expressions of the initiation and propagation of deterioration mechanisms (e.g. reinforcement corrosion) (Morcous and Lounis 2007; Nickless and Atadero 2018); hence, they require extensive physical measurements of bridge deterioration (e.g. chloride concentration, corrosion rate, crack width, etc). The collection of such measurements from bridge inspections is costly for large bridge populations; thus, such deterioration models are inefficient if

integrated with BMSs (Srikanth and Arockiasamy 2020). To address this issue, the current study proposes a new fuzzy-probabilistic framework that can predict bridge condition by knowing only information readily available from the inspection database (e.g. inspector ratings, bridge age, etc.) or any other existing databases (e.g. bridge inventory and meteorological databases). The proposed framework can be easily and efficiently integrated into BMSs.

In this framework, the aleatory component is handled using logistic regression and the epistemic component is handled using the principles of fuzzy set theory and membership functions. The current study demonstrates the application of the framework using the condition data of bridges owned by the Ministry of Transportation of Ontario (MTO) in Canada; however, other agencies can also apply this suggested framework using their data. Based on the predictions of the derived fuzzy-probabilistic deterioration model, life-cycle cost (LCC) analysis is conducted to optimize maintenance and inspection decisions from a safety and cost perspective while considering both aleatory and epistemic uncertainties.

3.3. Inspection Data

3.3.1. Bridge Condition Index (BCI)

This study utilizes the bridge condition data provided by the MTO (Government of Ontario 2018). The MTO manages over 2800 bridges in the province of Ontario and each bridge is inspected every two years (MTO 2008). First, inspectors evaluate the condition of each bridge element, and then the bridge is assigned a Bridge Condition Index (BCI) score representing the ratio between the current value of the bridge and the replacement cost. Depending on the BCI value, the following actions could take place: (1) for the range 70-100, no maintenance action is needed; (2) for the range 60-70,

maintenance is required within five years; and (3) for values less than 60, maintenance is necessary within a year (MTO 2015).

3.3.2. Influencing Parameters for BCI

Identifying the influencing parameters for BCI is the first step for predicting the future bridge condition. Abdelmaksoud et al. (2021) investigated the parameters available in the MTO bridge database (Government of Ontario 2018) and identified the bridge age, maintenance history, and location as primary parameters affecting the BCI. The BCI diminishes with age due to material degradation from environmental and climatic conditions (Stewart et al. 2011), and the BCI increases following bridge maintenance. The bridge location was used as an indicator for the local environment and it was found that bridges in northern regions of Ontario experience faster BCI degradation rates given the harsher climate which may be a consequence of higher concentrations of de-icing chemicals (Shi et al. 2009).

The significant parameters are included in the formulation of the proposed fuzzy-probabilistic models. However, to better understand the impact of local environment, the bridge location is replaced with several meteorological parameters obtained from the climate database (ECCC 2019) such as the number of days of snow fall (DOSF), number of days of ground snow (DOGS), and the snow fall per year (SFPY) (cm/year). The bridge maintenance is modelled by two parameters: time to last major maintenance (T_{major}) and time to last minor maintenance (T_{minor}) similar to Abdelmaksoud et al. (2021). Major maintenance includes retrofit of the bridge deck and extensive rehabilitation or replacement of other elements, whereas minor maintenance includes work on any element other than the deck (MTO 2008). If the

bridge has had only major maintenance, T_{minor} is assumed to be equal to T_{major} ; if only minor maintenance has occurred, T_{major} is measured from the construction date; if the bridge has no maintenance history, T_{major} and T_{minor} are both measured from the construction date.

3.3.3. Sources of Epistemic Uncertainty

Two sources of epistemic uncertainty are investigated: the subjectivity of the assigned BCI value and the meteorological conditions at the bridge site. The subjective nature of the BCI is due to the inspector's judgement which is related to several hard-to-measure factors including (1) inspector related factors such as practical experience and level of training, (2) inspection environment related factors such as the type and size of the inspected bridge element and the complexity of identifying the degree of deterioration, and (3) managerial related factors such as the time allocated for the inspection process (Megaw 1979).

The meteorological conditions at bridge site are based on the available meteorological data from 1981 to 2010 which were recorded at 151 stations positioned across Ontario, each with a minimum of 15 years of records (ECCC 2019). Out of the over 2800 bridges managed by MTO, 39 are located within 1 km of a meteorological station; the remaining bridges are located at distances of up to 162 km from the nearest station. For those 39 bridges, the BCI and the recorded meteorological parameters share a high correlation coefficient (ρ) (e.g. $\rho = -0.58$ for DOSF). However, as the distance between the bridge and the station grows, the correlation decreases. As such, all investigated meteorological parameters are treated as imprecise parameters if the distance between the bridge and the station is more than 1 km.

3.3.4. Data Pre-Processing

The bridge inspection records are available from 2000 to 2017. All records in or prior to 2015 are used for training the proposed fuzzy-probabilistic models, and the most recent records are used for testing the models. Prior to the analysis, all outlier bridges and bridges with missing information are excluded. An outlier bridge is defined as that whose BCI fell below 85 within 5 years following construction which may be caused by accidents, extreme events, or inaccurate data entry.

3.4. Methodology

3.4.1. Logistic Regression

Previous studies have shown that logistic regression can successfully incorporate aleatory uncertainty into infrastructure management decisions under extreme events. Examples include the assessment of the uplift failure risks during hurricanes for ports (Balomenos and Padgett 2018) and bridges (Balomenos et al. 2020) and risk based assessment of post-hazard accessibility of infrastructure such as petrochemical facilities (Bernier et al. 2019) and health facilities (Balomenos et al. 2019). The current study uses logistic regression to incorporate the aleatory uncertainty in the scheduling of bridge maintenance and inspection while considering time-dependent deterioration. As such, a logistic model is used to predict the probability of exceeding a limit state, beyond which a maintenance or inspection action is triggered, given a set of input parameters. The probability of exceeding the limit state, P_{LS} , is expressed as

$$P_{LS} = \frac{\exp[\beta_o + \sum_{j=1}^n \beta_j x_j^{\gamma_j}]}{1 + \exp[\beta_o + \sum_{j=1}^n \beta_j x_j^{\gamma_j}]} \quad (1)$$

where n is the number of input parameters, β_o is the model intercept, and β_j and γ_j are the regression and exponent coefficients for the input parameters x_j , respectively.

A separate limit state is defined for maintenance and inspection, each based on MTO guidelines (MTO 2015). For maintenance, the limit state is defined as the bridge reaching a BCI of 70 at a specific time instance. This BCI value is chosen to give early warning regarding the bridge condition as noticeable signs of deterioration may appear at this BCI. For scheduling inspections, the limit state is defined as the BCI reaching 70 within a given inspection interval (Δt). Inspection intervals can reach up to 6 years (Everett et al. 2008). Here, three common values of Δt are investigated during the analysis: 2, 4, and 6 years.

3.4.2. LASSO Regularization

The logistic regression is integrated with the least absolute shrinkage and selection operator (LASSO) regularization (Tibshirani 1996) which uses a regularization tuning parameter (λ) to constrain the summation of regression coefficients in order to exclude less significant parameters, minimize overfitting, and simplify the model input. The regularized logistic objective function is formulated as

$$\min \left[\frac{1}{N} \text{Deviance}(\beta_o, \beta_j, \gamma_j) + \lambda \sum_{j=1}^n |\beta_j| \right] \quad (2)$$

where N is the number of data points, and the deviance is a goodness-of-fit statistic inversely proportional to the likelihood function (Nelder and Wedderburn 1972).

3.4.3. Fuzzy Set Theory

Fuzzy set theory is a common approach for dealing with epistemic uncertainty (Zadeh 1965). Based on this theory, any subjective or imprecise parameter X obtained from bridge inspections (e.g. condition rating, measurement of defects, etc.) can be represented by fuzzy sets \tilde{X} . Each fuzzy set is modelled using a membership function

$\mu(x)$, ranging from 0 to 1, which describes the degree of membership in the fuzzy set given parameter value of x . A $\mu(x)$ value of 0 indicates the absolute confidence that the parameter value x does not belong to the fuzzy set, whereas a value of 1 indicates the absolute confidence that the parameter value x belongs to the fuzzy set. The functions can be defined using expert opinion, available data, clustering, neural networks, etc. (Medasani et al. 1998) and can be then processed to obtain the bridge condition. In the current study, membership functions are defined for the inspection BCI and the meteorological parameters and are then integrated with logistic regression to formulate the fuzzy-logistic deterioration models.

3.4.3.1. Membership Function of the BCI

A triangular membership function is adopted for the BCI as shown in Fig. 3.1. This membership function describes the degree of confidence in the BCI value assigned by the inspector. The value of $BCI_{\mu=1}$ is assumed to be that assigned by the inspector. $BCI_{\mu=0,max}$ and $BCI_{\mu=0,min}$ can be determined based on the expert opinion of inspectors from the relevant bridge agency or approximated based on available studies. Due to the lack of expert opinion data on bridges in Ontario, the $BCI_{\mu=0,max}$ and $BCI_{\mu=0,min}$ are herewithin estimated based on general insights from Moore et al.'s study (2001).

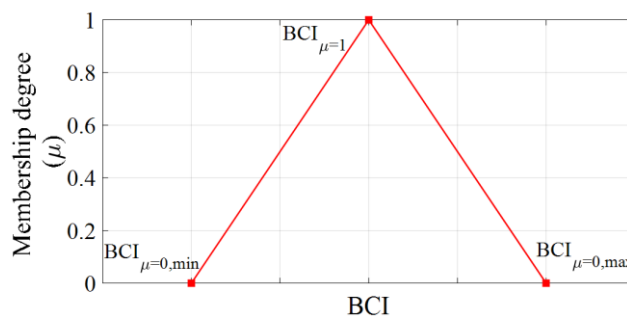


Fig. 3.1 Membership function of the BCI

Moore et al. (2001) tasked a group of inspectors to inspect and rate the deck, superstructure, and substructure of seven test bridges managed by the Non-destructive Evaluation Validation Center (NDEVC). The inspectors' ratings were compared to reference ratings. The results revealed that the discrepancy in inspector-assigned condition ratings is inversely related to the average condition ratings. Bridges with excellent condition (average condition rating of 8 or above) had almost no discrepancy in the ratings, whereas, bridges with poor condition (average condition rating of 4) had the highest discrepancy due to the complexity of identifying the degree of damages in a severely deteriorated bridge. In the latter case, the average rating of the deck, superstructure, and substructure could be actually 40% higher or lower than the average inspector-assigned ratings. Thus, $BCI_{\mu=0,max}$ and $BCI_{\mu=0,min}$ are assigned as in Fig. 3.2. For a newly constructed bridge with $BCI_{inspector}$ of 100, there is no uncertainty, and $BCI_{\mu=0,max} = BCI_{\mu=0,min} = BCI_{inspector}$. For a poorly conditioned bridge with $BCI_{inspector}$ of 60 or less, it is assumed that the actual BCI ranges up to 40% higher or lower than that assigned by the inspector (i.e. $BCI_{\mu=0,max} = 1.4 \times BCI_{inspector}$ and $BCI_{\mu=0,min} = 0.6 \times BCI_{inspector}$).

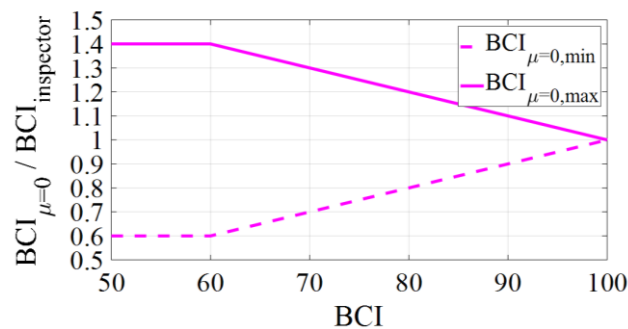


Fig. 3.2 Estimation of $BCI_{\mu=0,max}$ and $BCI_{\mu=0,min}$

3.4.3.2. Membership Function of the Meteorological Parameters

The current study assumes that the meteorological parameters (MP) at the bridge site

can be represented by that of the nearest station (MP_{nms}) (i.e. no epistemic uncertainty) if the distance separating the bridge and the station (d) is less than 1 km. However, if d is larger than 1 km, the MP is modelled using a trapezoidal membership function to describe the degree of confidence in MP_{nms} as shown in Fig. 3.3. A trapezoidal, rather than a triangular, function is adopted to show that even with the highest degree of confidence (i.e. $\mu = 1$) the MP_{nms} may not be viewed as a reliable representation of the MP at bridge site especially when the station is several kilometres away from the bridge. Rather, for μ equal to 1, it is assumed that the MP varies within a narrow range ($MP_{\mu=1,min}$ to $MP_{\mu=1,max}$), and this range varies depending on the distance separating the bridge and the station (d). Meanwhile, for μ equal to 0, it is assumed that the MP ranges within the minimum and maximum recorded values of the meteorological or geographical zone in which the bridge is located ($MP_{\mu=0,min}$ to $MP_{\mu=0,max}$). This study expresses the range $MP_{\mu=1,min}$ to $MP_{\mu=1,max}$ as a percentage (α) of the range $MP_{\mu=0,min}$ to $MP_{\mu=0,max}$ as

$$MP_{\mu=1,max/min} = MP_{nms} \pm \frac{\alpha (MP_{\mu=0,max} - MP_{\mu=0,min})}{2} \quad (3)$$

subject to $MP_{\mu=1,max} \leq MP_{\mu=0,max}$, and $MP_{\mu=1,min} \geq MP_{\mu=0,min}$

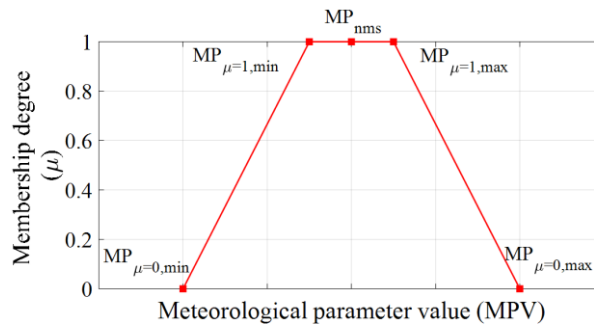


Fig. 3.3 Membership function for the meteorological parameters

To compute $MP_{\mu=0,\min}$ and $MP_{\mu=0,\max}$, the province of Ontario is divided into several meteorological zones using the k -means clustering method (MacQueen 1967; Wagstaff et al. 2001). The appropriate value of k was chosen based on a sensitivity analysis to minimize the variation of the MP, and four clusters were deemed to be sufficient. The four clusters are shown in Fig. 3.4a, and the extreme MP for each cluster is in Table 3.1. Each cluster of stations is used to divide Ontario into four meteorological zones. To account for the non-homogenous distribution of the meteorological station clusters resulting from localized climate conditions, a bridge location is classified into one of the four meteorological zones based on the dominant station cluster for the nearest 3 to 9 stations to the bridge location. Based on this assumption, the Ontario meteorological map is plotted in Fig. 3.4b.

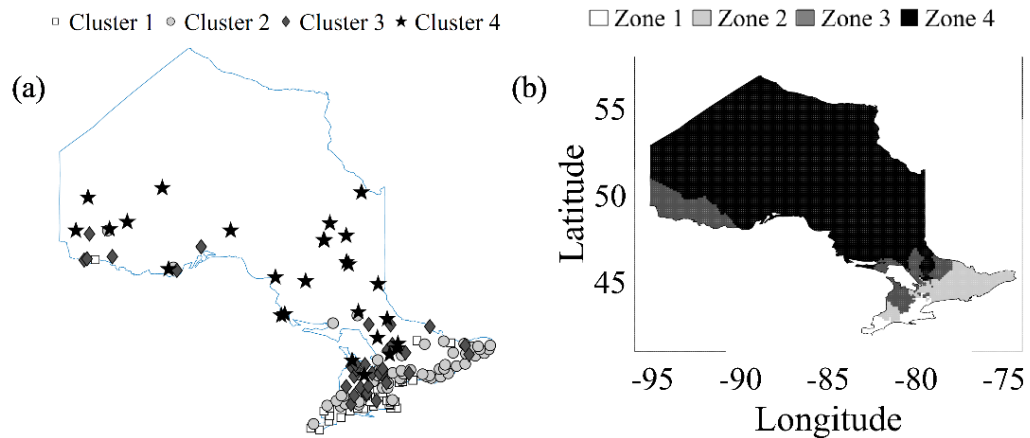


Fig. 3.4 (a) Meteorological stations clusters and (b) Meteorological map of Ontario, Canada

Table 3.1. Extreme values of MP for each meteorological cluster

MP	Cluster 1		Cluster 2		Cluster 3		Cluster 4	
	min	max	min	max	min	max	min	max
DOSF (days)	17.6	36.8	37.6	52.0	53.0	80.1	69.4	101.1
DOGS (days)	53.2	121.0	53.2	121.0	81.3	131.0	112.4	170.5
SFPY (cm/yr)	79.2	179.2	108.5	294.9	137.1	447.2	164.1	404.8

To compute $MP_{\mu=1,\min}$ and $MP_{\mu=1,\max}$, it is assumed that α shares a bilinear relationship with the distance separating the bridge and the nearest station (d) as follows

$$\alpha = \begin{cases} 0 & d = 1 \\ (d-1)/39 & 1 < d < 40 \\ 1 & d \geq 40 \end{cases} \quad (4)$$

The value of α is assumed to have a bilinear pattern, i.e., α increases from 0 to 1 when d increases from 1 to 40 km and then it is constant, based on the observed pattern between the coefficient of variation (COV) of the DOSF and the distance d between a bridge and the station as shown in Fig. 3.5. The COV of DOSF increases rapidly until d is roughly equal to 40 km after which the COV plateaus. A higher COV necessitates a higher α .

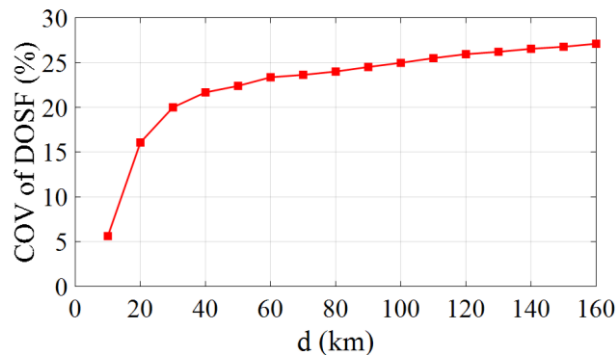


Fig. 3.5 COV of DOSF versus d

3.4.4. Formulation of Fuzzy-Logistic Models

Given the range of possible input parameters, as shown in Fig. 3.1 and Fig. 3.3, it would be expected to have a range of possible nonlinear logistic models bound by a worst- and a best-case scenario model. As the input parameters vary with each μ degree, each μ degree has a unique worst-case scenario model. First, for each recorded bridge inspection, the inspector-assigned BCI is replaced with a BCI membership function; the bridge-specific MP membership functions are defined based on the records of the

nearest station and the meteorological zone. Given a μ degree, the possible range of BCI and MP values is estimated from the membership functions. Then, m random BCI and MP values are generated from within these ranges using Monte Carlo simulation, combined with Latin hypercube sampling (McKay et al. 2000). The generated BCI values are transformed into a binary variable, with outcomes of repair and no-repair, based on the two limit states. Then, for each investigated μ degree, m nonlinear LASSO-regularized logistic models are formulated, each relating the probability of a bridge being in a specific state (i.e. repair or no-repair) to the age, T_{major} , T_{minor} , and MPs using a unique set of regression and exponent coefficients (β_j and γ_j). The value of m is taken as 4000 based on a sensitivity analysis.

The worst case scenario model for a given μ degree is defined as the model that maximizes the sum of limit state exceedance probabilities. This is done using the following objective function

$$\text{for a given } \mu: \max \left[\sum_{k=1}^{N_t} P_{\text{LS},k} \right] \quad (5)$$

where N_t is the number of testing data points and $P_{\text{LS},k}$ is the limit state exceedance probability for the k^{th} testing data point. $P_{\text{LS},k}$ is computed for each of the m investigated models by substituting the following inputs into Eq. (1):

1. The regression and exponent coefficients (β_j and γ_j) for the investigated model.
2. The values of the bridge parameters (i.e. age, T_{major} , and T_{minor}) associated with the k^{th} testing data point.
3. The maximum values of the MPs associated with the k^{th} testing data point at the investigated μ degree ($\text{MP}_{\mu,\text{max},k}$)

The regression and exponent coefficients (β_j and γ_j) for each of the m models are

estimated as shown in the next section.

3.5. Fuzzy-Logistic Models

3.5.1. Maintenance Limit State (MLS)

The fuzzy-logistic models that predict the probability of exceeding the MLS (i.e. probability of the BCI falling below 70) are constructed as follows. The exponent coefficients γ_j are estimated for all parameters (i.e. age, T_{major} , T_{minor} , DOSF, DOGS, and SFPY) in two stages. First, initial values of γ_j are estimated via non-regularized logistic regression analysis in which each parameter is separately related to the probability of exceeding the MLS (P_{MLS}). Second, γ_j are varied within ± 0.2 from the initial estimates with a 0.1 step and all permutations are examined via LASSO-regularized logistic regression. For each permutation, a range of λ is examined resulting in a range of deviance. Initially, the deviance is correlated to λ but then plateaus as shown in Fig. 3.6. To balance the model's accuracy and interpretability, the λ corresponding to 0.1% reduction in deviance is compared across all permutation to select the simplest model while minimizing the deviance. The aforementioned second step is repeated m times for each μ degree and the worst-case scenario model is identified using Eq. (5).

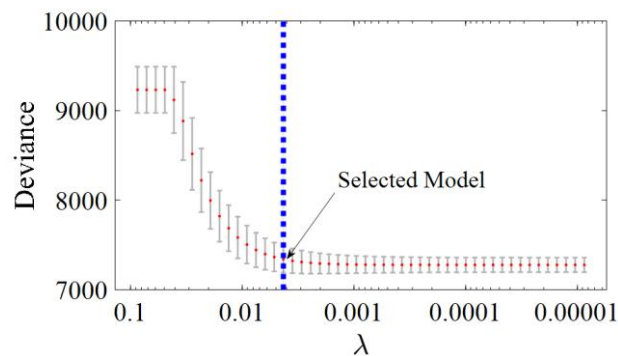


Fig. 3.6 Deviance versus λ

The proposed MLS fuzzy-logistic model is found as

$$P_{\text{MLS}} = \frac{\exp [\beta_0 + \beta_1 * \text{age}^{\gamma_1} + \beta_2 * T_{\text{major}}^{\gamma_2} + \beta_3 * \text{DOSF} + \beta_4 * \text{DOGS}]}{1 + \exp [\beta_0 + \beta_1 * \text{age}^{\gamma_1} + \beta_2 * T_{\text{major}}^{\gamma_2} + \beta_3 * \text{DOSF} + \beta_4 * \text{DOGS}]} \quad (6)$$

where the regression coefficients (β_0 to β_4) and the exponent coefficients (γ_1 and γ_2) for given μ levels are shown in Table 3.2. The analysis results agree with the initial speculation that bridge condition is controlled by bridge aging, maintenance history, and climate conditions. For MTO owned bridges, T_{major} is more detrimental to the bridge condition compared to T_{minor} , and DOSF and DOGS are the most relevant meteorological parameters to the bridge condition. The probabilistic nature of logistic models enables the aleatoric uncertainty to be captured, whereas the epistemic uncertainty is captured by the variability of the regression and exponent coefficients as shown in Table 3.2.

Table 3.2. Regression and exponent coefficients for MLS fuzzy-logistic models

μ	β_0	β_1	γ_1	β_2	γ_2	β_3	β_4
0	-10.600	6.500	0.1	0.0279	0.9	0.0026	0
0.2	-11.594	6.814	0.1	0.1669	0.5	0.0034	0.0015
0.4	-13.072	7.668	0.1	0.0733	0.7	0.0019	0.0056
0.6	-16.653	9.641	0.1	0.1239	0.6	0.0076	0.0065
0.8	-23.809	13.896	0.1	0.0925	0.7	0.0037	0.0156
1	-25.635	14.964	0.1	0.1391	0.6	0.0145	0.0109

3.5.2. Inspection Limit State (ILS)

The ILS fuzzy-logistic models are constructed similarly to the MLS fuzzy-logistic models with the difference of the limit state definition. The probability of exceeding the ILS (P_{ILS}) is expressed as a function of the bridge age and maintenance history, at the beginning of an inspection interval (Δt), as well as the meteorological conditions.

The ILS fuzzy-logistic model follows the same formulation as Eq. (6), with regression coefficients (β_0 to β_4) and exponent coefficients (γ_1 and γ_2) for given μ levels are shown in Table 3.3, Table 3.4, and Table 3.5 for Δt of 2, 4, and 6 years, respectively.

Table 3.3. Regression and exponent coefficients for ILS fuzzy-logistic models for Δt of 2 years

μ	β_0	β_1	γ_1	β_2	γ_2	β_3	β_4
0	-5.470	1.596	0.2	0.142	0.5	0	0
0.2	-5.671	1.592	0.2	0.170	0.5	0	0
0.4	-10.576	5.482	0.1	0.209	0.5	0	0
0.6	-13.814	7.273	0.1	0.219	0.5	0.0009	0.0009
0.8	-11.200	3.133	0.2	0.334	0.4	0	0.0072
1	-10.995	3.125	0.2	0.197	0.5	0.0044	0.0021

Table 3.4. Regression and exponent coefficients for ILS fuzzy-logistic models for Δt of 4 years

μ	β_0	β_1	γ_1	β_2	γ_2	β_3	β_4
0	-5.743	1.742	0.2	0.140	0.6	0	0
0.2	-6.261	1.930	0.2	0.144	0.6	0	0
0.4	-7.370	2.355	0.2	0.233	0.5	0	0
0.6	-10.640	3.549	0.2	0.264	0.5	0.005	0
0.8	-21.392	11.925	0.1	0.239	0.5	0	0.0079
1	-25.561	13.595	0.1	0.800	0.3	0.0008	0.0105

Table 3.5. Regression and exponent coefficients for ILS fuzzy-logistic models for Δt of 6 years

μ	β_0	β_1	γ_1	β_2	γ_2	β_3	β_4
0	-5.604	1.702	0.2	0.166	0.6	0	0
0.2	-6.545	1.907	0.2	0.320	0.5	0	0
0.4	-7.370	2.263	0.2	0.222	0.6	0	0
0.6	-10.904	3.550	0.2	0.548	0.4	0.0039	0
0.8	-15.280	5.161	0.2	0.363	0.5	0.0081	0.0027
1	-25.038	13.964	0.1	0.324	0.5	0.0035	0.0067

3.6. Case Study

The application of the proposed fuzzy-logistic models for scheduling maintenance and

inspections is demonstrated using a case study bridge. P_{MLS} and P_{ILS} can be tracked over the bridge service life using Eq. (6) and a given μ degree. Bridge authorities can impose probability thresholds ($P_{MLS\text{-threshold}}$ and $P_{ILS\text{-threshold}}$) beyond which a maintenance action or inspection action (e.g. reduce inspection intervals) are triggered. Preliminary maintenance and inspection schedules can then be established for planning purposes.

The case study is a steel girder bridge, constructed in 2016 at latitude and longitude coordinates of 43.4137 N and 80.3454 W, respectively, which has yet to receive any major maintenance. First, the bridge-specific membership functions for DOSF and DOGS (Fig. 3.7) are constructed using the following steps:

1. Identify the meteorological zone of the bridge (region 3).
2. Determine the $DOSF_{nms}$ and $DOGS_{nms}$ from the nearest station which is 5.06 km away from the bridge (62.2 and 95.3 days, respectively).
3. Determine $DOSF_{\mu=0,min/max}$ and $DOGS_{\mu=0,min/max}$ from Table 3.1 (53 and 80.1 days for DOSF; 81.3 and 131 days for DOGS).
4. Compute α from Eq. (4) based on the distance to the nearest stations (0.104).
5. Compute $DOSF_{\mu=1,min/max}$ and $DOGS_{\mu=1,min/max}$ based on Eq. (3) (60.8 and 63.6 for DOSF; 92.7 and 97.9 for DOGS).

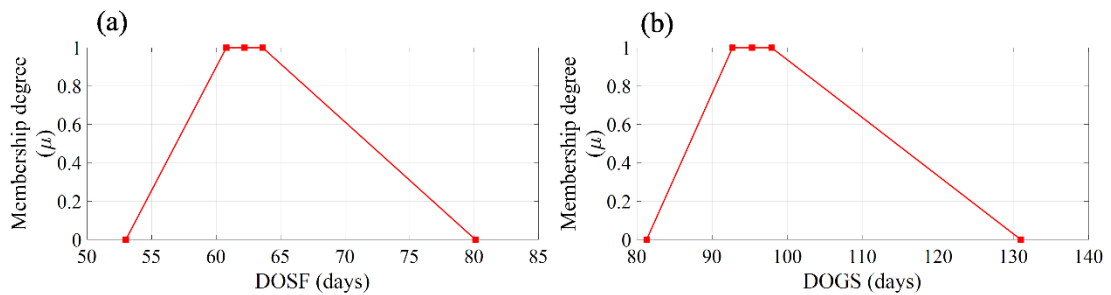


Fig. 3.7 Membership functions for (a) DOSF and (b) DOGS

Substituting the maximum DOSF and DOGS, at a given μ degree, into Eq. (6) will result in the worst-case scenario for P_{MLS} and P_{ILS} for that μ degree (e.g. $DOSF_{\mu=1,max} = 63.6$ and $DOGS_{\mu=1,max} = 97.9$). Given a $P_{MLS-threshold}$ of 0.35 and a μ_{MLS} degree of 1, the P_{MLS} is tracked as shown in Fig. 3.8a using the following steps (the optimum μ_{MLS} degree and $P_{MLS-threshold}$ are determined in the LCC section):

1. Find the regression and exponent coefficients for Eq. (6) for the μ_{MLS} degree (Table 3.2).
2. Track the P_{MLS} starting at the construction date in 2016 (age = $T_{major} = 0$, and $P_{MLS} = 0$).
3. Increase age and T_{major} incrementally until P_{MLS} approaches the threshold (age = $T_{major} = 41$ years, and $P_{MLS} = 0.34$).
4. Assume that maintenance is applied five years after reaching the threshold and extend the profile until 2062 (age = $T_{major} = 46$ years, and $P_{MLS} = 0.42$), then reset T_{major} to zero. This leads to an instantaneous drop in P_{MLS} (age = 46 years, $T_{major} = 0$, and $P_{MLS} = 0.154$).
5. Repeat step 3 and 4 to find the timing of all interventions.
6. Repeat step 1 to 5 to track P_{MLS} for μ_{MLS} degree of 0 (Fig. 3.8b).

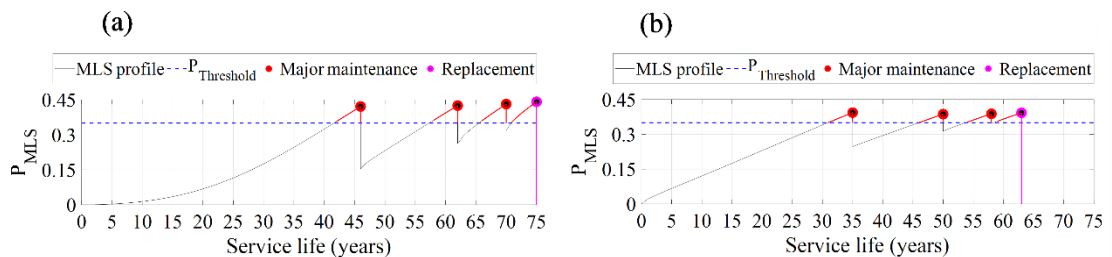


Fig. 3.8 P_{MLS} profile for $P_{MLS-threshold} = 0.35$ with (a) $\mu_{MLS} = 1$ and (b) $\mu_{MLS} = 0$

For μ_{MLS} degree of 1 (Fig. 3.8a), three major maintenances are expected, at 46 years after construction of the bridge, 16 years following the first major maintenance, and 8 years following the second major maintenance. The bridge is expected to be partially or fully replaced after a service life of 75 years to maintain the P_{MLS} -threshold of 0.35. For the lowest μ_{MLS} degree of 0 (Fig. 3.8b), the first major maintenance is expected 35 years after the construction of the bridge; the second major maintenance is expected 15 years following the first major maintenance, and the third major maintenance is expected 8 years following the second major maintenance. The bridge is expected to be partially or fully replaced after a service life of 63 years to maintain the P_{MLS} -threshold of 0.35. Thus, a lower μ_{MLS} indicates a prediction of a faster deterioration rate which in turn leads to a shorter service life and to a shorter time between the construction of the bridge and each major maintenance.

After identifying maintenance timings, the worst-case scenario P_{ILS} can be plotted. As an example, the P_{ILS} is plotted over time for μ_{ILS} degrees of 1 and 0.5. A P_{ILS} -threshold of 0.15 is selected and inspection intervals are shortened whenever this threshold is reached (the optimum μ_{ILS} degree and P_{ILS} -threshold are determined in the LCC section). The P_{ILS} can be plotted as follows:

1. Find the regression and exponent coefficients for Eq. (6) for $\Delta t = 2$ years and the μ_{ILS} degree (Table 3.3).
2. Track the P_{ILS} starting at the construction date in 2016 (black dotted line in Fig. 3.9).
3. Increase age and T_{major} incrementally until first maintenance is reached then reset T_{major} to zero. Repeat for all maintenance interventions until bridge

replacement (e.g. for $\mu_{MLS} = 1$ and $P_{MLS\text{-threshold}} = 0.35$, maintenance is expected at age of 46, 62, and 70 years, whereas replacement is expected at an age of 75 years as shown in Fig. 3.9).

4. Repeat step 2 and 3 for $\Delta t = 4$ and 6 years using the coefficients in Table 3.4 and Table 3.5, respectively.

Note that larger inspection intervals (Δt) are accompanied with higher risks of exceeding the limit state (i.e. higher P_{ILS}) as shown in Fig. 3.9. To plan an inspection schedule, the envelope P_{ILS} profile (magenta line in Fig. 3.9) is plotted as follows:

1. Start by tracking the profile of $\Delta t = 6$ years.
2. Upon reaching $P_{ILS\text{-threshold}}$, drop down and start tracking the next lower Δt .
3. Repeat step (2) until reaching the first maintenance.
4. Drop down and start tracking the profile of $\Delta t = 6$ years again.
5. Repeat previous steps until the end of the service life.

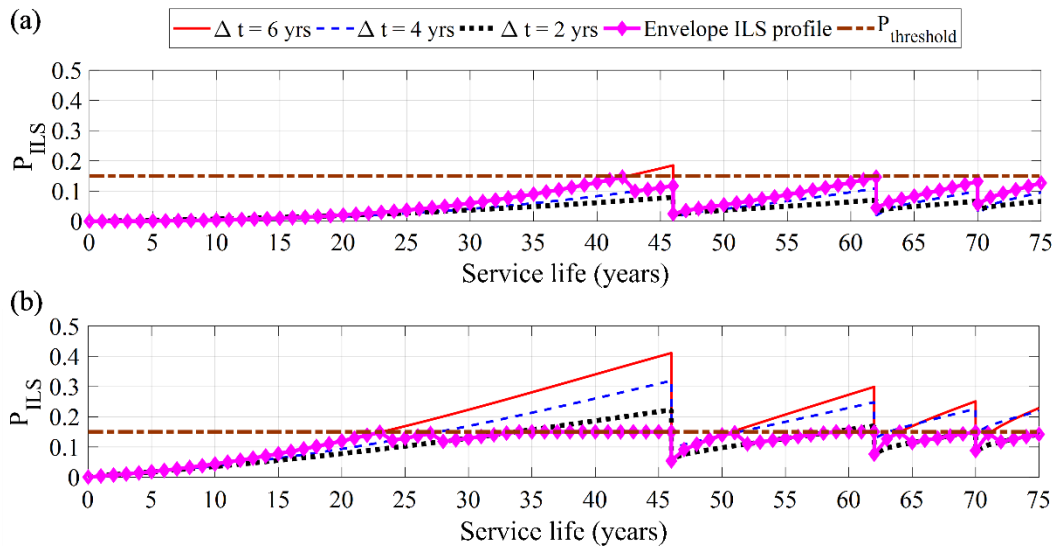


Fig. 3.9 P_{ILS} profile for $P_{ILS\text{-threshold}} = 0.15$ with (a) $\mu_{ILS} = 1$ and (b) $\mu_{ILS} = 0.5$ (maintenance timings based on $\mu_{MLS} = 1$ and $P_{MLS\text{-threshold}} = 0.35$)

The theoretical changes in suggested inspection intervals can be found from the envelope P_{ILS} profile. Generally, the bridge service life can be divided into several segments, each ending with bridge maintenance or replacement. Initially for each segment, a large inspection interval is sufficient to keep P_{ILS} below $P_{ILS\text{-threshold}}$; however, as the bridge ages, the inspection intervals should become shorter. The theoretical changes in inspection intervals can be adjusted according to the bridge-specific deterioration rates identified from future inspections.

For μ_{ILS} degree of 1 (Fig. 3.9a), an inspection interval of 6 years is adequate for the first 42 years, and afterwards the interval shortened to 4 years until the first major maintenance (i.e. at age of 46 years). For μ_{ILS} degree of 0.5 (Fig. 3.9b), an inspection interval of 6 years should be used for the first 23 years followed by inspection intervals of 4 and 2 years until 27 and 33 years after bridge construction, respectively. From the age of 33 years until the first major maintenance (i.e. at age of 46 years), an inspection interval of 2 years is no longer adequate and it is assumed that annual inspections will be required to limit P_{ILS} to the $P_{ILS\text{-threshold}}$. Note that a lower μ_{ILS} prompts faster transition from large to short inspection intervals during each segment of the bridge service life.

3.7. Life Cycle Cost (LCC) Analysis

The bridge management strategies, devised by the proposed fuzzy-logistic models, are dependent on the chosen probability thresholds ($P_{MLS\text{-threshold}}$ and $P_{ILS\text{-threshold}}$) and μ degrees (μ_{MLS} and μ_{ILS}). Strategies with low probability thresholds or low μ degrees have lower service failure risks but higher operational costs. To ensure cost-effective strategies with acceptable risk, LCC analysis can be used to select the optimum

thresholds and μ degrees. A two-stage LCC analysis is applied separately for each type of work (i.e. maintenance or inspection). First, the study explores the optimum probability threshold and corresponding strategy for selected μ degrees. Then, the strategies are compared across all selected μ degrees to choose the most cost-effective strategy while minimizing service failure risk. The same case study bridge is used as an example, and the LCC required for 75 years of service life is computed. The LCC is computed in present value (Yanev 1994) using a discount rate r of 5% (MTO 2013).

3.7.1. Maintenance Limit State (MLS)

The LCC for MLS includes construction, operating, and failure costs. For a given μ degree, LCC_{MLS} is calculated as

$$C_C + [C_{MM} + C_{MM-U} + C_{BR} + C_{BR-U}] + [C_{F-MLS} + C_{F-MLS-U}] \quad (7)$$

where C_C is the construction cost, and C_{MM} is the cost of major maintenance, C_{BR} is the cost of partial or full bridge replacement, and C_{F-MLS} is the probabilistic service failure cost arising from exceeding the MLS. The associated user delay costs, due to traffic congestions and detouring, are C_{MM-U} , C_{BR-U} and $C_{F-MLS-U}$, for maintenance, bridge replacement, and failure, respectively. The considered service life is 75 years regardless of maintenance or replacement needs.

The Parametric Estimating Guide (MTO 2016) is used to estimate the base year costs of construction, major maintenance, and bridge replacement. For the examined steel girder bridge with deck area of 2,048 m², the base year costs are estimated as 8, 3.1, and 8.8 million CAD\$, respectively. C_{MM} and C_{BR} are then estimated as

$$\sum_1^S C_{MM-base} \frac{1}{(1+r)^t} \quad (8)$$

$$\sum_1^s C_{\text{BR-base}} \frac{1}{(1+r)^t} \quad (9)$$

where s is the number of times the cost is incurred and t is the year when the cost is incurred. The user delay costs associated with maintenance or replacement work, $C_{\text{MM-U}}$, $C_{\text{BR-U}}$, are estimated based on the research of Chang and Shinozuka (1996) as

$$\sum_1^s t_m b_m u \frac{1}{(1+r)^t} \quad (10)$$

where t_m is the duration of the work in years, b_m is the percentage of closed lanes during the work, and u is the unit user cost. Major maintenance is assumed to take 2 months with closure of half of the bridge lanes ($t_m = 2/12$, $b_m = 0.5$) (Manning and Bye 1984), whereas bridge replacement is assumed to take 1 year with full bridge closure ($t_m = 1$, $b_m = 1$). The user unit cost is estimated as

$$u = \text{delay cost per hour} \times \text{average delay per user} \times \text{annual traffic or truck volume} \quad (11)$$

where the delay cost is taken as 15 and 75 CAD\$ per hour for vehicles and trucks, respectively (Armstrong et al. 2008). The average delay per user is assumed to be 1 hour (Chang and Shinozuka 1996). Finally, the annual traffic and truck volumes are estimated based on an annual average daily traffic and truck traffic of 137,300 vehicles and 23,341 trucks, respectively (MTO 2019).

The service failure cost $C_{\text{F-MLS}}$ is defined as the probabilistic cost incurred to repair the bridge after exceeding the MLS. $C_{\text{F-MLS}}$ is found as

$$\sum_{t=1}^{t=75} P_{\text{MLS}}(t) C_{\text{F-MLS-base}} \frac{1}{(1+r)^t} \quad (12)$$

where the base year failure cost $C_{F-MLS-base}$ is taken the same as $C_{MM-base}$. The expected C_{F-MLS} is then computed by accumulating the probabilistic service failure cost ($P_{MLS}(t) \times C_{F-MLS-base}$) every year in the service life (Ghosh and Padgett 2011), where $P_{MLS}(t)$ is computed from Eq. (6). The user cost $C_{F-MLS-U}$ is computed similarly to C_{MM-U} while multiplying by $P_{MLS}(t)$.

Based on Eqs. (7) to (12), the LCC_{MLS} can be computed for a range of $P_{MLS-threshold}$. The results for LCC_{MLS} given $\mu_{MLS}=1$ are shown as an example in Fig. 3.10. For μ_{MLS} of 1, the optimum $P_{MLS-threshold}$ that balances service failure and operational costs is 0.2. Similarly, the optimum thresholds are computed for other selected values of μ_{MLS} as shown in Table 3.6; resulting in multiple possible maintenance strategies.

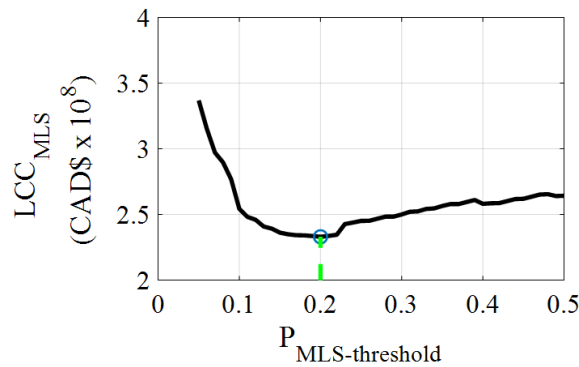


Fig. 3.10 LCC_{MLS} given $\mu_{MLS}=1$ versus $P_{MLS-threshold}$

Table 3.6. Optimum $P_{MLS-threshold}$ for various μ_{MLS} degrees

Strategy	1	2	3	4	5	6	7	8	9	10	11
μ_{MLS}	0	0.1	0.2	0.3	0.4	0.5	0.6	0.7	0.8	0.9	1
$P_{MLS-threshold}$	0.34	0.35	0.28	0.32	0.32	0.28	0.25	0.23	0.21	0.22	0.20

The availability of multiple optima maintenance strategies (Table 3.6) reflects the epistemic uncertainty in bridge condition and its maintenance requirements. This uncertainty may lead to additional service failure and user costs. Maintenance strategies

corresponding to high μ_{MLS} tend to have lower operational costs, but also pose the risk of incurring higher additional failure and user costs. The optima strategies in Table 3.6 are compared in terms of operational costs and additional service failure and user costs. The additional service failure and user costs are defined as those incurred if the maintenance strategy is planned using a value of μ_{MLS} greater than 0 but the bridge deteriorates in accordance with μ_{MLS} of 0.

For example, if maintenance is planned in accordance with μ_{MLS} of 1 and P_{MLS} -threshold of 0.2, then maintenance timings can be predicted from the corresponding P_{MLS} profile (solid line in Fig. 3.11) which is plotted using the steps explained in the case study section. Two major maintenances are expected at ages of 36 and 47, respectively, before partial or full replacement takes place at an age of 54 years. Afterwards, a second P_{MLS} profile (dashed line in Fig. 3.11) is plotted parallel to the first one but in accordance with μ_{MLS} of 0. The highlighted area between these two profiles (Fig. 3.11) represents the additional failure risks. The additional failure costs can then be computed as the difference between the two profiles in terms of the probabilistic service failure and associated user costs, respectively.

The total cost (i.e. construction + operational + additional failure costs) is computed for all strategies in Table 3.6 and plotted in Fig. 3.12a. The optimum maintenance strategy has μ_{MLS} of 0.1 and P_{MLS} -threshold of 0.35. This optimum maintenance strategy predicts the need for two major maintenances at ages of 36 and 52 years, respectively, before partial or total bridge replacement takes place at an age of 60 years (Fig. 3.12b).

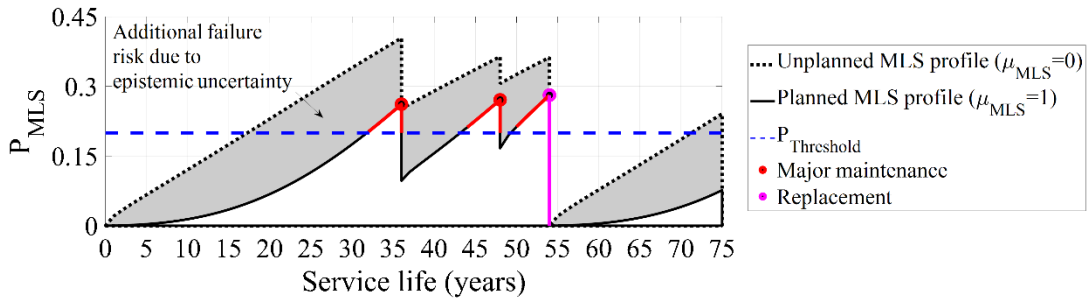


Fig. 3.11 Planned versus unplanned MLS profile

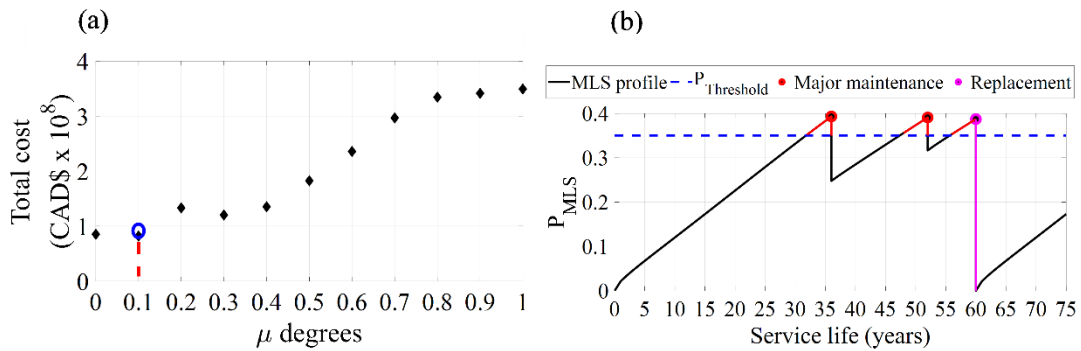


Fig. 3.12 (a) Total cost for maintenance strategies in Table 3.6 and (b) optimum maintenance strategy for the case study bridge ($\mu_{MLS} = 0.1$ and $P_{MLS\text{-threshold}} = 0.35$)

3.7.2. Inspection Limit State (ILS)

The LCC for ILS includes inspection and failure costs. Inspection is classified as either ordinary or enhanced. The first is done for well-conditioned bridges and includes only visual examination of its elements, whereas the second is for fair- or bad-conditioned bridges and involves close-up examination of elements using specialized equipment which often requires partial lane closures (MTO 2008). For a given μ degree, LCC_{ILS} can be calculated as

$$[C_{I-O} + C_{I-E} + C_{I-E-U}] + [C_{F-ILS} + C_{F-ILS-U}] \quad (13)$$

where C_{I-O} is the cost of ordinary inspections, C_{I-E} is the cost of enhanced inspections, and C_{F-ILS} is the probabilistic service failure costs due to ILS exceedance. The associated user delay costs with enhanced inspections and service failure are C_{I-E-U} and $C_{F-ILS-U}$, respectively.

The base year costs for ordinary and enhanced inspections are assumed to be 0.5% and 1.5% of construction costs, respectively. It is also assumed that all inspections are of ordinary type except for those within the 5 years prior to a planned maintenance intervention. C_{I-E-U} is computed similarly to Eq. (10) assuming that enhanced inspection requires 1 day with half bridge closure ($t_m = 1/365$, $b_m = 0.5$). C_{F-ILS} and $C_{F-ILS-U}$ are computed similar to those of MLS while replacing $P_{MLS}(t)$ with $P_{ILS}(t)$. Finally, it is assumed that if biennial inspection is not sufficient to maintain $P_{ILS-threshold}$, then annual inspection will be required.

The analysis follows the same steps as for the MLS, resulting in multiple optima inspection strategies as shown in Table 3.7. Next, the total cost (i.e. inspection + additional failure costs) is computed for all strategies in Table 3.7 and plotted in Fig. 3.13a. The optimum inspection strategy has μ_{ILS} of 0.7 and $P_{ILS-threshold}$ of 0.09 (Fig. 3.13b). The theoretical bridge-age ranges for different inspection intervals can be found from the envelope P_{ILS} profile in Fig. 3.13b.

Table 3.7. Optimum $P_{ILS-threshold}$ for various μ_{ILS} degrees

Strategy	1	2	3	4	5	6	7	8	9	10	11
μ_{ILS}	0	0.1	0.2	0.3	0.4	0.5	0.6	0.7	0.8	0.9	1
$P_{ILS-threshold}$	0.2	0.2	0.19	0.18	0.22	0.19	0.11	0.09	0.09	0.11	0.09

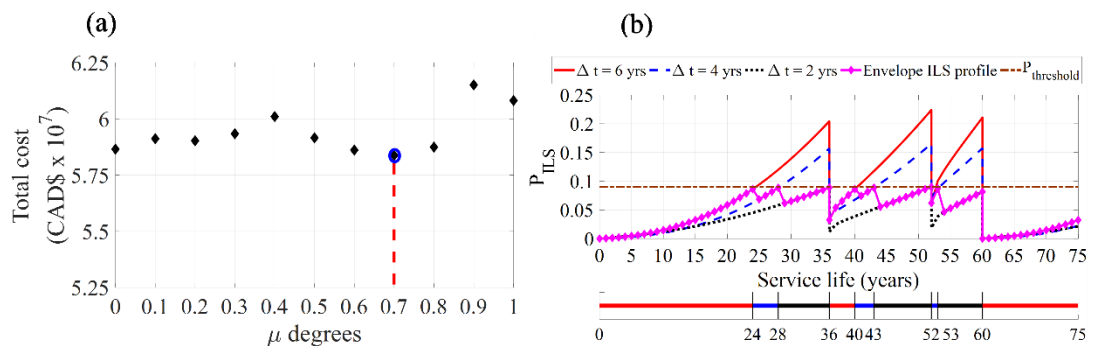


Fig. 3.13 (a) Total cost for inspection strategies in Table 3.7 and (b) optimum inspection strategy for the case study bridge ($\mu_{ILS} = 0.7$ and $P_{ILS-threshold} = 0.09$)

3.8. Development of Maintenance and Inspection Strategies

For the case study bridge, the optimum maintenance strategy corresponds to P_{MLS} -threshold of 0.35 and μ_{MLS} of 0.1, whereas the optimum inspection strategy corresponds to P_{ILS} -threshold of 0.09 and μ_{ILS} of 0.7. The bridge is expected to need two major maintenances during a service life of 60 years after which it should be partially or fully replaced as shown in Fig. 3.14. Based on the predicted theoretical changes in inspection intervals in Fig. 3.13b, a preliminary inspection schedule is proposed in Fig. 3.14. It is expected that 22 inspections (13 and 9 of ordinary and enhanced type, respectively) would be needed to adequately monitor the bridge condition over a service life of 60 years. This represents about 70% of the requirements of the current biennial inspection system used by the MTO which shows potential for saving valuable resources.

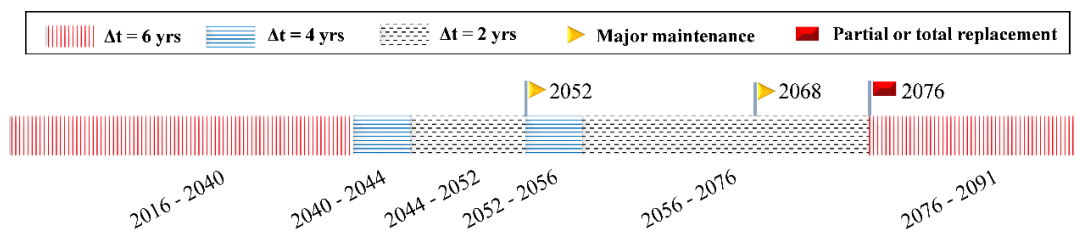


Fig. 3.14 Optimum maintenance and inspection strategy for the case study bridge

3.8.1. Potential Extensions for Network Level Strategies

The proposed framework can be extended to support bridge network level decisions. Network level decisions are influenced by both the individual bridge condition as well as the effect of the condition of the bridge on the functionality of the network (Hegazy et al. 2004; Zhang and Wang 2017). The functionality of the network can be measured using the average vehicle travel time (Zhang and Wang 2017) or the flow capacity (Chen et al. 2002). The importance of each bridge in the network is proportional to the change in the functionality of the network with reduced condition of the bridge. The

importance of the bridges to the network can be used as weighting functions with the probabilities from Eq. (6) (i.e. P_{MLS} or P_{ILS}) to support network level decisions.

3.8.2. Updating Maintenance and Inspection Strategies

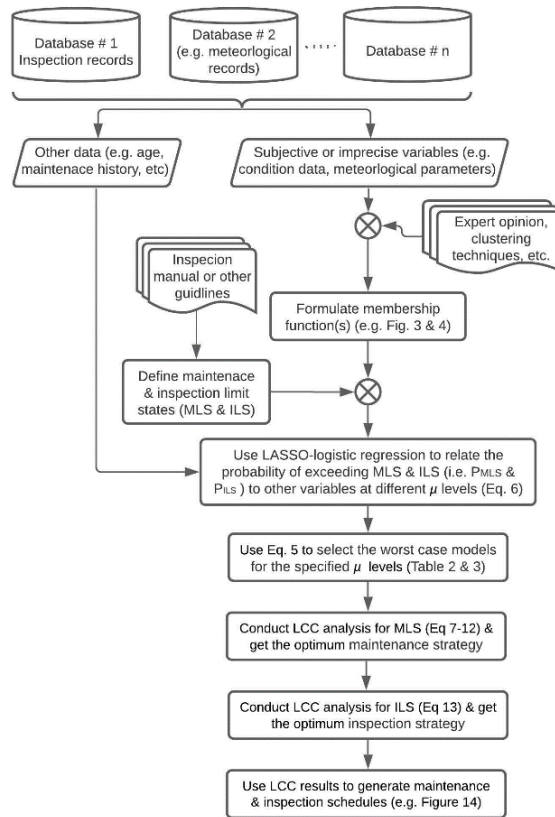


Fig. 3.15 Flowchart for the proposed fuzzy-probabilistic framework

The proposed maintenance and inspection strategies can be improved by incorporating any additional bridge-specific information into the proposed fuzzy-logistic model using one or more updating factors. The gained improvements can be quantified as an increase in the rate of true repair predictions (Abdelmaksoud et al. 2021), reduction in expected costs (Fauriat and Zio 2020), or increase in functionality (Zhang et al., 2021). For example, Abdelmaksoud et al. (2021) used the BCI deterioration rate as an updating factor and showed that it can improve the ability of logistic models to detect bridges in

need of maintenance and inspection. A summary of the proposed fuzzy-probabilistic framework used to create the preliminary maintenance and inspection strategies can be found in the flowchart in Fig. 3.15.

3.9. Conclusions

A simple-yet-efficient fuzzy-probabilistic framework is proposed to aid bridge owners to account for aleatory and epistemic uncertainties when developing maintenance and inspection strategies. Unlike existing fuzzy-probabilistic approaches, the proposed framework does not require extensive measurements of bridge deterioration (e.g. chloride concentration, reinforcement corrosion rate, etc.). Rather, the framework only uses information readily available from the inspection database (e.g. age and maintenance history) or any other existing databases (e.g. meteorological databases); hence, it can be efficiently integrated into BMSs.

Aleatory uncertainty, arising from randomness, is handled using logistic regression which predicts the probability of exceeding the defined maintenance or inspection limit states, P_{MLS} and P_{ILS} , respectively. For MTO owned bridges, P_{MLS} and P_{ILS} are expressed using fuzzy-logistic models function of bridge age, time since last major maintenance (T_{major}), days of snow fall (DOSF), and days of ground snow (DOGS). Meanwhile, epistemic uncertainty, arising from subjectivity or imprecise data, is handled using fuzzy logic principles in which subjective and imprecise parameters are modelled using membership functions. For a given μ degree, each subjective or imprecise parameter is assigned a specific range of values, where the lower the μ degree the wider the range. This results in a specific range of logistic models for each μ degree; however, only the worst-case scenario model is of interest as it

predicts the highest probabilities of exceeding the limit states. The lower the μ degree the more conservative the model and the higher the operational costs.

The proposed fuzzy-logistic models can be used to track the bridge condition throughout its service life, and a range of maintenance and inspection strategies can be suggested depending on the probability thresholds ($P_{MLS\text{-threshold}}$ and $P_{ILS\text{-threshold}}$) and μ degree. The optimum strategies can be chosen based on a two-stage LCC analysis. First, the optimum probability thresholds and corresponding strategies are computed separately for given μ degrees by minimizing the summation of operational and probabilistic failure costs. Then, the strategies are compared across all μ degrees. Strategies corresponding to high μ degrees have higher additional failure risks, whereas those corresponding to low μ degrees have higher operational costs. As such, the optimum maintenance and inspection strategies will tend to be associated with mid-range values of μ degree. For the examined bridge, the methodology has the potential for reducing bridge inspections by about 30% throughout the service life, compared to biennial inspection practices.

While the proposed fuzzy-logistic models are directed towards capturing time-dependent deterioration of bridge condition, they do not account for the effect of accidents or extreme events. Hence, future work could focus on developing similar models to predict the drop in bridge condition following such events.

3.10. Data Availability Statement

All data, models, or code that support the findings of this study are available from the corresponding author upon reasonable request.

3.11. Acknowledgments

The authors gratefully acknowledge the support from the Ontario Graduate Scholarship provided by the Government of Ontario, and the start-up funding provided by the Faculty of Engineering at McMaster University. Any opinions, findings, and conclusions or recommendations expressed in this material are those of the authors and do not necessarily reflect the views of the sponsor.

3.12. References

- Abdelmaksoud, A. M., G. P. Balomenos, and T. C. Becker. 2021. "Parameterized logistic models for bridge inspection and maintenance scheduling." *J. Bridge Eng.* 26 (10): 04021072. [https://doi.org/10.1061/\(ASCE\)BE.1943-5592.0001774](https://doi.org/10.1061/(ASCE)BE.1943-5592.0001774).
- Armstrong, J., J. Loftus, J. Weir, and W. Roy. 2008. "The highway element investment review (HEIR) guidelines: Making the right decisions in Ontario." In *Proc., Annual Conf. the Transportation Association of Canada (TAC): Transportation—A Key to a Sustainable Future*. Ottawa: Transportation Association of Canada.
- Balomenos, G. P., Y. Hu, J. E. Padgett, and K. Shelton. 2019. "Impact of coastal hazards on residents' spatial accessibility to health services." *J. Infrastruct. Syst.* 25 (4): 04019028. [https://doi.org/10.1061/\(ASCE\)IS.1943-555X.0000509](https://doi.org/10.1061/(ASCE)IS.1943-555X.0000509).
- Balomenos, G. P., S. Kameshwar, and J. E. Padgett. 2020. "Parameterized fragility models for multi-bridge classes subjected to hurricane loads." *Eng. Struct.* 208 (Apr): 110213. <https://doi.org/10.1016/j.engstruct.2020.110213>.
- Balomenos, G. P., and J. E. Padgett. 2018. "Fragility analysis of pile-supported wharves and piers exposed to storm surge and waves." *J. Waterw. Port Coastal Ocean Eng.* 144 (2): 04017046. [https://doi.org/10.1061/\(ASCE\)WW.1943-5460.0000436](https://doi.org/10.1061/(ASCE)WW.1943-5460.0000436).
- Bernier, C., I. Gidaris, G. P. Balomenos, and J. E. Padgett. 2019. "Assessing the

- accessibility of petrochemical facilities during storm surge events.” *Reliab. Eng. Syst. Saf.* 188 (Aug): 155–167. <https://doi.org/10.1016/j.ress.2019.03.021>.
- Brown, C. B., and J. T. P. Yao. 1983. “Fuzzy sets and structural engineering.” *J. Struct. Eng.* 109 (5): 1211–1225. [https://doi.org/10.1061/\(ASCE\)0733-9445\(1983\)109:5\(1211\)](https://doi.org/10.1061/(ASCE)0733-9445(1983)109:5(1211)).
- Chang, S. E., and M. Shinozuka. 1996. “Life-cycle cost analysis with natural hazard risk.” *J. Infrastruct. Syst.* 2 (3): 118–126. [https://doi.org/10.1061/\(ASCE\)1076-0342\(1996\)2:3\(118\)](https://doi.org/10.1061/(ASCE)1076-0342(1996)2:3(118)).
- Chen, A., H. Yang, H. K. Lo, and W. H. Tang. 2002. “Capacity reliability of a road network: An assessment methodology and numerical results.” *Transp. Res. Part B Methodol.* 36 (3): 225–252. [https://doi.org/10.1016/S0191-2615\(00\)00048-5](https://doi.org/10.1016/S0191-2615(00)00048-5).
- ECCC (Environment and Climate Change Canada). 2019. “1981-2010 Canadian climate normals and averages.” https://climate.weather.gc.ca/climate_normals/index_e.html.
- Everett, T. D., P. Weykamp, H. A. Capers Jr., W. R. Cox, T. S. Drda, L. Hummel, P. Jensen, D. A. Juntunen, T. Kimball, and G. A. Washer. 2008. *Bridge evaluation quality assurance in Europe*. Rep. No. FHWA-PL-08-016. Washington, DC: Federal Highway Administration.
- Fauriat, W., and E. Zio. 2020. “Optimization of an aperiodic sequential inspection and condition-based maintenance policy driven by value of information.” *Reliab. Eng. Syst. Saf.* 204 (Dec): 107133. <https://doi.org/10.1016/j.ress.2020.107133>.
- Frangopol, D. M., M.-J. Kallen, and J. M. van Noortwijk. 2004. “Probabilistic models for life-cycle performance of deteriorating structures: Review and future

- directions.” *Prog. Struct. Eng. Mater.* 6 (4): 197–212. <https://doi.org/10.1002/pse.180>.
- Ghosh, J., and J. E. Padgett. 2011. “Probabilistic seismic loss assessment of aging bridges using a component-level cost estimation approach.” *Earthquake Eng. Struct. Dyn.* 40 (15): 1743–1761. <https://doi.org/10.1002/eqe.1114>.
- Golabi, K., and R. Shepard. 1997. “Pontis: A system for maintenance optimization and improvement of US bridge networks.” *Interfaces* 27 (1): 71–88. <https://doi.org/10.1287/inte.27.1.71>.
- Government of Ontario. 2018. “Bridge condition dataset.” Accessed October 2018. <https://data.ontario.ca/dataset/bridge-conditions>.
- Hawk, H., and E. P. Small. 1998. “The BRIDGIT bridge management system.” *Struct. Eng. Int.* 8 (4): 309–314. <https://doi.org/10.2749/101686698780488712>.
- Hegazy, T., E. Elbeltagi, and H. El-Behairy. 2004. “Bridge deck management system with integrated life-cycle cost optimization.” *Transp. Res. Rec.* 1866 (1): 44–50. <https://doi.org/10.3141/1866-06>.
- Kiureghian, A. D., and O. Ditlevsen. 2009. “Aleatory or epistemic? Does it matter?” *Struct. Saf.* 31 (2): 105–112. <https://doi.org/10.1016/j.strusafe.2008.06.020>.
- Kwakernaak, H. 1978. “Fuzzy random variables—I. Definitions and theorems.” *Inf. Sci.* 15 (1): 1–29. [https://doi.org/10.1016/0020-0255\(78\)90019-1](https://doi.org/10.1016/0020-0255(78)90019-1).
- Li, Z., and R. Burguen~o. 2010. “Using soft computing to analyze inspection results for bridge evaluation and management.” *J. Bridge Eng.* 15 (4): 430–438. [https://doi.org/10.1061/\(ASCE\)BE.1943-5592.0000072](https://doi.org/10.1061/(ASCE)BE.1943-5592.0000072).
- Ma, Y., L. Wang, J. Zhang, Y. Xiang, T. Peng, and Y. Liu. 2015. “Hybrid uncertainty

quantification for probabilistic corrosion damage prediction for aging RC bridges.”

J. Mater. Civ. Eng. 27 (4): 04014152. [https://doi.org/10.1061/\(ASCE\)MT.1943-5533.0001096](https://doi.org/10.1061/(ASCE)MT.1943-5533.0001096).

MacQueen, J. 1967. “Some methods for classification and analysis of multivariate observations.” In Vol. 1 of Proc., 5th Berkeley Symp. on Mathematical Statistics and Probability, 281–297. Oakland, CA.

Manning, D. G., and D. H. Bye. 1984. “Bridge deck rehabilitation manual (Part two: Contract preparation).” <https://www.library.mto.gov.on.ca/SydneyPLUS/Sydney/Portal/default.aspx?lang=en-US>.

McKay, M. D., R. J. Beckman, and W. J. Conover. 2000. “A comparison of three methods for selecting values of input variables in the analysis of output from a computer code.” Technometrics 42 (1): 55–61. <https://doi.org/10.1080/00401706.2000.10485979>.

Medasani, S., J. Kim, and R. Krishnapuram. 1998. “An overview of membership function generation techniques for pattern recognition.” Int. J. Approximate Reasoning 19 (3–4): 391–417. [https://doi.org/10.1016/S0888-613X\(98\)10017-8](https://doi.org/10.1016/S0888-613X(98)10017-8).

Megaw, E. D. 1979. “Factors affecting visual inspection accuracy.” Appl. Ergon. 10 (1): 27–32. [https://doi.org/10.1016/0003-6870\(79\)90006-1](https://doi.org/10.1016/0003-6870(79)90006-1).

Moore, M., B. M. Phares, B. Graybeal, D. Rolander, G. Washer, and J. Wiss. 2001. Reliability of visual inspection for highway bridges, volume I. Rep. No. FHWA-RD-01-105. McLean, VA: Turner-Fairbank Highway Research Center.

Morcous, G., and Z. Lounis. 2007. “Probabilistic and mechanistic deterioration models for bridge management.” In Computing in civil engineering (2007), 364–373.

- MTO (Ministry of Transportation Ontario). 2008. “Ontario structure inspection manual (OSIM).” <https://www.ogra.org/files/OSIMApril2008.pdf>.
- MTO (Ministry of Transportation Ontario). 2013. “Pavement design and rehabilitation manual.” <http://www.bv.transports.gouv.qc.ca/mono/1165561.pdf>.
- MTO (Ministry of Transportation Ontario). 2015. “Bridge repairs.” Accessed October 2018. <http://www.mto.gov.on.ca/english/highway-bridges/ontario-bridges.shtml>.
- MTO (Ministry of Transportation Ontario). 2016. “Parametric estimating guide (PEG).” <http://www.mto.gov.on.ca/phmpmbp/ReferenceMaterials/EstCon-ParametricEstimatingGuide-2016.pdf>.
- MTO (Ministry of Transportation Ontario). 2019. “MTO ICorridor: Historical provincial highways traffic volumes.” Accessed October, 2020. <http://www.maps.mto.gov.on.ca/icorridor/index.html>.
- Nelder, J. A., and R. W. M. Wedderburn. 1972. “Generalized linear models.” *J. R. Stat. Soc.* 135 (3): 370–84. <https://doi.org/10.2307/2344614>.
- Nickless, K., and R. A. Atadero. 2018. “Mechanistic deterioration modelling for bridge design and management.” *J. Bridge Eng.* 23 (5): 04018018. [https://doi.org/10.1061/\(ASCE\)BE.1943-5592.0001223](https://doi.org/10.1061/(ASCE)BE.1943-5592.0001223).
- Omar, T., M. L. Nehdi, and T. Zayed. 2017. “Integrated condition rating model for reinforced concrete bridge decks.” *J. Perform. Constr. Facil.* 31 (5): 04017090. [https://doi.org/10.1061/\(ASCE\)CF.1943-5509.0001084](https://doi.org/10.1061/(ASCE)CF.1943-5509.0001084).
- Puri, M. L., and D. A. Ralescu. 1986. “Fuzzy random variables.” *J. Math. Anal. Appl.* 114 (2): 409–422. [https://doi.org/10.1016/0022-247X\(86\)90093-4](https://doi.org/10.1016/0022-247X(86)90093-4).
- Sasmal, S., K. Ramanjaneyulu, S. Gopalakrishnan, and N. Lakshmanan. 2006. “Fuzzy

- logic based condition rating of existing reinforced concrete bridges.” *J. Perform. Constr. Facil.* 20 (3): 261–273. [https://doi.org/10.1061/\(ASCE\)0887-3828\(2006\)20:3\(261\)](https://doi.org/10.1061/(ASCE)0887-3828(2006)20:3(261)).
- Shi, X., M. Akin, T. Pan, L. Fay, Y. Liu, and Z. Yang. 2009. “Deicer impacts on pavement materials: Introduction and recent developments.” *Open Civ. Eng. J.* 3 (1). <https://doi.org/10.2174/1874149500903010016>.
- Srikanth, I., and M. Arockiasamy. 2020. “Deterioration models for prediction of remaining useful life of timber and concrete bridges: A review.” *J. Traffic Transp. Eng. English Ed.* 7 (2): 152–173. <https://doi.org/10.1016/j.jtte.2019.09.005>.
- Stewart, M. G., X. Wang, and M. N. Nguyen. 2011. “Climate change impact and risks of concrete infrastructure deterioration.” *Eng. Struct.* 33 (4): 1326–1337. <https://doi.org/10.1016/j.engstruct.2011.01.010>.
- Tarighat, A., and A. Miyamoto. 2009. “Fuzzy concrete bridge deck condition rating method for practical bridge management system.” *Expert Syst. Appl.* 36 (10): 12077–12085. <https://doi.org/10.1016/j.eswa.2009.04.043>.
- Tee, A. B., M. D. Bowman, and K. C. Sinha. 1988a. “Application of fuzzy logic to condition assessment of concrete slab bridges.” *Transp. Res. Rec.* 1184.
- Tee, A. B., M. D. Bowman, and K. C. Sinha. 1988b. “A fuzzy mathematical approach for bridge condition evaluation.” *Civ. Eng. Syst.* 5 (1): 17–24. <https://doi.org/10.1080/02630258808970498>.
- Thompson, P. D., T. Merlo, B. Kerr, A. Cheetham, and R. Ellis. 1999. “The New Ontario bridge management system.” In Vol. 153 of *Proc., 8th Int. Bridge Management Conf.* Washington, DC: Transportation Research Board.

- Tibshirani, R. 1996. “Regression shrinkage and selection via the Lasso.” *J. R. Stat. Soc.* 58 (1): 267–288.
- Wagstaff, K., C. Cardie, S. Rogers, and S. Schrödl. 2001. “Constrained K-means clustering with background knowledge.” *ICML 1 (Jun)*: 577–584.
- Wang, L., Y. Ma, J. Zhang, and Y. Liu. 2013. “Probabilistic analysis of corrosion of reinforcement in RC bridges considering fuzziness and randomness.” *J. Struct. Eng.* 139 (9): 1529–1540. [https://doi.org/10.1061/\(ASCE\)ST.1943-541X.0000738](https://doi.org/10.1061/(ASCE)ST.1943-541X.0000738).
- Wang, L., Y. Ma, J. Zhang, X. Zhang, and Y. Liu. 2015. “Uncertainty quantification and structural reliability estimation considering inspection data scarcity.” *ASCE-ASME J. Risk Uncertainty Eng. Syst. Part A: Civ. Eng.* 1 (2): 04015004. <https://doi.org/10.1061/AJRUA6.0000818>.
- Yanev, B. 1994. “User costs in a bridge management system.” *Transp. Res. Circ.* 423 (Apr): 130–138.
- Yuan, Y., W. Han, T. Guo, X. Chen, and Q. Xie. 2020. “Establishment and updating of nonstationary resistance deterioration model of existing concrete bridge component.” *J. Perform. Constr. Facil.* 34 (6): 04020104. [https://doi.org/10.1061/\(ASCE\)CF.1943-5509.0001517](https://doi.org/10.1061/(ASCE)CF.1943-5509.0001517).
- Zadeh, L. A. 1965. “Fuzzy sets.” *Inf. Control* 8 (3): 338–353. [https://doi.org/10.1016/S0019-9958\(65\)90241-X](https://doi.org/10.1016/S0019-9958(65)90241-X).
- Zhang, W., and N. Wang. 2017. “Bridge network maintenance prioritization under budget constraint.” *Struct. Saf.* 67 (Jul): 96–104. <https://doi.org/10.1016/j.strusafe.2017.05.001>.
- Zhang, W.-H., D.-G. Lu, J. Qin, S. Thöns, and M. Havbro Faber. 2021. “Value of

information analysis in civil and infrastructure engineering: A review.” J. Infrastruct. Preserv. Resilience 3 (1): 1–21. <https://doi.org/10.1186/s43065-021-00047-w>.

4. Parameterized Models for Prediction of Lifetime Bearing Demands

Reprinted with permission from Journal of Engineering Structures, Elsevier

Abdelmaksoud, Ahmed M., Minesh K. Patel, Tracy C. Becker, and Georgios P. Balomenos. "Parameterized models for prediction of lifetime bearing demands." *Engineering Structures* 252 (2022): 113649.

4.1. Abstract

A good replacement and maintenance policy for bridge bearings is essential for bridge integrity and functionality. This requires proper estimation of the bearing life expectancy which in turn is dependent on the working condition demands. The lifetime travel and peak displacement demands are highly sensitive to the loading, bridge geometry, and bearing properties. Hence, predicting when bearings should be replaced is difficult. To facilitate the decision making process, this study proposes prediction models for the annual demands of elastomeric bearings. First, random bridge configurations (e.g. elements geometry, deck type, and number of spans) and random loading conditions (e.g. temperature profiles, earthquake records, and traffic loading scenarios) are generated using Monte Carlo simulation, combined with Latin hypercube sampling, and the bearing demands are computed. Bearing demand prediction models are then developed via regression analysis and used to create a general fatigue loading protocol. This protocol can be used for testing and rating sample bearings. This would aid in predicting the bearing life expectancy, allowing for better replacement scheduling, and budget estimation. The application of the proposed demand prediction models for generating fatigue loading protocols is demonstrated through a case study bridge.

Keywords: Bridge bearings, Elastomeric bearings, Bearing demands, Parametric demand models, Fatigue loading protocol, Bearing life expectancy

4.2. Introduction

Bridge bearings are vital load transferring components which accommodate the longitudinal and rotational deformations of the superstructure resulting from loads, such as temperature fluctuations, traffic, and seismic events. In this way, the bearings reduce design forces throughout the structure. While bridge bearings are widely used, there is still minimal information available on their performance lifespan and behavior. Such lack of information not only adds uncertainty to bridge maintenance, but it can also lead to potential structural damages. One example is the Birmingham Bridge in Pennsylvania which suffered \$8 million worth of damages when the undetected deterioration of its rocker bearings led to the partial collapse of the deck [1]. Also, a large scale investigation of the performance of elastomeric bearings of concrete bridges in Maryland, US revealed that aging elastomeric bearings are more susceptible to noticeable fatigue deterioration which may lead to structural damage [2]. Therefore, a good management policy for bearing maintenance and replacement can help mitigate damage or failure. However, current design codes, such as the *Canadian Highway Bridge Design Code* (CHBDC) [3] and *AASHTO LRFD Bridge Design Specification* C14.8.1 [4] provide limited guidance regarding replacement criteria or timing, leaving replacement decisions to be primarily based on engineering judgement and visual inspections.

To understand the bearing life expectancy, the lifetime demands must be well estimated. Bearings experience small displacements from daily loads, such as

temperature fluctuation and traffic, and larger displacements from extreme loads, such as earthquakes. Although small displacement cycles may not be critical individually, their accumulation over time can lead to fatigue and reduced bearing performance [5],[6]. Roeder et al. [7] observed that elastomeric bearing damage can be also observed at moderate displacement cycles given a large cycle count. Hence, capturing the lifetime displacements is as critical as capturing extreme displacements when predicting the bearing life expectancy. Most standard bearing testing procedures listed in design codes, such as CHBDC [3] and AASHTO [4], are mainly directed towards evaluating the bearing material. The loading protocols in such tests are not representative of the lifetime loading, hence, the bearing on-site behavior and life expectancy are not properly assessed in these tests.

Roeder et al. [7] experimentally investigated the parameters affecting the fatigue of laminated elastomeric bearings and developed fatigue loading protocol under cyclic compression and shear. However, the developed loading protocol does not reflect the amplitude-variant cyclic loading pattern experienced in practice. Furthermore, the experimental program was directed towards assessing the impact of loading and bearing parameters while ignoring other factors such as bridge geometry and bridge aging. The impact of bridge geometry on bearing demands was highlighted by Aria and Akbari [8] based on the results of a wide scale bridge inspection campaign in Iran. Ala et al. [9] proposed prediction equations for the service life of sliding bearings through experimental research on the wearing rate of the sliding surface material when subjected to temperature and traffic loading.

Recently, Noade and Becker [10] proposed a framework for determining

lifetime demands of elastomeric bearings. They estimated the attributes of the on-site bearing displacement cycles (e.g. mean, amplitudes, no. of occurrence, etc.) based on elastic analysis of an existing three span concrete girder bridge subjected to temperature, traffic, and seismic loading. With this information, they proposed a loading protocol representative of the bearing lifetime loading. However, the proposed protocol is tailored to a single bridge and, thus, does not provide information on the demands for bridges with different design parameters or loading conditions. Thus, the current study generalizes the framework to be applicable for various bridge configurations (e.g., geometry of pier, deck, superstructure, construction materials, etc.) and bearing properties (e.g. vertical and horizontal stiffness), while incorporating uncertainties in material properties and aging of the bridge deck and piers. First, Monte Carlo simulation, combined with Latin hypercube sampling, is used to generate random bridge configurations and loading conditions. The demands are evaluated through nonlinear OpenSees models and then related to the loading condition, bridge configuration, and bearing properties via regression analysis. Based on the predicted demands, a general fatigue loading protocol is proposed which can be used for testing and rating sample bearings. This protocol can aid in predicting the bearing life expectancy, and allow for economic replacement scheduling.

4.3. Bridge Design and Modelling

4.3.1. Bridge Design Parameters

The original bridge configuration utilized by Noade and Becker [10] was that of the Chemin des Dalles Bridge located in Trois Rivières, Quebec City. The superstructure consists of three 35.5 m long spans with a 0.165 m thick reinforced concrete slab deck, and six AASHTO V-Type precast prestressed concrete girders of depth 1.6 m and

spaced at 2.2 m from each other. The substructure consists of two piers, each with three 0.9 m diameter circular reinforced concrete columns connected by a bent beam. All dimensions and section properties are specified in Roy et al. [11] and Tavares et al. [12]. Laminated elastomeric bearings are located at the abutments and piers, with one directly below each of the six precast girders. However, only those at the abutments are horizontally unrestricted while the remainder are horizontally restricted, as shown in Fig. 4.1.

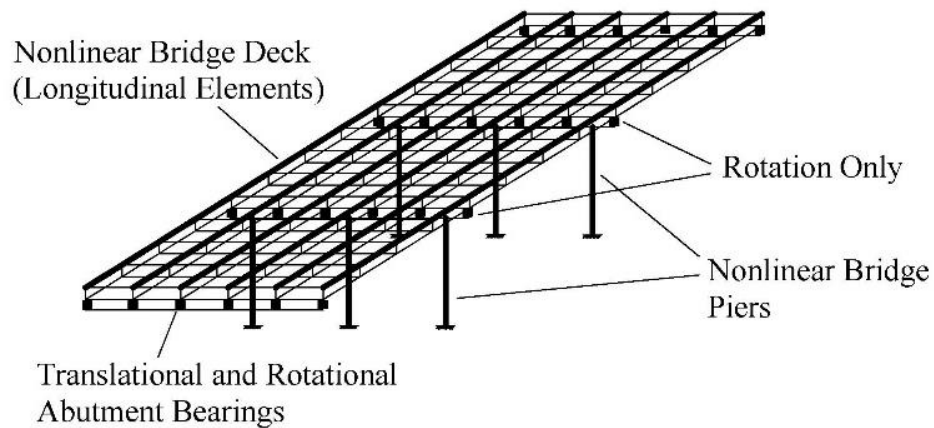


Fig. 4.1 Nonlinear OpenSees model

The current study uses the same bridge configuration for the validation of the bridge model. However, this study investigates also five more commonly found bridge configurations, varying the number of spans and construction material. Two-span and single-span bridges based on the initial three span Chemin des Dalles model, shown with the bearing fixities in Fig. 4.2, are investigated to explore the impact of variation in the number of bridge spans on the bearing demands. A second deck construction material, slab on steel girders, is also examined with single, two, and three spans. For each bridge configuration, the bearings' properties are selected based on their governing longitudinal design displacements which are controlled by the local

temperature variations. The steel girder bridges have higher design displacements compared to the concrete girder bridges because of the higher coefficient of thermal expansion. In addition, the three span configuration for both steel and concrete girder bridges has higher design displacements due to a larger expansion length than the two or one span.

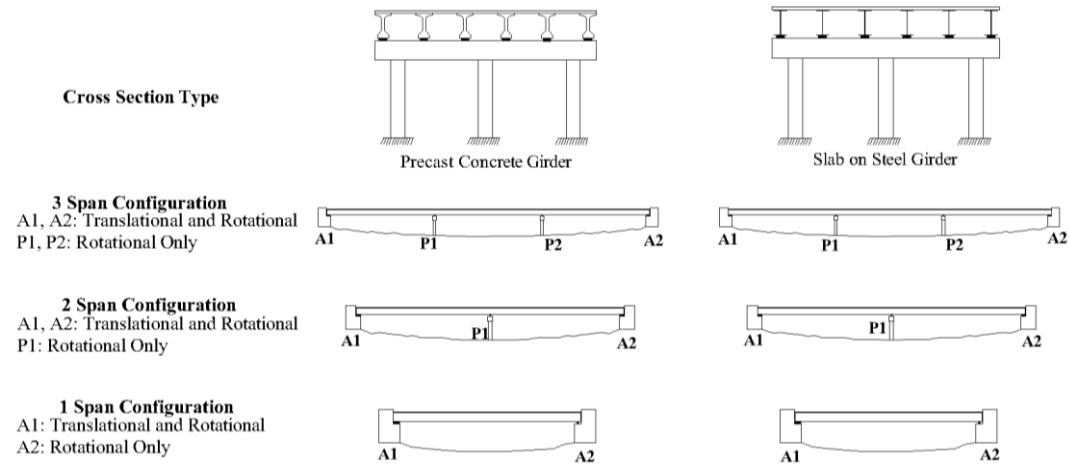


Fig. 4.2 Bridge deck and span variation models

A parametric study is conducted using Monte Carlo simulations combined with Latin hypercube sampling [13] to understand how the bridge design parameters (Table 4.1) affect the bearing demands for each of the six bridge configurations. The investigated parameters include bridge geometric features, such as depth-to-span ratio and width-to-span ratio, whose values are assumed to be uniformly distributed within the ranges in Table 4.1. The ranges are taken from similar configurations in bridge inventories, such as that of the Ontario Bridge Management System, as described in Balomenos et al. [14]. The depth of the concrete girders and steel girders are kept constant at the initial design depths of 1.6 m and 1 m, respectively. The spans are then varied from 30 to 40 m to achieve the depth-to-span ratio range in Table 4.1. The girder

spacing is varied from 1 m to 2.7 m and the deck thickness is varied from 0.15 to 0.18 m to generate random width-to-span ratios and deck stiffness properties. All configurations have three columns per bent with a constant diameter of 0.9 m and a height varying from 3 to 7 m to examine various inertia-to-height ratios for the pier bents.

Table 4.1. Distribution of bridge design parameters

Parameter	Distribution	Value Range
Depth-to-span ratio	Uniform	0.029 – 0.059
Width-to-span ratio	Uniform	0.15 – 0.54
Girder spacing	Uniform	1 – 2.7 m
Deck thickness	Uniform	0.15 – 0.18 m
Inertia-to-height ratio of a single bent	Uniform	0.0138 – 0.0322 m ³
Young's modulus of concrete (E_c)	Normal	$\mu=26100$ MPa, cov = 10%

To include uncertainties in construction material properties, a normal distribution was assumed for the Young's modulus of concrete (E_c) with the same mean value reported by Tavares et al. [12], and a coefficient of variation (cov) of 10%. Finally, the bridge bearing's dimensions, vertical, and horizontal stiffness properties ($k_{v \text{ bearing}}$ and $k_{h \text{ bearing}}$) are chosen based on the longitudinal design temperature demands in each simulation.

4.3.2. Bridge Modelling Elements

The bridge configurations are modelled in OpenSees [15] using the grillage model [16] shown in Fig. 4.1. The bridge deck is modelled as a grillage to be able to account for multi-lane vehicle loading. Stiffness losses of the bridge elements with aging combined with earthquake loading can cause the bridge to undergo larger displacements and nonlinear behavior. To model this stiffness reduction and potential nonlinear behavior,

the piers and the slab deck are modelled using nonlinear fibre elements for all of the investigated bridge configurations.

The laminated bridge bearings are modelled using zero length elements where the bearings' rotational stiffness properties are determined following the analytical formula for multilayer rubber bearings with rectangular cross sections [17]. The stiffness in the vertical direction is modelled as a linear spring. To match the on-site measured periods [11] and to represent the slight nonlinear shear behavior experienced by the bearings located at the abutments, a bilinear model with low yield strength is used in the horizontal direction. Pin connections are located between the superstructure and the bents which allow only rotation about the out of plane axis. The first mode period of the modelled original bridge configuration is 0.43 sec in the transverse direction which is a close match to the results reported by Tavares et al. [12].

4.3.3. Bridge Aging

With age, bridges are susceptible to corrosion due to deicing salts or atmospheric conditions which may reduce the stiffness properties over time [18]; potentially affecting the bearing demands. Thus, this study accounts for the corrosion in deck, piers, and steel girders. However, corrosion in precast prestressed beams is neglected given their uncracked sections and their higher fabrication quality compared to conventional reinforced concrete elements [19],[20]. Given that corrosion propagation is time variant, the bridge age is used to indicate the degree of corrosion. The age is assumed to be uniformly distributed within zero to 100 years when conducting the simulations. Then, the corrosion degree corresponding to the selected age in each simulation is estimated from the following corrosion models.

4.3.3.1. Concrete Corrosion Models

For bridge deck, the study adopts the following corrosion initiation model [21],[22] to calculate the time to corrosion initiation (T_{corr}) assuming a uniform rebar corrosion [23]

$$T_{corr} = \frac{d^2}{4D} \frac{1}{\left[erf^{-1}\left(1 - \frac{C_{cr}}{C_s}\right)\right]^2} \quad (1)$$

where d is the depth of cover, C_{cr} is the critical chloride concentration, C_s is the chloride concentration at concrete surface, $erf(.)$ is the error function, and D is the diffusion coefficient. For the current study, C_{cr} is assumed to be 5.818 N/m^3 , whereas C_s and D are assumed to be uniformly distributed within $23.27 - 69.82 \text{ N/m}^3$ and $39.5 - 131.6 \text{ mm}^2/\text{yr}$ respectively [22]. The cover depth is also assumed to be uniformly distributed within $45 - 55 \text{ mm}$ [3].

For concrete piers, a modified version of Eq. (1) was proposed by DuraCrete [24]

$$T_{corr} = X_1 \left[\frac{d^2}{4k_e k_t k_c D_0 (t_0)^n} \left[erf^{-1}\left(1 - \frac{C_{cr}}{C_s}\right)\right]^{-2} \right]^{1/(1-n)} \quad (2)$$

where X_1 is a model uncertainty coefficient, k_e , k_t , and k_c are factors related to environment, assessment methods of diffusion, and concrete curing respectively, D_0 and t_0 are the empirical diffusion coefficient and reference period to diffusion respectively, and n is an age factor. All factors are treated as discrete variables based on their mean values from DuraCrete [24].

The time variant diameter of corroded reinforcement in decks and piers can then be determined using the following corrosion propagation model [25]

$$d_b(t, T_{\text{corr}}) \begin{cases} d_{bi} & t \leq T_{\text{corr}} \\ d_{bi} - \frac{1.0508 \left(1 - \frac{w}{c}\right)^{-1.64}}{d} (t - T_{\text{corr}})^{0.71} & t > T_{\text{corr}} \end{cases} \quad (3)$$

where $d_b(t, T_{\text{corr}})$ is the reduced bar diameter at time t , d_{bi} is the initial bar diameter, and w/c is the water-cement ratio. The w/c ratio is treated as a uniformly distributed variable within the range 0.4 - 0.5 [3],[26]. Finally, the effect of cover spalling and cracking associated with corrosion is incorporated by reducing the unconfined strength of the concrete cover [27].

4.3.3.2. Steel Corrosion Model

Steel girders are assumed to uniformly corrode using the following power law [28],[29]

$$C(t) = At^B \quad (4)$$

where $C(t)$ is the average corrosion penetration. A and B are environment and steel type parameters which are treated as normal variates with parameters values corresponding to urban environment ($\mu_A = 80.2 \cdot 10^{-6}$ m, $\sigma_A = 0.42 \cdot 10^{-6}$ m) and carbon steel girders ($\mu_B = 0.59$, $\sigma_B = 0.4$) [29]. Carbon steel is assumed as it is more affected by corrosion than weathering steel.

4.4. Bridge Loading

This study examines the three primary loads (i.e. temperature, traffic, and seismic loading) used by Noade and Becker [10]. However, for the temperature loading this study investigates the effect of vertical temperature gradients on the bearing demands in addition to the uniform thermal expansion and contraction of the bridge investigated by Noade and Becker [10]. For the traffic loading, this study proposes a general approach to simulate any possible traffic loading scenarios. Finally, for the earthquake

loading this study investigates several earthquake types to examine how the bearing demands are affected by the earthquake properties.

4.4.1. Temperature Loading

Daily fluctuations in bridge temperature cause the bridge deck to uniformly expand and contract resulting in bearing displacement in the longitudinal direction. Measurement of the bridge temperature requires extensive instrumentation, hence, several simplified methods have been proposed to estimate the bridge temperature from air temperature records at meteorological stations [30],[31],[32]. This study adopts the Emerson method [30] as it is more suited for estimating the daily bridge temperature fluctuation [33] and it is applicable for both concrete and steel girder bridges with concrete decks. This method predicts the minimum daily bridge temperature from the average air temperature in the previous 48 hours for concrete bridges and 24 hours for steel girder bridges with concrete decks. To find the maximum daily bridge temperature, a range is added to the minimum daily temperature, dependent on the type of bridge, season, and cloud cover as shown in Table 4.2.

Table 4.2. Bridge temperature ranges taken from [30]

	Concrete girder bridge			Steel girder bridge with concrete deck		
	Cloudy	Partial	Clear	Cloudy	Partial	Clear
Winter	< 2 C	2 – 4 C	4 C	< 4 C	4 – 8 C	8 C
Spring/Autumn	< 2.5 C	2.5 – 5 C	5 C	< 6 C	6 – 12 C	12 C
Summer	< 3 C	3 – 6 C	6 C	< 7 C	7 – 14 C	14 C

The air temperature data are obtained from over 1,000 meteorological stations across Canada [34]. Table 4.3 and Fig. 4.3a show a sample annual temperature profile from a meteorological station in Quebec. The temperature profile is defined based on monthly averages of daily maximum and minimum temperatures (T_{\max} and T_{\min}) and monthly standard deviations. By analyzing the statistical distribution of these values

and their correlations, a random annual air temperature profile is generated for each simulation. The percentage of days in cloudy, partial cloudy, or clear conditions are randomly assumed and then the air temperature profile is converted to an annual bridge temperature profile as shown in shown in Fig. 4.3b. Finally, the annual bearing longitudinal displacement history due to uniform temperature variation is evaluated.

Table 4.3. Meteorological data for the “JEAN LESAGE INTL A” station in Quebec

Month	Jan	Feb	Mar	Apr	May	Jun	July	Aug	Sep	Oct	Nov	Dec
Aver. T_{\max}	-7.9	-5.6	0.2	8.3	17	22.3	25	23.6	17.9	11.1	2.9	-4.2
Aver. T_{\min}	-17.7	-15.6	-9.4	-1	5.4	10.5	13.5	12.5	7.5	2	-4.2	-12.8
σ	3.2	2.9	1.9	1.5	1.1	1.1	1.1	1.3	1.2	1.4	1.5	3.0

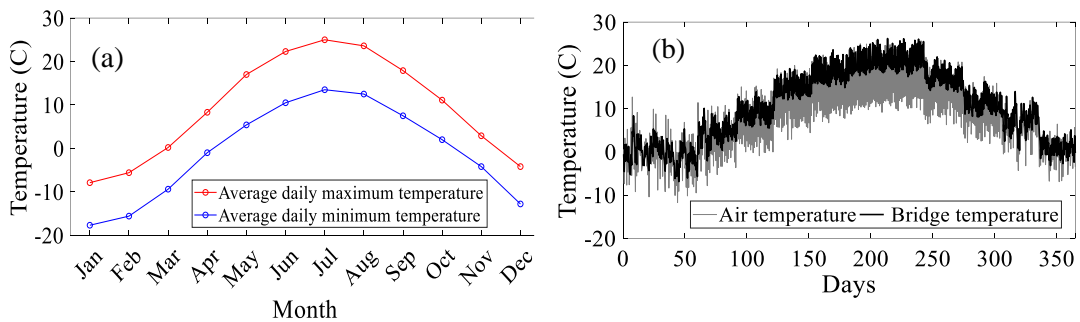


Fig. 4.3 (a) Air temperature data from the “JEAN LESAGE INTL A” station in Quebec and (b) random annual air temperature and bridge temperature profiles for a concrete bridge.

Aside from the uniform expansion or contraction of the bridge deck, additional bearing displacements can occur due to the vertical thermal gradients over the deck depth. For example, when the top surface of the deck is warmer than the soffit, there is a positive thermal gradient. The temperature differential ΔT between the top surface of the deck and deck soffit results in a bending moment in the deck calculated as

$$M = \frac{EI\alpha\Delta T}{h} \quad (5)$$

where EI is the bending rigidity of the superstructure, α is the coefficient of thermal expansion, ΔT is the temperature differential, and h is the superstructure depth. The

resulting moment causes additional longitudinal displacement in the bearings.

Many design codes and standards provide design temperature differential profiles for the bridge deck. For example, given the depth of the deck of the original Chemin des Dalles Bridge configuration, CSA S6-19 (CSA 2019) gives a 10°C summer positive and 5°C winter positive or negative temperature differential (Fig. 4.4a). For bridges with steel systems and concrete decks, CSA S6-19 (CSA 2019) only considers positive temperature differentials and only in the reinforcing slab. Nevertheless, significant uncertainty still remains in the actual temperature differentials experienced by a bridge in practice. Hedegaard et al. (Hedegaard, French, and Shield 2013) measured the on-site temperature differentials for a concrete bridge over the course of three years and concluded that the temperature differentials can vary significantly depending on the climate, material properties, and the shape of deck cross section. Kennedy and Soliman (Kennedy and Soliman 1987) reached a similar conclusion regarding the slab on steel girder bridges and proposed temperature differentials for the Middle Atlantic States and Southern Ontario as shown in Fig. 4.4b. The positive differential values were given as 22.2°C during the summer and 11.1°C during winter, with a 4.2°C negative differential to occur over the year as shown in Fig. 4.4b.

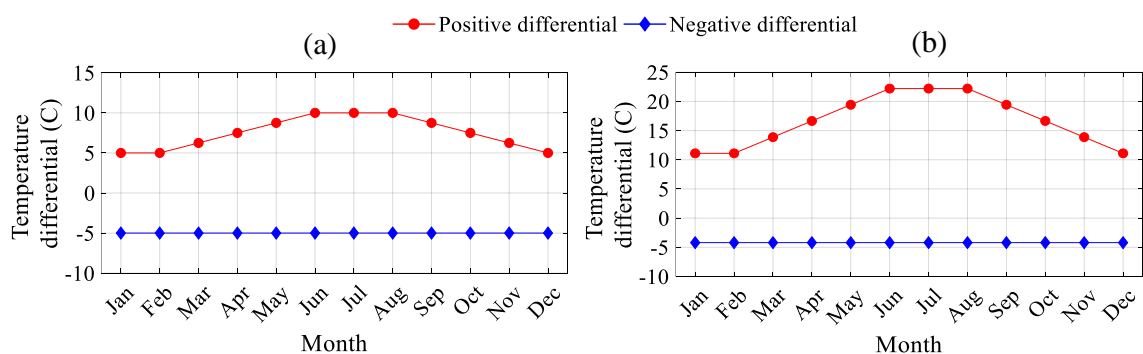


Fig. 4.4 Average differential temperature profile for (a) concrete girder bridges and (b) concrete slab on steel girder bridges

Considering that the temperature differential is uncertain and may exceed the design code limits, the value of ΔT for each month is assumed as a random variable with a mean centred around the values shown in Fig. 4.4 and with a coefficient of variation of 10% [37]. From this a random annual temperature differential profile is generated for each simulation. Then using Eq. (5), an annual moment loading profile is generated and applied to the OpenSees model to find the annual bearing displacement demands from temperature differential. Considering that the maximum positive and negative differentials are expected to occur during the warmest (T_{\max}) and coolest (T_{\min}) daily temperatures. Then, the extreme daily bearing displacements from temperature differentials are concurrent with their counterparts from uniform temperature variation. Hence, the total bearing longitudinal displacement history can be evaluated as the summation of those from the uniform temperature variation and temperature differential.

4.4.2. Traffic Loading

Similar to Noade and Becker [10], only multiunit trucks are considered for the traffic loading. To estimate the bearing demands, it is required to identify the truck type, truck traffic volume, and the number of trucks that could be present simultaneously on a bridge (i.e. truck scenario). This study uses the CL-625 truck load type [3], i.e., the heaviest vehicle loading in Canadian standards. A truck traffic volume of 610 trucks/day/direction [10] is used as an example; however, in practice the volume can be estimated from traffic analysis. A bridge could experience several traffic loading scenarios depending on factors such as the bridge length and the number of traffic lanes. Therefore, the current study proposes a general methodology that gives the flexibility

to compute the bearing traffic demands given any possible truck scenario. For example, consider the bridge configuration shown in Fig. 4.5a where a single wheel axle is moving along a loading line located at a distance x from the edge of the deck. At any given time instant, the bearings experience the horizontal and vertical displacement profiles shown in Fig. 4.5a. The maximum displacement that a bearing can experience, whether in the horizontal or vertical direction, occurs when the bearing is directly beneath the loading line. In the current work, the bearing displacement profiles are normalized so that the displacement demand of a specific bearing i , caused by a single wheel axle j , is expressed as a percentage (p_{ij}) of the maximum bearing displacement as shown in Fig. 4.5b.

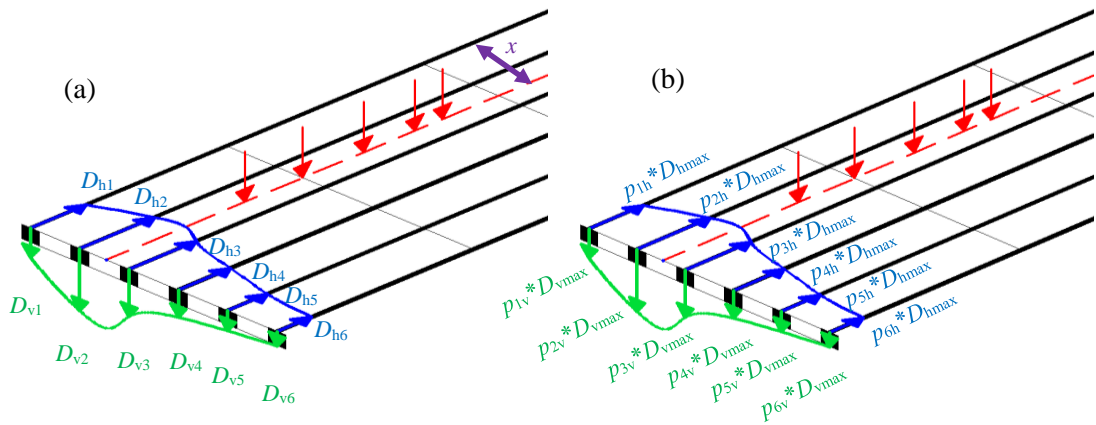


Fig. 4.5 (a) Bearing displacement profiles and (b) normalized bearing displacement profiles at a given time instant.

The bearing displacement demands due to a given truck scenario can then be computed by superposition of the effects of all wheel axles. Thus, the displacement demand of a specific bearing i can be expressed as

$$\text{Displacement of bearing } i = \sum_{j=1}^{j=m} p_{ij} * \text{maximum bearing displacement} \quad (6)$$

where m is the number of wheel axles in the considered loading scenario. The value of p_{ij} is dependent on the deck's geometry in addition to the distance between the bearing i and the loading line of wheel axle j in the direction of the bridge width. The maximum bearing displacement demand can be also estimated given the superstructure type and geometry.

Bridge deck can also experience horizontal braking force frequently if the bridge is on or near a highway entrance or exit ramp. This force can induce significant bearing displacements in the longitudinal direction. To account for this force, an impact factor (IF) is used to amplify the displacement computed from Eq. (6). The truck is assumed to start braking at a random location on the bridge with a random deceleration (a), and then the horizontal force is computed as $m_{truck} * a$ where m_{truck} is the truck mass. Given a random initial velocity (V_o), the braking distance, during which the horizontal force is applied, is computed. Next, the IF is computed as the ratio of the bearing displacement in braking and no-braking scenarios. Finally, the IF is related to the braking force parameters (i.e. a and V_o) and the deck's geometry. The parameters a and V_o are assumed to be uniformly distributed within 0.25g-0.75g and 50-100 km/hr, respectively [4],[38],[39].

4.4.3. Seismic Loading

To evaluate the bearing displacement demands from seismic loading, several earthquake types are used. Fifty-nine eastern seismic records and 55 shallow crustal seismic records were selected from the Pacific Earthquake Engineering Research Center (PEER) strong motion database [40] based on the seismic hazard deaggregation values of several eastern and western Canadian cities reported by Halchuk et al. [41]

for the 2% probability of exceedance in 50 years. Similarly, 46 subduction records from the Cascadia zone were chosen for the analysis from the NGA-Subduction database [42]. A single three-component ground motion is selected and scaled for each simulation run in the Monte Carlo analysis for each earthquake type.

The eastern and shallow crustal records were scaled to cover the expected range of design spectra in the eastern and western zones of Canada, respectively [43], with the assumption that the bridges are on site Class C, very dense soil or soft rock. The records were scaled from 0.2 times the minimum first mode period from all possible bridge configurations to 1.5 s as required in the commentary of CHBDC [38]. The subduction records were scaled to match the expected range of design spectra of several Canadian cities in the Cascadia zone [43]. Given that the Cascadia subduction events mostly dominate at a larger period range [41], the records were scaled from 0.5 s to 1.5 s. The bearing demands are evaluated through dynamic analysis, and then related to the pseudo accelerations for the periods 0.2 s and 1 sec and bridge geometry.

4.5. Bearing Demands

Monte Carlo simulations are conducted to quantify the longitudinal bearing demands due to temperature, traffic, and seismic loading. These demands are then related to the loading condition and bridge design parameters through regression prediction models which are used to develop a general loading protocol. The focus of this paper will be on the longitudinal, rather than the transverse, bearing demands as it was shown by a preliminary analysis that the former significantly exceeds the latter for the examined bridge configurations.

Monte Carlo simulation requires a sufficient number of simulations to produce

a reliable model; thus, sensitivity analysis is conducted using the original bridge configuration. A training to validation simulation ratio of 4 to 1 was used for the sensitivity analysis and validating the prediction models.

Despite the widespread application of regression techniques in the engineering field, such as multiple linear regression [44], dynamic linear regression [45,46], and nonlinear regression [47], most of these techniques require a predefined form for the demand prediction models. The choice of the most appropriate form for the demand prediction models is an iterative and time consuming process. To address this, the study adopts tree-based regression analysis in which the demand is related to different combinations (i.e. trees) of the regression variables. All trees are tested and the optimum one is defined as that balancing the goodness-of-fit and complexity. Many methodologies were proposed to develop tree-based regression models such as CART [48], RETIS [49], M5 [50], random forest [51,52], and genetic programming [53,54]. This study uses genetic programming with the GPTIPS2 toolbox in Matlab [54]. The main advantage of GPTIPS2 is its ability to quickly generate and test multiple iteration models with various degrees of complexity starting from a simple linear to highly nonlinear models. The goodness-of-fit versus the complexity of the tested models result in Pareto fronts, from which, a model is chosen to balance the goodness-of-fit and complexity. To further facilitate reaching an explicit form for the prediction models, GPTIPS2 can be also fed with any previously known relationships (e.g. linear, exponential, power, etc.) between the dependant and regression variables.

4.5.1. Temperature Demands

For each simulation, the annual bearing displacement history due to the uniform

temperature variation and the temperature differential is evaluated as shown in Fig. 4.6. Then the annual cumulative displacement demand of the bearing (CDDT) is related to the loading and bridge parameters. The data used for the regression analysis is from 150 simulations for each bridge configuration. This number of simulations was determined from the sensitivity analysis results shown in Fig. 4.7. The ratio of the root mean squared error to the demand mean (normalized RMSE) fluctuates with increasing simulations until it plateaus at roughly 10%.

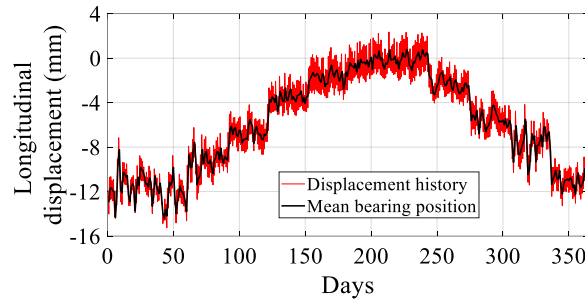


Fig. 4.6 Total longitudinal displacement history of bearings

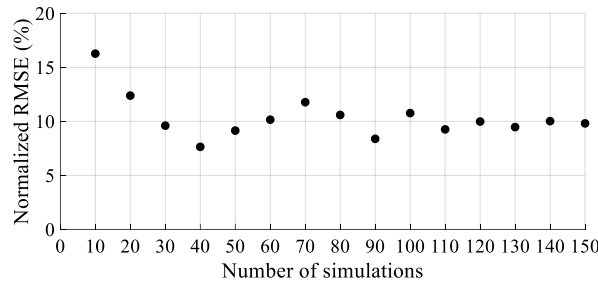


Fig. 4.7 Normalized RMSE vs. number of simulations for the temperature loading

Genetic programming is then used to find the best form for the CDD_T prediction model using the GPTIPS2 program [54]. The CDD_T model is expressed as

$$CDD_T = -1.5 - 12.85 * P_{\text{cloudy}} + 7.21 * P_{\text{clear}} + 29.51 * \frac{MF_u * L}{N_{\text{UBS}}} + 10.96 * \frac{M * N_s^{0.1}}{N_{\text{UBS}}^3 * k_{\text{h bearing}}^{0.1} * MF_d} \quad (7)$$

where CDD_T is in mm, P_{cloudy} and P_{clear} are the percentage of days with cloudy and clear weather, respectively, N_{UBS} is the number of horizontally unrestricted bearing supports, L is the bridge length (m), M is the end moment caused by the yearly average temperature differential fluctuation (kN.m) and is equal to $(\alpha_{girder}E_{girder}I/h)*(\Delta T_{pos} - \Delta T_{neg})_{average}$ where α_{girder} and E_{girder} are the girder's coefficient of thermal expansion and Young's modulus (kN/m²), respectively, I is the moment inertia of one girder plus the portion of the deck between the mid-points of girder spacing (m⁴), h is the height of the girder plus deck (m), N_s is the number of spans, and $k_{h\ bearing}$ is the horizontal bearing stiffness (kN/m). MF_u and MF_d are material factors related to the uniform temperature variation and temperature differential, respectively. For concrete girders, $MF_u = 1$ and $MF_d = 1$, whereas for steel girders, $MF_u = 3$ and $MF_d = 2.85$. These factors are calibrated to maximize the goodness-of-fit of the CDD_T model. Within the genetic programming, the complexity of the tested prediction models is computed from their tree representations. For example, the CDD_T model (i.e. Eq. (7)) has a complexity equal to 53 which is the summation of leaves in the tree and all possible sub-trees as shown in Fig. 4.8a. This form balances accuracy and complexity as inferred from the Pareto plots (Fig. 4.8b).

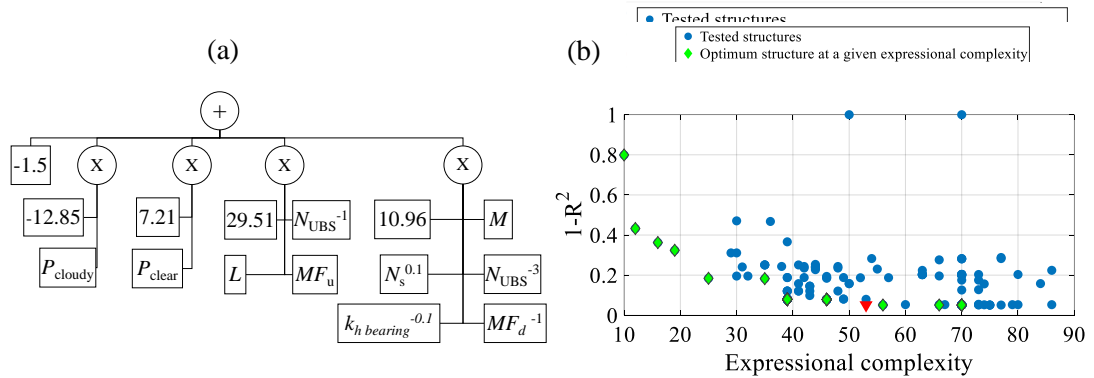


Fig. 4.8 (a) Genome tree representation of the CDD_T model and (b) Pareto optimal plot

Steel girder bridges experience higher bearing displacements from uniform temperature variation compared to concrete girder bridges. This is due to the fact that steel girders have thinner sections, lower thermal mass, and larger coefficient of thermal expansion compared to concrete girders. This demand component is also dependent on the bridge length, the number of unrestricted end supports, and the cloud cover.

For the temperature differential component, Fig. 4.9 shows its variation with the loading magnitude (end moment) for the investigated bridge configurations. Given that steel girders have more slender sections in comparison to concrete girders, they experience lower end moments and displacements from temperature differentials. For one span bridges, the displacements from temperature differential far exceed that of the two and three spans bridges. This is attributed to the lack of span continuity which makes the superstructure more flexible, increasing the end rotation of the superstructure and the accompanied longitudinal bearing displacements. For all bridge configurations, the demands are not time sensitive (i.e. not affected by bridge aging) given the limited corrosion-induced stiffness losses of the superstructure elements (deck and steel girder).

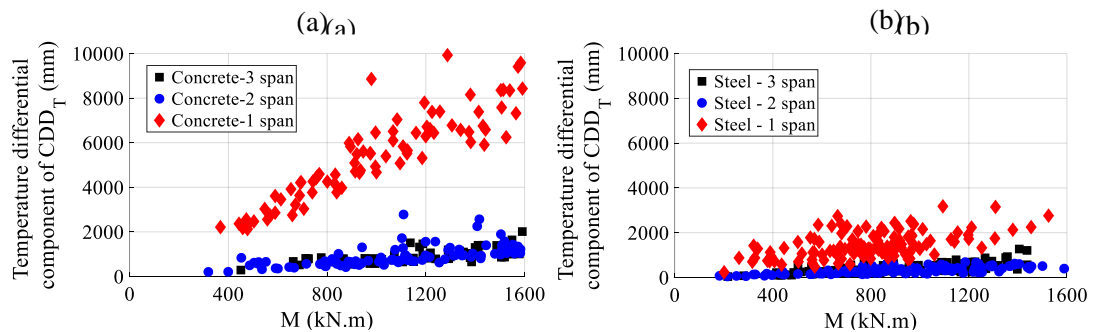


Fig. 4.9 Temperature differential component of CDD_T for bridges with (a) concrete girders and (b) steel girders.

Based on the predicted annual cumulative demands, the study estimates the average bearing displacement amplitude about the mean position (i.e. black line in Fig. 4.6) and uses it as a reference amplitude ($A_{ref T}$). Assuming that the bearing undergoes one displacement loading cycle per day about its mean position, $A_{ref T}$ is computed as CDD_T divided by 365 days and then divided by four, which is then used for the calibration of the proposed loading protocol as follows. First, based on the bearing displacement histories (Fig. 4.6), the bearing displacements relative to the mean bearing position are derived as shown in Fig. 4.10a. Then, the relative displacements are normalized using $A_{ref T}$ as shown in Fig. 4.10b. Afterwards, the distribution of the normalized cycle amplitudes is established as shown in Fig. 4.10c. The cycle amplitudes due to temperature loading follow a normal distribution, with mean and standard deviation as described below, but not less than zero; hence, the cycle count N for a given amplitude range x_1 to x_2 can be expressed as

$$N_{x_1-x_2} = \frac{\Phi \left[\frac{x_2 - \mu}{\sigma} \right] - \Phi \left[\frac{x_1 - \mu}{\sigma} \right]}{1 - \Phi \left[\frac{-\mu}{\sigma} \right]} * N_{annual} \quad (8)$$

where μ is equal to 100% of $A_{ref T}$, N_{annual} is the number of annual cycles which is 365, and σ is estimated as

$$\sigma = \left(\sqrt{-18479 + 5613 * MF_{\sigma} + 1624 * N_s^{-3}} \right) \% * A_{ref T} \quad (9)$$

where MF_{σ} is a material factor, calibrated to maximize the goodness-of-fit, equal to 3.6 for concrete and 3.5 steel girder.

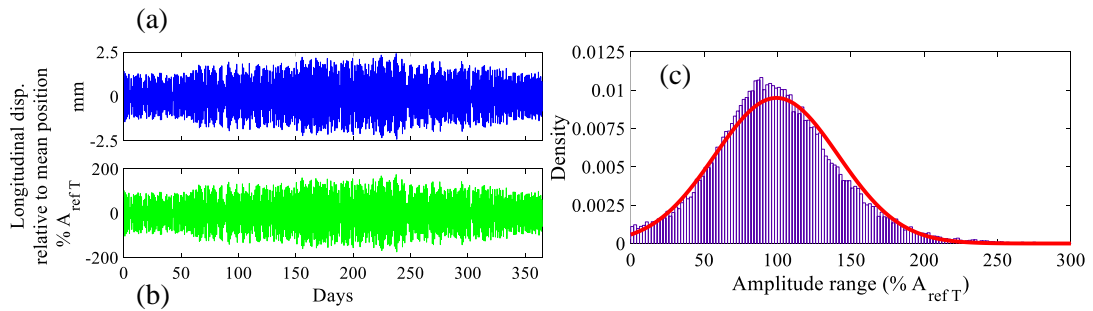


Fig. 4.10 (a) Bearing displacement history relative to the mean bearing position (mm), (b) bearing displacement history relative to the mean bearing position (normalized by the $A_{ref T}$), and (c) distribution of the normalized temperature cycle amplitudes

4.5.2. Traffic Demands

For each simulation, the analysis is conducted once with no-braking scenario and another with a braking scenario. For the no-braking scenarios, the loading line of a single axle of a CL-625 truck is positioned (a) directly over a line of bearings to find maximum displacement demands, and (b) at a random position across the width of the deck to find the displacements of all bearings along the width. The first loading line and the resulting bearing longitudinal displacements are shown in Fig. 4.11.

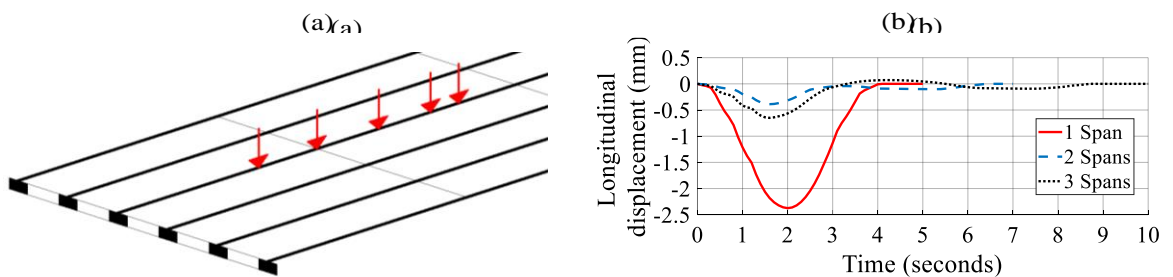


Fig. 4.11 (a) Loading line of a single axle of a CL-625 truck in alignment with a bearing and (b) longitudinal displacement history of the bearing directly below the loading line (no-braking).

Based on the displacement histories, the maximum cumulative displacement demand due to a single axle (CDD_{ho}) directly over the line of bearings is computed and related to the design parameters. Per the results of a sensitivity analysis, 300

simulations per bridge configuration are used for the regression analysis. The GPTIPS2 toolbox [54] is then used to find the form of the CDD_{ho} prediction model as

$$CDD_{ho} = 15.55 - 1.36 * k_{h \text{ bearing}}^{0.1} - 0.19 * k_{deck}^{0.1} + 0.68 * N_s - 3.27 * N_{UBS} - 110 * \left(\frac{h}{S}\right) - 8.17 * \left(\frac{E_{girder}}{10^9}\right) \quad (10)$$

where CDD_{ho} is in mm, k_{deck} is equal to $E_{deck} * (t_{deck}/GS)^3$, E_{deck} and E_{girder} are the Young modulus values (kN/m^2), t_{deck} is the deck thickness (m), GS is the girders spacing (m), h is the height of the girder plus deck (m), and S is the span length (m). For the displacement due to loading at a random position across the deck, the demands are expressed as a percentage p of the CDD_{ho}

$$p = 145.12 - 3.51 * \left(\frac{d_i}{t_{deck}/GS}\right)^{0.6} + 7.74 * N_s - 25.28 * N_{UBS} - 110.52 * \left(\frac{E_{girder}}{10^9}\right) \leq 100\% \quad (11)$$

where d_i is the distance between bearing i and the loading line in the deck width direction.

For the braking scenarios, the loading line is positioned directly over a line of bearings while applying the braking force. The bearing longitudinal displacement is then compared for the no-braking and braking scenarios as shown in Fig. 4.12.

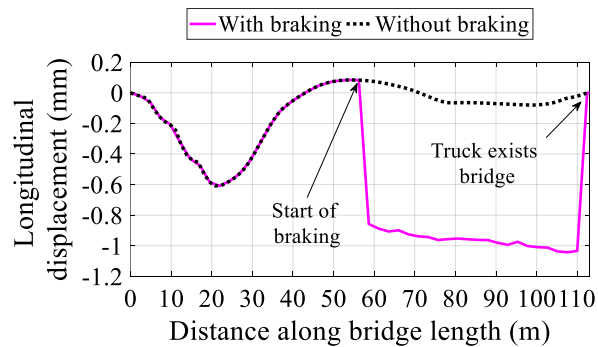


Fig. 4.12 Longitudinal displacement with and without braking on a three span bridge

The impact factor (IF) is then computed as the ratio between the cumulative displacement with and without braking. The IF is evaluated separately for multi- and single-span bridges; for the multi-span bridges

$$IF = 18.14 + 4.13*(a)^2 + 49.9 \left(\frac{h}{S}\right)^{0.9} - 14.1*\left(\frac{k_h \text{ bearing}}{1000}\right)^{0.1} - 1.31*k_{\text{piers}}^{0.1} \geq 1 \quad (12)$$

where a is the deceleration in units of g and k_{piers} is the summation of the stiffness of all the piers (kN/m). For the single-span bridges, IF is equal to 1.5 across all input parameters.

Based on Eq. (10) to (12), the annual cumulative displacement demands due to truck loading (CDD_{Traffic}) for a given loading scenario are expressed as

$$CDD_{\text{Traffic}} = IF * CDD_{\text{ho}} * N_{\text{scenario occurrence}} \sum_{j=1}^{j=m} P_{ij} \quad (13)$$

where IF is the impact factor for the scenario (taken as 1 if braking is not considered), m is the number of wheel axles in the scenario, and $N_{\text{scenario occurrence}}$ is number of times that the scenario occurs per year. For simplicity, the number of scenarios can be assumed to be finite. For example, a two-lane bridge can be assumed to carry either one or two trucks at a given time. As such, four loading scenarios can be considered (two scenarios with braking and two scenarios without braking). For each scenario, $N_{\text{scenario occurrence}}$ can be estimated as

$$N_{\text{scenario occurrence}} = \frac{\ell_{\text{scenario}} * N_{\text{trucks annual}}}{N_{\text{trucks scenario}}} \quad (14)$$

where ℓ_{scenario} is the likelihood of the loading scenario to occur, $N_{\text{trucks annual}}$ is the number of trucks passing the bridge per year, and $N_{\text{trucks scenario}}$ is the number of trucks in the

loading scenario. The values of ℓ_{scenario} , $N_{\text{trucks annual}}$ and, $N_{\text{trucks scenario}}$ are assumed in this study; however, in practice they can be estimated from traffic analysis.

Fig. 4.13 and Fig. 4.14 show how the cumulative displacement demand (CDD_{ho}) is affected by the geometry of the superstructure and the loading line location for each of the investigated bridge configurations. For all configurations, the demands are highly sensitive to the geometry of the superstructure and deck and the distance between the bearings and the loading line (d_i). Configurations with steel girders have higher displacement demands given their slender sections in comparison to concrete girders. Also, the demands in one span configurations far exceed that of the two and three spans configurations. This is attributed to the lack of span continuity which makes the superstructure much more flexible, thus increasing the end rotation of the superstructure and the resulting bearing displacements. For all bridge configurations, the demands are not time sensitive (i.e. not affected by bridge aging) given the limited corrosion-induced stiffness losses of the superstructure elements (deck and steel girder).

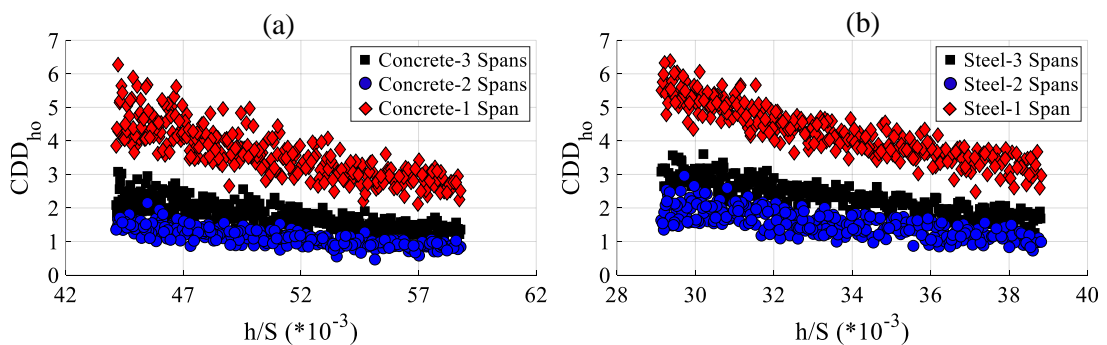


Fig. 4.13 CDD_{ho} vs. depth-to-span ratio for (a) concrete and (b) steel girders configurations

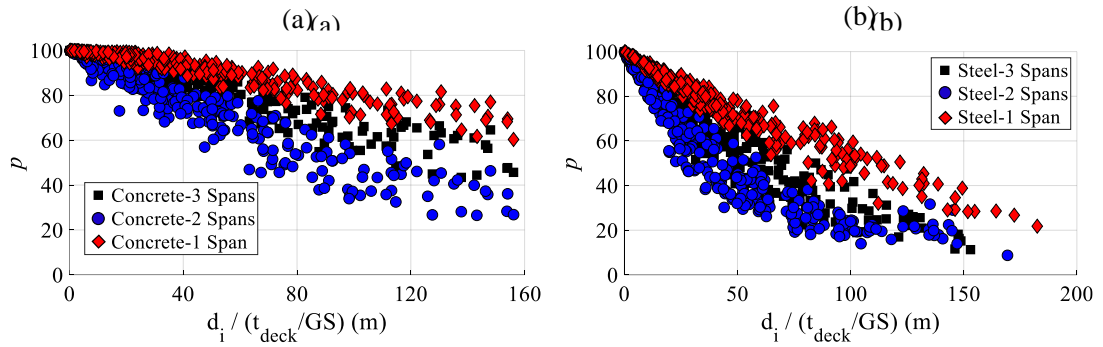


Fig. 4.14 Displacement percentage p for (a) concrete and (b) steel girders configurations

For multi-span bridges, the bearing displacement due to the braking force is dependent on the deceleration, bearing stiffness, pier stiffness, and height-to-span ratio. For the single-span bridges, as one of the two end bearing supports is horizontally restricted, the displacement of the other bearing is mainly dependent on longitudinal stiffness of the superstructure. As such, both types of displacements (i.e. cumulative displacements with or without braking) are correlated to each other and the IF is roughly constant at a value of 1.5.

Based on the predicted annual cumulative demands and assuming that the bearing undergoes one displacement loading cycle per scenario occurrence, the reference bearing displacement amplitude is estimated as

$$A_{\text{ref Tr}} = \frac{\text{CDD}_{\text{traffic}}}{4 * \text{Scenario occurrences}} \quad (15)$$

Then, the displacement histories (Fig. 4.11b) are normalized using $A_{\text{ref Tr}}$, and the distribution of the normalized cycle amplitudes is estimated as shown in Fig. 4.15. The cycle amplitudes due to traffic loading roughly follow an exponential distribution with a maximum observed value of 200% of $A_{\text{ref Tr}}$; hence, the cycle count for a given

amplitude range is expressed as

$$N_{x1-x2} = \frac{(e^{-\frac{x1}{z}} - e^{-\frac{x2}{z}})}{(1 - e^{-\frac{200\% A_{ref Tr}}{z}})} * N_{annual} \quad (16)$$

where z is equal to 70%, 50%, and 32% of $A_{ref Tr}$ for the one, two, and three span configurations respectively. The number of annual cycles (N_{annual}) can be estimated given the annual number of truck scenario occurrences ($N_{scenario\ occurrence}$) computed from Eq. (14) and the number of bearing cycles caused by a single scenario occurrence. The latter is estimated from bearing displacement histories using the rainflow cycle counting. For no-braking scenarios, it is found to be on average 1, 2.5, and 2.5 cycles per occurrence for the one, two, and three span configurations respectively. For braking scenarios, it is found to be on average 2, 3.5, and 3.5 cycles per occurrence, respectively.

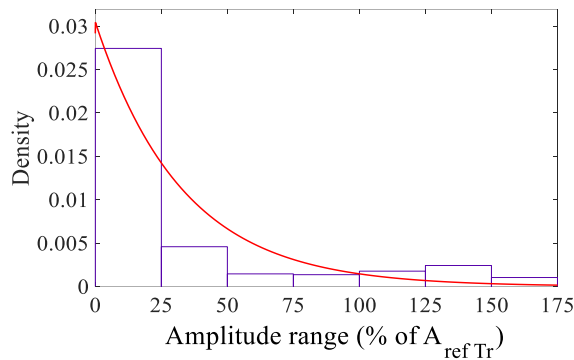


Fig. 4.15 Distribution of traffic cycle amplitudes

4.5.3. Seismic Demands

Unlike the temperature and traffic loading cases the seismic loading results in much fewer cycles but larger cycle amplitudes, furthermore, earthquake occurrence is far less common. Thus, the risk of exceeding design limits, rather than fatigue, is of interest

when it comes to seismic loading. Hence, the seismic demand models are for predicting the maximum bearing displacement ($D_{L \max}$) rather than the cumulative travelled displacement. The regression analysis is based on the results of 150 simulations per bridge configuration per earthquake type. Two prediction models are generated for $D_{L \max}$; for the multi-span bridges

$$\ln(D_{L \max \text{ multi}}) = a_0 + a_1 * \text{Sa}(0.2)^{b_1} + a_2 * \text{Sa}(1.0)^{b_2} + a_3 * \left(\frac{m_{\text{supstr}}}{k_{\text{piers}}}\right)^{b_3} + a_4 * \left(\frac{k_{\text{h bearing}}}{10^3}\right)^{b_4} \quad (17)$$

and for the single-span bridges

$$\ln(D_{L \max \text{ single}}) = a_0 + a_1 * \text{Sa}(0.2)^{b_1} + a_2 * \text{Sa}(1.0)^{b_2} + a_3 * \left(\frac{m_{\text{supstr}}}{10^6}\right)^{b_3} + a_4 * \left(\frac{k_{\text{h bearing}}}{10^3}\right)^{b_4} \quad (18)$$

where $D_{L \max}$ is the maximum bearing displacement in the longitudinal direction (mm), $\text{Sa}(0.2)$ and $\text{Sa}(1.0)$ are the spectral accelerations at 0.2 and 1 sec respectively in units of g , m_{supstr} is the mass of the superstructure (kg), k_{piers} is the summation of all piers stiffness (kN/m) computed as $\Sigma 12EI/H^3$, and $k_{\text{h bearing}}$ is the horizontal bearing stiffness (kN/m). The values of the regression coefficients (a_0 to a_4) and power coefficients (b_1 to b_4) are presented in Table 4.4 and Table 4.5 for the multi-span and the single-span bridges, respectively.

Table 4.4. $D_{L \max \text{ multi}}$ model coefficients for multi-span bridges

EQ type	a_0	a_1	a_2	a_3	a_4	b_1	b_2	b_3	b_4
Eastern	-5.19	2.03	6.13	0.5	-0.08	0.1	0.1	0.4	1
Shallow Crustal	-2.25	0.55	5.02	0.15	-0.08	0.1	0.1	0.9	1
Subduction	-5.51	0.47	7.82	1.12	-0.01	0.1	0.1	0.2	1

Table 4.5. $D_{L \max \text{ single}}$ model coefficients for single-span bridges

EQ type	a_0	a_1	a_2	a_3	a_4	b_1	b_2	b_3	b_4
Eastern	-5.68	4.22	2.75	1.66	-0.22	0.1	0.3	1	0.8
Shallow Crustal	-5.32	6.12	2.96	1.32	-2.55	0.1	0.1	1	0.1
Subduction	-8.03	5.13	5.21	0.75	-0.38	0.1	0.1	1	0.3

Fig. 4.16 shows the increase in seismic demands with the increase of $Sa(0.2)$ for both multi and single-span bridges. However, the demands for multi-span bridges are significantly higher than that of single-span bridges due to their different mode shapes. For the multi-span bridges, the superstructure is supported by the piers and the unrestricted end bearings, both of which allow lateral deformations. When subjected to seismic forces, the superstructure undergoes rigid body motion, resulting in relatively large lateral deformation in the end bearings. In the single-span bridges, the superstructure is only supported on the two end bearing supports, and one of these supports is horizontally restricted. This increases the longitudinal stiffness of the superstructure, limiting the lateral movement. For all bridge configurations, the demands are not time sensitive (i.e. not affected by bridge aging) due to the limited corrosion-induced stiffness losses of the superstructure elements (deck and steel girder) and the piers.

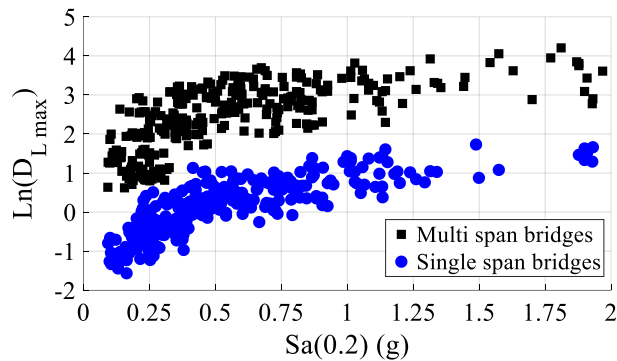


Fig. 4.16 $\ln(D_{L\max})$ vs. $Sa(0.2)$ for multi- and single-span bridge configurations (Eastern EQ)

Using the predicted maximum displacement, the bearing displacement histories are normalized and the distribution of the normalized cycle amplitudes is found. Given that the interest is mainly in the large seismic displacements that may exceed the design limits, only the expected cycles with amplitudes larger than 50% of $D_{L\max}$ are reported

(Table 4.6). The distribution of the cycle amplitudes varies significantly between the multi- and single-span bridges. The single-span bridges have higher longitudinal stiffness leading to higher number of cycles with low displacement amplitudes in comparison to multi-span bridges. This is clear from Table 4.6 which shows that at the lower amplitude ranges (50%-60% $D_{L\max}$), the cycle count for bearings in single-span bridges can be 50% to 100% higher than that in multi-span bridges depending on the EQ type.

Table 4.6. Expected cycle count for amplitudes larger than 50% of $D_{L\max}$

Amplitudes (% of $D_{L\max}$)	Eastern EQ		Shallow Crustal EQ		Subduction EQ	
	MS ^a	SS ^a	MS ^a	SS ^a	MS ^a	SS ^a
50%-60%	7	17	5	9	8	12
60%-70%	4	9	3	6	5	7
70%-80%	3	5	2	4	3	4
80%-90%	2	3	2	2	2	2
90%-100%	1	1	1	1	1	1
100%	1	1	1	1	1	1

^a MS and SS denote multi-span and single-span bridges, respectively.

4.6. Case Study

A case study is presented to demonstrate the application of the demand models for generating annual bearing demands and an associated loading protocol. Consider a bridge located in Quebec carrying two traffic lanes. The superstructure has a total depth of 2 m, a total mass of 2×10^6 kg, three 40 m long spans, and a 0.16 m thick reinforced concrete slab deck resting on six AASHTO V-Type precast prestressed concrete girders spaced at 2.2 m. The superstructure is supported on two horizontally unrestricted bearing supports and two piers. Each pier has three circular reinforced concrete columns, with a diameter of 0.9 m and a height of 6 m, connected by a bent beam. The bearings are initially designed for the difference between the maximum and minimum

temperatures shown in Table 4.3. The design displacement is 25.6 mm based on which the bearing properties are selected [55]. Table 4.7 shows the design parameters required for generating the bearing loading protocol.

Table 4.7. Design parameters for the case study bridge

Parameter	Value	Parameter	Value
N_s	3	I	0.42 m ⁴
N_{UBS}	2	k_h bearing	2,300 kN/m
L	120 m	k_v bearing	391,600 kN/m
MF_u and MF_d	1	h/S	0.05
E_{girder} and E_{deck}	2.41*10 ⁷ kN/m ²	k_{deck}	9270.6 kN/m ²
α_{girder}	1*10 ⁻⁵	m_{supstr}/k_{piers}	7.72 kg.m/kN

The steps for finding the annual loading protocol of the bearing due to temperature loads, together with the values for the case study shown inside the parenthesis, are:

1. Estimate the yearly average temperature differential fluctuation (ΔT_{pos} – ΔT_{neg})_{average} from the temperature differential profile (12.5 °C from CSA S6-19 [3] for concrete bridges shown in Fig. 4.4a).
2. Estimate P_{cloudy} and P_{clear} (assumed as 20% and 60%, respectively. In practice, field monitoring data can be used).
3. Compute the CDD_T from Eq. (7) (2390.8 mm).
4. Estimate the parameters of the cycle amplitude probability distribution (μ and σ). In this study, μ is estimated by $CDD_T/365/4$ (1.64 mm) with a standard deviation σ estimated from Eq. (9) (0.69 mm).
5. Establish the cycle count for given amplitude intervals using Eq. (8) (e.g. 2 mm intervals as shown in Table 4.9).

For the traffic loading, two loading scenarios are examined with and without

braking (S1-B, S1-NB, S2-B, and S2-NB), shown in Fig. 4.17. The first has two trucks (four loading lines spaced at 2 m across the width the bridge) while the second has one truck (two loading lines spaced at 2 m). To ensure that the maximum bearing demands are found, one loading line (LL1) is positioned directly above an interior bearing. The loading for that bearing is found as follows, where inside the parentheses are the values for the case study:

1. Compute CDD_{ho} from Eq. (10) (1.93 mm)
2. Compute the displacement percentages p for each loading line from Eq. (11) (results shown in Table 4.8).
3. Assume an annual truck count $N_{trucks\ annual}$ (445,300 trucks/year from Noade and Becker [10]). In practice $N_{trucks\ annual}$ can be estimated from traffic analysis.
4. Estimate scenario likelihoods $\ell_{scenario}$ from traffic analysis (assumed here as 5%, 15%, 40%, and 40% for S1-B, S1-NB, S2-B, and S2-NB, respectively).
5. Compute the number of occurrences per year $N_{scenario\ occurrence}$ for each scenario from Eq. (14) (11,133; 33,397; 178,120; and 178,120 for S1-B, S1-NB, S2-B, and S2-NB, respectively).
6. Calculate the impact factor (IF) using Eq. (12) (assuming a deceleration of 0.5g, $IF = 2.65$ for S1-B and S2-B, $IF = 1$ for S1-NB and S2-NB)
7. Calculate the annual demands $CDD_{Traffic}$ for each scenario using Eq. (13) (202.3 m; 229 m; 1726.3 m and 651.5 m for S1-B, S1-NB, S2-B, and S2-NB, respectively).
8. Compute $A_{ref\ Tr}$ for each scenario using Eq. (15) (4.54 mm, 1.71 mm, 2.42 mm, and 0.91 mm for S1-B, S1-NB, S2-B, and S2-NB, respectively).

9. Estimate the parameter of the cycle amplitude distribution (z) for each scenario based on the bridge configuration. For three span bridges, z is equal to 32% of $A_{ref Tr}$ (1.453, 0.547, 0.774, and 0.291 mm for S1-B, S1-NB, S2-B, and S2-NB, respectively)
10. Establish the cycle count for given amplitude intervals using Eq. (16) (e.g. 2 mm intervals as shown in Table 4.9).

Table 4.8. Displacement percentages for traffic loading scenarios of the case study bridge

Loading line	S1-B/ S1-NB		S2-B/ S2-NB	
	d_i (m)	p	d_i (m)	p
LL1	0	100%	0	100%
LL2	2	89.5%	2	89.5%
LL3	2	89.5%	-	-
LL4	4	76.3%	-	-

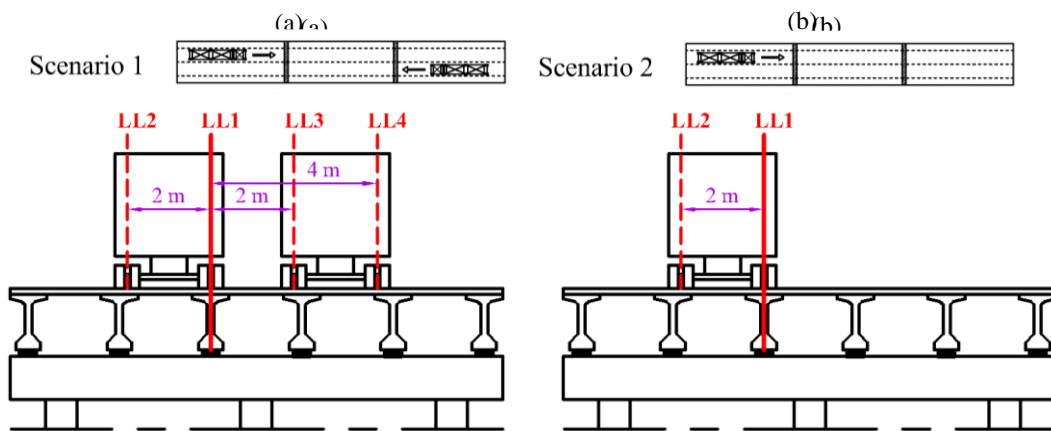


Fig. 4.17 Traffic loading scenarios considered in the case study bridge

Table 4.9. Expected cycle count for the case study bridge

Amplitude range (mm)	0-2	2-4	4-6	6-8	8-10
Temperature demands (cycles/year)	254	111	-	-	-
S1-B (cycles/year)	29,184	7,368	1,860	469	118
S1-NB (cycles/year)	81,493	2,105	54	1	-
S2-B (cycles/year)	577,480	43,584	3,289	248	19
S2-NB (cycles/year)	445,696	462	-	-	-
Total/year	1,134,107	53,630	5,203	718	137

In addition to the number and amplitude of cycles (Table 4.9), the mean position of the bearing is also required for the proposed loading protocol. For example, in this study the seasonal mean bearing displacements are found by:

1. Finding the average bridge seasonal temperatures from bridge temperature profile (-10, 5, 20, and 7 degrees for winter, spring, summer, and fall, respectively. For the case study, an air temperature profile is generated, based on data from the nearest meteorological station to the bridge, and converted into a bridge temperature profile).
2. Finding the effective construction temperature, also known as setting temperature (assumed as 15 °C)
3. Finding the seasonal mean bearing positions as $0.5 * \alpha_{\text{girder}} * L * (\text{average seasonal temperatures} - \text{setting temperature})$ (-15, -6, 3, and -4.8 mm for winter, spring, summer, and fall, respectively).

Based on the data in Table 4.9 and the seasonal mean bearing displacements, the annual fatigue loading protocol due to temperature and traffic loading is constructed. The constructed loading protocol consists of four segments, each with a mean corresponding to one of the four seasonal mean displacements as shown in Fig. 4.18. For simplicity, the cycle counts in Table 4.9 are assumed to be equally distributed among the four segments. Then, the cycles are superimposed on the mean displacements with the average amplitude of the corresponding amplitude range (e.g. for amplitude range of 0-2 mm, the average amplitude is 1 mm). The highest bearing displacements for the case study occur at the winter segment (Fig. 4.19) and can reach 24 mm (\approx 95% of the bearing design displacement).

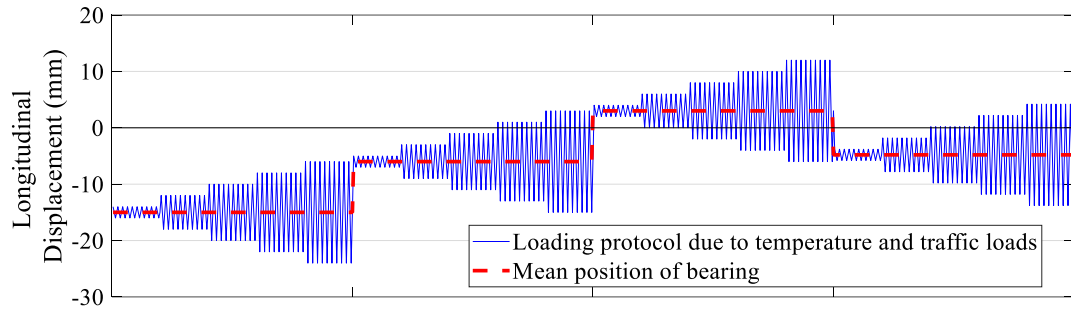


Fig. 4.18 Representative loading protocol due to the annual temperature and traffic loading

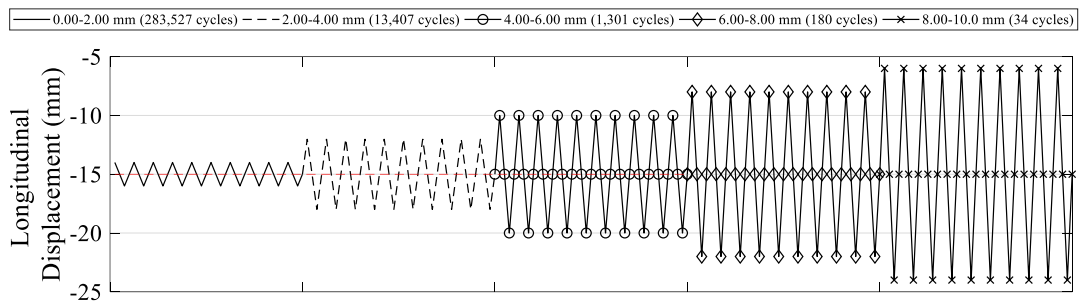


Fig. 4.19 Winter segment of the annual loading protocol due to temperature and traffic loading

After several years of cyclic displacement demands from temperature and traffic, it is expected that the bearing might experience performance degradation due to fatigue, which may affect the behavior and the performance of the bearing in seismic events. Thus, seismic loading (with amplitudes causing the bearing displacement to exceed its design value) can be added to the loading protocol to evaluate the impact of seismic events on a fatigued bearing as follows:

1. Find design spectrum [43] and get $S_a(0.2)$ and $S_a(1.0)$ (0.49 g and 0.13 g, respectively)
2. Compute $D_{L \max \text{ multi}}$ from Eq. (17) (14.1 mm)
3. Conservatively estimate the minimum considered seismic amplitude as the difference between the design displacement (25.6 mm) and the maximum absolute seasonal mean displacement (15 mm) ($10.6 \text{ mm} \approx 70\% D_{L \max \text{ multi}}$).

Select the number of cycles based on Table 4.6 and add them to the loading protocol as shown in Fig. 4.20 (for a multi-span bridge subjected to eastern seismic event, seven cycles, with amplitudes greater than 70% of $D_{L\ max\ multi}$, are added: three, two, one, and one cycles with amplitudes of 75%, 85%, 95%, and 100% of $D_{L\ max\ multi}$, respectively).

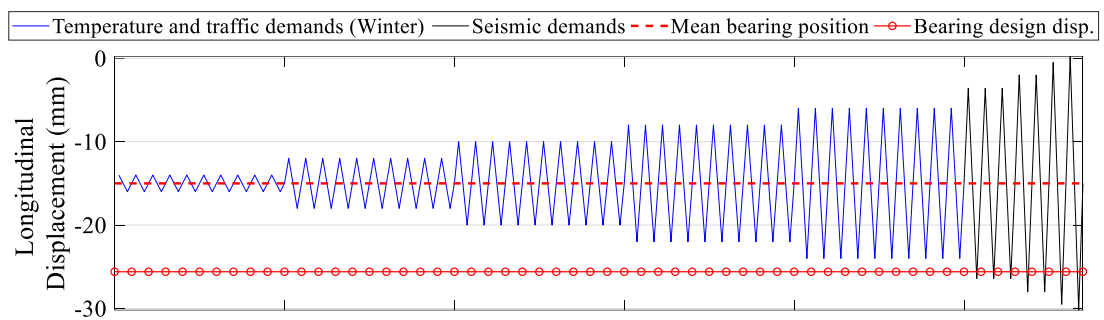


Fig. 4.20 Seismic cycles added to the winter segment of the loading protocol

The proposed loading protocol (Fig. 4.18 to Fig. 4.20) reflects in-practice loading of bearings including numerous small cycles from traffic and temperature, and few large cycles from seismic events. To avoid heating, testing would require slow loading rates (e.g. less than 12 cycles / minute [7]). While this would result in long fatigue tests, it would result in highly valuable knowledge on bearing lifetime and required replacement timing; furthermore, the testing would only be necessary for a handful of samples from which results for other bearings or applications can be extrapolated.

4.7. Conclusions

This study proposes a generalized approach for generating bridge bearing loading protocols representative of the lifetime bearing demands for three primary load types: temperature, traffic, and seismic. First, prediction models are developed through

regression analyses that relate the bearing demands to the bridge configuration (e.g. different number of spans and material type of girder) and loading parameters. These models are then used to generate a bearing loading protocol. The models in this study were based on a range of bridge configurations including concrete girder and steel girder bridges with one, two, and three spans. The effect of bridge aging on bearing demands was also included through corrosion models.

The bearing demands, and consequently the bearing loading protocol, have high sensitivity to the bridge configuration. For temperature loading, bearings in multi-span bridges undergo large cumulative displacement demands, compared to bearings in single-span bridges, from uniform temperature variation given their expansion length. However, bearings in single-span bridges, especially those with concrete girders, experience cumulative displacements of similar magnitudes from temperature differentials given the flexibility of their superstructures. For traffic loading, single-span bridges have a smaller number of cycles with higher displacement amplitudes compared to multi-span bridges. The traffic demands are highly sensitive to the superstructure geometry including the height-to-span ratio and deck stiffness. Furthermore, vehicle braking can significantly amplify the bearing displacements. For seismic loading, single-span bridges typically have one of their supporting ends restricted in the horizontal direction, limiting the displacement amplitudes and increasing the cycle count in comparison to multi-span bridges. For all of the investigated load types, the bearing response in terms of amplitude and cycle count is not significantly affected by bridge aging.

The presented demand prediction models can be used to develop experimental

fatigue loading protocols for bridge bearings. These protocols can be used for testing and rating sample bridge bearings to better understand bearing fatigue life. Additionally, this could be used to study the seismic performance of fatigued bearings. This future research will aid bridge owners and bearing manufacturers in predicting the bearing life expectancy, allowing for better replacement scheduling and budget estimation.

4.8. Acknowledgments

The authors gratefully acknowledge the support of this research by an Ontario Early Researcher Award as well as start-up funding provided by the Faculty of Engineering at McMaster University. Any opinions, findings, and conclusions or recommendations expressed in this material are those of the authors and do not necessarily reflect the views of the sponsor.

4.9. References

- [1] Grata J. Birmingham Bridge Report Confirms Rocker Bearing Failure; 2008. <https://www.post-gazette.com/breaking/2008/07/01/Birmingham-Bridge-report-confirms-rocker-bearing-failure/stories/200807010159> [accessed July 2020].
- [2] Angelilli C. Surveillance of the Performance of Elastomeric Bearings in Maryland's Concrete Bridges. Doctoral Dissertation, University of Maryland, College Park, Maryland, United States; 2007.
- [3] CSA (Canadian Standards Association). Canadian Highway Bridge Design Code. CSA S6-19. Toronto, Canada; 2019.
- [4] AASHTO. LRFD Bridge Design Specification. Washington, DC; 2017.
- [5] Kumar R, Gardoni P, Sanchez-Silva M. Effect of cumulative seismic damage and

corrosion on the life-cycle cost of reinforced concrete bridges. *Earthq Eng Struct Dyn* 2009;38(7):887–905.

[6] Deng P, Warn GP. Modeling the compression stiffness degradation in circular elastomeric bearings due to fatigue. *J Eng Mech* 2016; 142(1):04015057. [https://doi.org/10.1061/\(ASCE\)EM.1943-7889.0000947](https://doi.org/10.1061/(ASCE)EM.1943-7889.0000947).

[7] Roeder CW, Stanton JF, Taylor AW. Fatigue of steel-reinforced elastomeric bearings. *J Struct Eng* 1990;116(2):407–26.

[8] Aria M, Akbari R. Inspection, condition evaluation and replacement of elastomeric bearings in road bridges. *Struct Infrastruct Eng* 2013;9(9):918–34.

[9] Ala N, Power EH, Azizinamini A. Predicting the service life of sliding surfaces in bridge bearings. *J Bridg Eng* 2016; 21(2):04015035. [https://doi.org/10.1061/\(ASCE\)BE.1943-5592.0000767](https://doi.org/10.1061/(ASCE)BE.1943-5592.0000767).

[10] Noade BM, Becker TC. Probabilistic Framework for Lifetime Bridge-Bearing Demands. *J Bridg Eng* 2019;24(7):04019065. [https://doi.org/10.1061/\(ASCE\)BE.1943-5592.0001430](https://doi.org/10.1061/(ASCE)BE.1943-5592.0001430).

[11] Roy N, Paultre P, Proulx J. Performance-based seismic retrofit of a bridge bent: Design and experimental validation. *Can J Civ Eng* 2010;37(3):367–79.

[12] Tavares DH, Suescun JR, Paultre P, Padgett JE. Seismic fragility of a highway bridge in Quebec. *J Bridg Eng* 2013;18(11):1131–9.

[13] McKay MD, Beckman RJ, Conover WJ. A comparison of three methods for selecting values of input variables in the analysis of output from a computer code. *Technometrics* 2000; 42(1):55–61.

[14] Balomenos GP, Kameshwar S, Padgett JE. Parameterized fragility models for

multibrige classes subjected to hurricane loads. *Eng Struct* 2020; 208:110213.

<https://doi.org/10.1016/j.engstruct.2020.110213>.

[15] McKenna F, Scott MH, Fenves GL. Nonlinear finite-element analysis software architecture using object composition. *J Comput Civ Eng* 2010;24(1):95–107.

[16] Hambly EC. Bridge deck behavior. CRC Press; 1991.

[17] Kelly JM, Konstantinidis D. Mechanics of rubber bearings for seismic and vibration isolation. John Wiley & Sons; 2011.

[18] O’Flaherty F, Mangat P, Lambert P, Brown EH. Influence of steel reinforcement corrosion on the stiffness of simply supported concrete beams. *Biophys J* 2010.

[19] Smith JL, Virmani YP. Materials and methods for corrosion control of reinforced and prestressed concrete structures in new construction. United States: Federal Highway Administration; 2000.

[20] Hewson NR. Prestressed concrete bridges: design and construction. Thomas Telford; 2003.

[21] Stewart MG, Rosowsky DV. Structural safety and serviceability of concrete bridges subject to corrosion. *J Infrastruct Syst* 1998; 4(4):146–55.

[22] Kassir MK, Ghosn M. Chloride-induced corrosion of reinforced concrete bridge decks. *Cem Concr Res* 2002; 32(1):139–43.

[23] Rao AS, Lepech MD, Kiremidjian AS, Sun X-Y. Simplified structural deterioration model for reinforced concrete bridge piers under cyclic loading. *Struct Infrastruct Eng* 2017; 13(1):55–66.

[24] DuraCrete. Statistical quantification of the variables in the limit state functions. Eur Union-Brite EuRam III-Contract BRPR-CT95-0132-Project BE95-1347/R9; 2000.

- [25] Vu KAT, Stewart MG. Structural reliability of concrete bridges including improved chloride-induced corrosion models. *Struct Saf* 2000; 22(4):313–33.
- [26] Choe D-E, Gardoni P, Rosowsky D, Haukaas T. Probabilistic capacity models and seismic fragility estimates for RC columns subject to corrosion. *Reliab Eng Syst Saf* 2008; 93(3):383–93.
- [27] Coronelli D, Gambarova P. Structural assessment of corroded reinforced concrete beams: modeling guidelines. *J Struct Eng* 2004; 130(8):1214–24.
- [28] Jiang M, Corotis RB, Ellis JH. Optimal life-cycle costing with partial observability. *J Infrastruct Syst* 2000; 6(2):56–66.
- [29] Kayser JR, Nowak AS. Reliability of corroded steel girder bridges. *Struct Saf* 1989; 6(1):53–63.
- [30] Emerson M. Bridge temperatures estimated from the shade temperature. TRRL Report SR 696, Department of Transport, Crowthorne, England; 1976.
- [31] Kuppa S, Roeder C. Thermal movements in bridges. Final Rep NSF 1991; 181.
- [32] Rojas E. Uniform temperature predictions and temperature gradient effects on I-girder and box girder concrete bridges. Master Dissertation, Utah State University, Logan, Utah, United States; 2014.
- [33] Roeder CW. Proposed design method for thermal bridge movements. *J Bridg Eng* 2003; 8(1):12–9.
- [34] Government of Canada. Historical Data; 2017. https://climate.weather.gc.ca/climate_normals/index_e.html [accessed November 2018].
- [35] Hedegaard BD, French CEW, Shield CK. Investigation of thermal gradient effects in the I-35W St. Anthony Falls Bridge. *J Bridg Eng* 2013; 18(9):890–900.

- [36] Kennedy JB, Soliman MH. Temperature distribution in composite bridges. *J Struct Eng* 1987; 113(3):475–82.
- [37] Nowak AS, Collins KR. Reliability of structures. CRC Press; 2012.
- [38] CSA (Canadian Standards Association). Commentary on CSA S6-19, Canadian Highway Bridge Design Code. CSA S6-19. Toronto, Canada; 2019.
- [39] Martins J, F'enart M-A, Feltrin G, Dumont A-G, Beyer K. Deriving a Load Model for the Braking Force on Road Bridges: Comparison Between a Deterministic and a Probabilistic Approach. *Dev Int Bridg Eng*, Springer; 2016. p. 27–39.
- [40] Chiou B, Darragh R, Gregor N, Silva W. NGA project strong-motion database. *Earthq Spectra* 2008; 24(1):23–44.
- [41] Halchuk S, Adams J, Kolaj M, Allen T. Deaggregation of NBCC 2015 seismic hazard for selected Canadian cities. *Proc. 12th Can. Conf. Earthq. Eng. Quebec City, QC, Canada; 2019. p. 17–20.*
- [42] Bozorgnia Y, Kishida T, Abrahamson NA, Ahdi SK, Ancheta TD, Archuleta RJ, et al. NGA-Sub research program. *Proc, 11th US Natl Conf Earthq Eng* 2018:25–9.
- [43] NBCC. National Building Code of Canada 2015. National Research Council of Canada, Ottawa, NRCC 56190 Vol 1 & 2; 2015.
- [44] Weisberg S. Applied linear regression. vol. 528. John Wiley & Sons; 2005.
- [45] Zhang Y-M, Wang H, Wan H-P, Mao J-X, Xu Y-C. Anomaly detection of structural health monitoring data using the maximum likelihood estimation-based Bayesian dynamic linear model. *Struct Heal Monit* 2020:1475921720977020.
- [46] Goulet J-A, Koo K. Empirical validation of bayesian dynamic linear models in the context of structural health monitoring. *J Bridg Eng* 2018; 23(2):05017017.

[https://doi.org/10.1061/\(ASCE\)BE.1943-5592.0001190](https://doi.org/10.1061/(ASCE)BE.1943-5592.0001190).

- [47] Rhinehart RR. Nonlinear regression modeling for engineering applications: modeling, model validation, and enabling design of experiments. John Wiley & Sons; 2016.
- [48] Breiman L, Friedman J, Olshen R, Stone C. Classification and Regression Trees. Belmont, California, US: Wadsworth International Group; 1984.
- [49] Karalic A, Cestnik B. The bayesian approach to tree-structured regression. Proc ITI 1991; 91:155–60.
- [50] Quinlan JR. Learning with continuous classes. 5th Aust. Jt. Conf. Artif. Intell., vol 92, World Scientific; 1992. p. 343–8.
- [51] Zhang Y-M, Wang H, Mao J-X, Xu Z-D, Zhang Y-F. Probabilistic Framework with Bayesian Optimization for Predicting Typhoon-Induced Dynamic Responses of a Long-Span Bridge. J Struct Eng 2021; 147(1):04020297. [https://doi.org/10.1061/\(ASCE\)ST.1943-541X.0002881](https://doi.org/10.1061/(ASCE)ST.1943-541X.0002881).
- [52] Breiman L. Random forests. Mach Learn 2001; 45(1):5–32.
- [53] Koza JR. Genetic programming as a means for programming computers by natural selection. Stat Comput 1994; 4(2):87–112.
- [54] Searson DP. GPTIPS 2: an open-source software platform for symbolic data mining. Handb. Genet. Program. Appl., Springer; 2015. p. 551–73.
- [55] Z-Tech G. Elastomeric Bearings. Qu'ébec; 2010.

5. Fuzzy-Probabilistic Seismic Vulnerability Index for Deteriorating Multi-span Continuous Concrete Girders Bridges

Abdelmaksoud, Ahmed M., Tracy C. Becker, and Georgios P. Balomenos. “Fuzzy-Probabilistic Seismic Vulnerability Index for Deteriorating Multi-span Continuous Concrete Girders Bridges” (In preparation)

5.1. Abstract

Seismic performance evaluation of bridges is critical to ensure the post-earthquake integrity of transportation networks; however, systematic evaluations are very costly. To satisfy budget limitations, bridge management systems (BMSs) have developed seismic screening policies to identify the most vulnerable bridges, giving them the highest priorities. Such policies are typically qualitative and do not accurately reflect the seismic performance. Furthermore, performance deterioration with aging is often ignored. This results in significant uncertainty and underestimation of the seismic vulnerability. Thus, a new quantitative risk-based framework is proposed for screening bridges using fragility analysis of deteriorating critical components, specifically bridge bearings and columns. To capture the fragility trends with deterioration, new BMS-compatible condition indices are proposed. The indices can be evaluated from typical visual inspections and are calibrated using fuzzy logic principles to inform the predicted performance of the deteriorating bridge components. Based on the fuzzy-fragility analysis, parameterized models are formulated to predict the fragility of columns and bearings given the condition indices, design parameters, and seismic intensity. Based on these fragilities, a global risk-based seismic vulnerability index (SVI) is derived for the bridge to set its priority for detailed seismic investigation. The analysis revealed that the fragilities and bridge vulnerability are significantly dependent on the

components' deterioration level.

Keywords: Seismic vulnerability index, seismic screening, fuzzy set theory, fragility, Multiple-stripe analysis

5.2. Introduction

Seismic performance evaluation of bridges is critical to ensure the post-earthquake integrity of transportation networks. Bridge damage due to earthquakes can lead to catastrophic consequences beyond repair costs and extend to traffic, social, and financial disruptions (Moehle and Eberhard, 2003). Such consequences are highly likely for bridges built prior to modern seismic provisions (Filiatrault et al. 1994) or those with deterioration (Biezma and Schanack 2007; Bazzucchi et al. 2018), but even bridges designed for seismic events are not immune (Priestley et al. 1996; Mitchell et al. 2013). Systematic seismic evaluation is costly for most bridge management systems (BMSs) with large bridge populations (Hearn et al. 2005; Hammad et al. 2007; Markow and Hyman 2009). To accommodate budgetary limits, several preliminary seismic screening procedures have been proposed to select and prioritize bridges for detailed seismic evaluation.

In Canada, several BMSs implement preliminary seismic screening, such as those in Quebec (Filiatrault et al. 1994), Ontario (Bagnariol and Au, 2000), and British Columbia (Tesfamariam and Modirzadeh, 2009). The screening aims to compute a seismic vulnerability index (SVI) reflecting the bridge's importance and seismic damage susceptibility. The higher the SVI, the higher the bridge priority for detailed seismic evaluation. While each province uses its scale for the SVI, the calculation procedures are similar. The SVI is typically computed based on four sets of indicators:

(1) importance-related indicators, such as the road type and traffic volume, (2) structure-related indicators, such as the type of bearings, superstructure, and substructure, (3) seismic hazard-related indicators, such as the ground acceleration, and (4) soil-related indicators, such as the soil type and liquefaction potential. Based on expert opinion, each indicator is given a weight, reflecting its relative importance to the bridge owners, and a score, proportional to its contribution to the seismic damage susceptibility. Then, the SVI is computed as the weighted average of the scores.

The existing provincial seismic screening procedures allow for rapid estimation of the SVI, and can be adapted to any existing inspection practice (Filiatrault et al. 1994). However, at least one or more of the following limitations was noted. First, the deterioration of seismic performance with bridge aging is not considered (Tesfamariam and Modirzadeh, 2009), which may underestimate the SVI for older bridges. Secondly, the SVI assessment is often based on recognizing the presence of poor seismic details (e.g., high rocker bearings) rather than quantifying the actual seismic performance (Dicleli and Bruneau, 1996). Thirdly, the screening scores for the SVI indicators are based on a subjective expert-opinion-based scoring scheme (Filiatrault et al. 1994). The two latter limitations highlight that the procedures are qualitative rather than quantitative, resulting in significant epistemic uncertainty (Brown and Yao, 1983). Such uncertainty may result in an underestimated SVI (Der Kiureghian and Ditlevsen, 2009).

Studies have suggested using the bridge age as a direct proxy for deterioration when computing the SVI (Kenedi and Bagnariol, 2007; Tesfamariam and Modirzadeh, 2009; Bonthron et al., 2021). Kenedi and Bagnariol (2007) also incorporated the repair

history by taking the average of age and time since the last major maintenance (T_{major}) (MTO 2018) as a deterioration indicator. While age and repair history indicate deterioration, Abdelmaksoud et al. (2021) found that directly incorporating condition data (e.g., inspector-assigned condition index) from past inspections can improve condition assessment by about 10%.

Quantitative assessment of the seismic damage susceptibility requires estimating the seismic response (e.g., column drift) and comparing it to a pre-specified capacity or damage state. For example, Dicleli and Bruneau (1996) proposed a seismic damage index function of the demand-to-capacity ratios of the potentially critical bridge components during seismic events. Their work identified the bearings and the columns as the most critical components and derived complex analytical expressions for their demand-to-capacity ratios. The proposed damage index is rigorous and requires detailed knowledge of the structural properties of the bridge components; hence, it may be time-consuming for the preliminary screening stage. Recently, Bonthron et al. (2021) proposed a seismic vulnerability assessment procedure based on simplified dynamic analysis. The procedure first establishes a single degree of freedom (SDOF) bridge model based on the readily available information from the bridge inventory. Then, the elastic column drifts are estimated based on a response spectrum analysis. The nonlinear drifts are then approximated (Sozen, 2003) and compared to pre-defined damage states. Based on this, the bridge is classified into a low, moderate, or high vulnerability category. The California Department of Transportation (Caltrans) uses fragility analysis for assessing bridges' seismic vulnerabilities. First, the main classes of bridges owned by Caltrans were identified (Mangalathu et al., 2016). Then, a

framework was proposed for developing bridge-class-specific parameterized fragility models to predict the probability of exceeding a damage limit given the typical values of the design parameters for the investigated bridge class (Dukes et al., 2018). Despite such large advance in quantitative assessment of seismic vulnerability, a methodology for updating the vulnerability estimates with deterioration or current inspection data has yet to be established.

To address the highlighted limitations, a new quantitative risk-based framework for rapid SVI assessment of deteriorating bridges is developed. The proposed framework defines the SVI as the risk of a deteriorating critical bridge component exceeding a specified damage limit. The columns and bearings are regarded as the most critical components (Tavares et al. 2013). Their damage risks are quantified from seismic fragility analysis (Mackie and Stojadinović, 2003) while considering the following deterioration mechanisms: column reinforcement corrosion and bearing aging. Based on the components' fragilities, a risk-based SVI is derived for the bridge to rank its priority for detailed seismic investigations. For demonstration, the proposed framework is developed for the multi-span continuous (MSC) concrete bridge class; however, it can be later extended to include other bridge classes. Here, the fragility analysis is conducted using a 3D nonlinear model in OpenSees (McKenna et al. 2010) of the Chemin des Dalles Bridge located in Trois Rivieres, Quebec. This bridge was chosen as its properties are well documented in the literature. Furthermore, the bridge is representative of MSC concrete bridges in the region (Tavares et al. 2012; Bandini et al. 2022).

The proposed framework has two main contributions. First, new condition

indices are proposed to capture the trends in seismic damage risk (i.e., the SVI) with the deterioration of columns and bearings. These indices are formulated so that they can be evaluated from visual inspection. Also, they are specifically calibrated using fuzzy logic (Zadeh, 1965) to correlate with the seismic response of the deteriorating components of MSC concrete girders bridges class. Secondly, a parametric study is conducted from which a simplified formula is generated using genetic programming (Searson, 2015) to relate the damage risks from the fragility analysis (i.e., the SVI) to the proposed condition indices and other bridge design parameters, such as pier stiffness, soil properties, and foundation dimensions. This proposed SVI model can facilitate rapid risk-based seismic screening of deteriorating bridges with minimal modifications to current inspection practice.

5.3. Methodology

The proposed framework for seismic vulnerability assessment of deteriorating bridges are shown in Fig. 5.1. The framework development (Fig. 5.1a) starts by relating the visually-inspected damages of critical components (i.e., columns and bearings) to seismic performance degradation. Damage identified from visual inspections is mapped onto quantitative deterioration values and input into a numerical model to assess the seismic performance. The performance is then traced back to the visually-inspected damages to formulate condition indices for the critical components. The proposed indices are then used as a part of a parametric fragility analysis to formulate parameterized models for the components fragilities with different levels of deterioration. Bridge owners can apply the framework (Fig. 5.1b) by first estimating the condition indices of their bridge components as well as other bridge parameters.

Based on this information, the component fragilities can be computed and aggregated to evaluate the bridge’s global seismic vulnerability index (SVI) which can be used to rank the importance for a more detailed inspection.

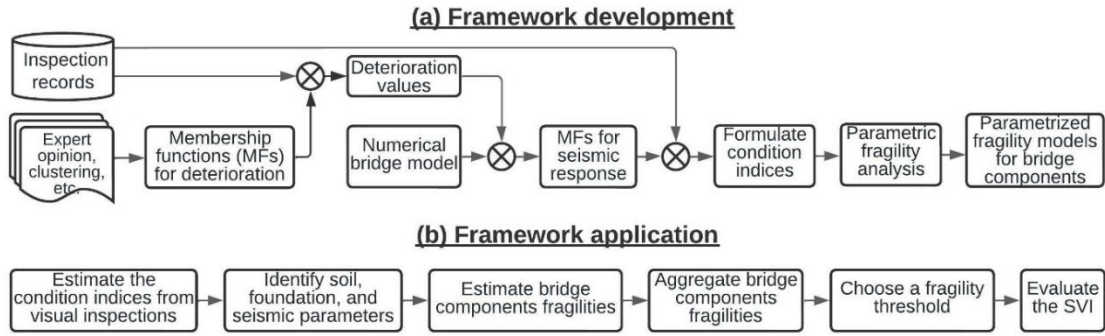


Fig. 5.1 Proposed framework for seismic vulnerability assessment of deteriorating bridges

5.3.1. Condition Indices for Critical Bridge Components

BMSs monitor bridge deterioration primarily through routine inspections. For example, bridge inspections in Ontario involve component-by-component visual assessments to identify any apparent signs of deterioration or material defects (MTO 2018). Based on these assessments, portions of the bridge are assigned condition ratings (e.g., poor, fair, good, or excellent). Then a bridge condition index (BCI) (scale 0-100) is computed as the weighted average of the ratings

$$BCI = \frac{\sum_{i=1}^{i=4} W_i * A_i}{\sum_{i=1}^{i=4} A_i} * 100 \quad (1)$$

where W_i is the weight for condition i (i.e., poor, fair, good, or excellent), representing its relative economic value compared to the as-good-as-new condition. Areas with excellent and poor conditions have the highest and lowest weights, respectively. A_i is the number of individual elements (e.g., bearings) or the surface area of individual

elements (e.g., columns) in condition *i*. While the BCI provides an overall indication of the bridge condition, it does not reflect the bridge's safety or performance (MTO 2015). The BCI captures the surface deterioration but not potential subsurface deterioration in bridge components. Also, the weights are assigned without clear reasoning and without reflecting the relative effects on seismic performance.

To address this, local condition indices for the critical bridge components are proposed. These indices will be used to quantify the variation in bridge seismic vulnerability with component deterioration. While virtually all bridge components will have some level of deterioration, this study focuses on corrosion of column reinforcement and aging of bearings, because damage or deterioration of these components is significantly detrimental to seismic performance (Oyado et al. 2007; Alipour et al. 2013; Biondini et al. 2014; Song et al. 2021; Fang et al. 2022).

For compatibility with current BMSs practices, the proposed indices are formulated similar to Eq. (1) but with few modifications. This includes recalibrating the condition weights to better inform the seismic performance of columns and bearings. For the column's condition index, a new factor is added to account for the impact of deterioration location (e.g., top, middle, or bottom of column). For the condition indices to indicate the seismic performance of the critical components, the condition ratings identified from visual inspections must be mapped into a range of possible subsurface deterioration values given past observations, inspection guidelines, or experimental data. For example, a column with relatively wide cracks containing rust stains, can be linked to severe corrosion with a 10%-20% loss of reinforcement area (MTO 2018). Combined with fuzzy logic (Zadeh, 1965), such information can be used

as an input (e.g., reduced reinforcement area) to a numerical bridge model. Hence, the seismic performance of the deteriorating critical components can be assessed. The performance can then be traced back to the observations from visual inspections.

5.3.1.1. Fuzzy Logic and Membership Functions

Fuzzy logic is a common approach for mapping imprecise or qualitative visual assessments of bridge components into a range of quantitative deterioration values (Tee et al. 1988). The values are expressed in a membership function $\mu(x)$, ranging from 0 to 1, which describes the degree of confidence that a value of x is the actual value. A $\mu(x)$ value of 0 indicates no confidence in a value x , whereas a value of 1 indicates complete confidence. In structural applications, the functions are typically assumed to have a triangular or trapezoidal shape (Sasmal and Ramanjaneyulu, 2008). They can be formulated using clustering, expert opinion, or other methods (Medasani et al. 1998).

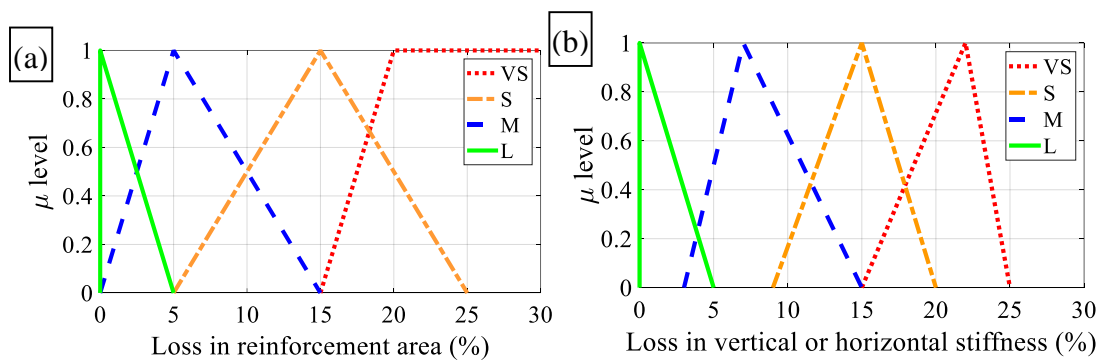
The membership functions for reinforcement corrosion in columns (Fig. 5.2a) were created based on the corrosion degree classifications in the Ontario Structure Inspection Manual (OSIM) (MTO 2018), whereas those for bearing aging (Fig. 5.2b and 2c) were formulated based on experimental data (Roeder et al., 1990; Fan, 2014; Deng et al., 2016). Four degrees of deterioration severity can be assigned based on visual inspection: light (L), medium (M), severe (S), and very severe (VS).

OSIM classifies corrosion based on the percentage loss in reinforcement area as: L (0%), M (<10%), S (10~20%), and VS (>20%). Differentiating between these classes during a visual inspection is not always clear and depends on the inspector's perception of the amount of corrosion. Consequently, it is assumed that corrosion membership functions will overlap between the mid-points of the corrosion ranges

defined by OSIM (Fig. 5.2a).

Bridge bearings experience fatigue due to the daily displacement cycles induced by temperature and traffic loads which may significantly degrade their horizontal and vertical stiffness. Despite the lack of clear understanding of in-practice bearing stiffness degradation (Abdelmaksoud et al., 2022), studies have estimated that elastomeric bearings lose 20%~25% of the initial stiffness over their life-span when subjected to cyclic shear and compression loading (Roeder et al. 1990; Deng and Warn 2016). The stiffness loss measurements were grouped into four severity clusters via the k-means method (MacQueen, 1967; Wagstaff et al., 2001), using the total protrusions in the bearings as a clustering criterion (Roeder et al. 1990). For each group, the minimum, maximum, and average values are used to construct a membership function (Fig. 5.2b).

Fan (2014) tested steel high rocker bearings retrieved from an in-service bridge and showed that severe corrosion could lead to at least 30% loss of the initial stiffness, subject to increase if the rust peels off. Based on the available experiments, the stiffness loss severities are reasonably assumed as: L (0%), M (~10%), S (10~20%), and VS (20~30%). Then, membership functions for the stiffness losses are formulated with the overlaps extending between the mid-points of the defined intervals (Fig. 5.2c).



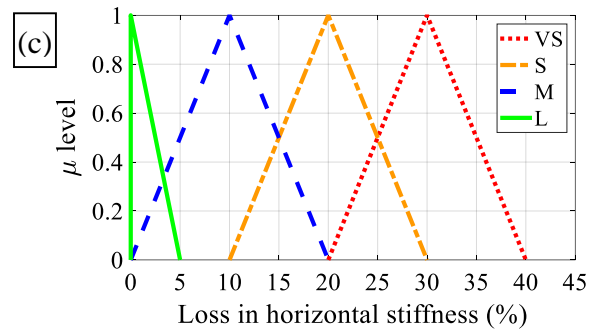


Fig. 5.2 Membership functions for (a) reinforcement corrosion in columns, (b) stiffness losses in elastomeric bearings, and (c) stiffness losses in high rocker bearings.

5.3.1.2. Modelling Deterioration

Monte Carlo simulations, combined with Latin hyper cube sampling (McKay et al. 2000), are used to generate various levels of deterioration for columns and bearings based on deterioration patterns observed from several inspection reports from the Ministry of Transportation in Ontario (MTO). The generated conditions are then converted into numerical values (e.g., reduction in reinforcement area or bearing stiffness) via the membership functions (Fig. 5.2) and input into the bridge model.

In the bridge model, each column is meshed into several elements with variable lengths. For each Monte Carlo simulation, one or two of these elements is selected to be the worst conditioned element(s) in the column and are assigned one of the four degrees of severity (i.e., L, M, S, or VS), where the random element selection and condition assignment follow a uniform distribution. The adjacent elements are then assigned the next lower degree of severity until reaching the lighter (i.e., L) degree of severity. As each degree of severity corresponds to a range of possible losses in the reinforcement area, each simulation was repeated three times to get the worst, best, and most probable scenarios. The worst and best-case scenarios occur at $\mu = 0$ when all column elements are assigned the highest or lowest possible loss in the reinforcement

area for their respective corrosion severity degrees. The most probable scenario occurs when all elements are assigned the reinforcement area loss corresponding to the highest confidence level (i.e., $\mu = 1$). The effect of cover spalling and cracking associated with corrosion is incorporated by reducing the unconfined strength of the concrete cover (Coronelli and Gambarova, 2004). Similarly, each of the bearings is assigned a random deterioration level, and then the worst, best, and most probable scenarios are evaluated.

5.3.1.3. Formulating the Condition Indices

After modelling the worst, best, and most probable deteriorated bridge, a time history analysis is conducted to find the range of values for the maximum column drift (δ_{col}) and bearing displacement (Δ_b). Then, for these three evaluations, a membership function is obtained for δ_{col} and Δ_b per simulation. These membership functions of δ_{col} and Δ_b are defuzzified into a crisp value using the centroid method (Chakraverty et al. 2019). Afterwards, the defuzzified values of δ_{col} and Δ_b are related to a column condition index (CCI) and a bearing condition index (BeCI), respectively. The BeCI is expressed similarly to Eq. (1), whereas the CCI is formulated as

$$CCI = \frac{\sum_{j=1}^{j=4} \sum_{k=1}^{k=3} C_o * A_{jk} * W_j * Lo_k}{\sum_{j=1}^{j=4} A_j} * 100 \quad (2)$$

where C_o is a scaling factor to convert the CCI into the 0-100 scale. A_{jk} is the length of the column section with a given degree of severity j (i.e., L, M, S, or VS) at a given location k (i.e., top, middle, or bottom of column). W_j is the corrosion severity weight in the range 0~1, the higher the severity degree the lower the weight. Lo_k is a corrosion location factor in the range 0~1, reflecting the relative impact of corrosion location on the column drift. The highest Lo_k is assigned to the most critical locations where the

reduction of the shear capacity and the confinement of columns due to reinforcement corrosion leads to significantly larger column drift (δ_{col}). The factors in the above equations are calibrated to maximize the correlation between the condition indices (i.e., BeCI and CCI) and their corresponding component response (i.e., Δ_b and δ_{col}).

5.3.2. Seismic Performance Assessment

5.3.2.1. Fragility Analysis

The seismic fragility is defined as the confidence level (CL_o) that the demand of each critical bridge component will not exceed its capacity. The higher the CL_o , the less fragile the bridge. To determine the CL_o , the demand and capacity distributions are estimated for each component, as discussed in later sections. For any given confidence level (CL), a safety margin can be computed between the demand and the capacity (Fig. 5.3). The value of CL_o is equal to the confidence level corresponding to a safety margin of zero. The CL_o values of the critical bridge components are later used to compute the global SVI for the bridge.

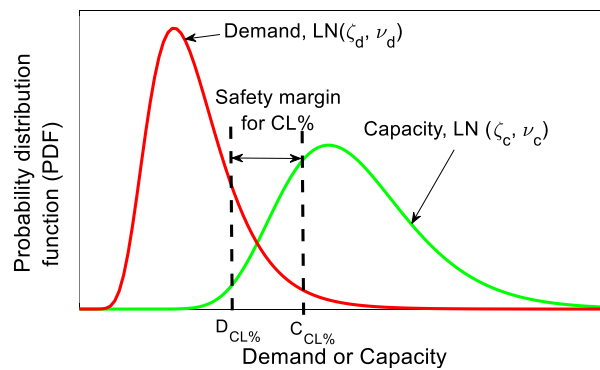


Fig. 5.3 Safety margin between demand and capacity for a confidence level (CL %)

A parametric study is conducted to evaluate the variation in CL_o with 11 selected parameters (Table 5.1) related to the seismic intensity, soil properties, material properties, and bridge geometry. The spectral acceleration at the fundamental period

$Sa(T_1)$ is adopted as the seismic intensity measure (IM) (Luco and Cornell, 2007). Six IM levels are investigated (Table 5.1) from 0.25g to 1.50g at increments of 0.25g. Variations of the other parameters are investigated at $Sa(T_1)$ of 0.50g and 1.25g, representing moderate and high seismic intensities. Soil properties of interest include the effective shear modulus (G_e) and the soil type (clay or sand). Ideally, the effective shear modulus (G_e) is evaluated based on a free-field ground response analysis over a depth of 1.5 to 2 times the shorter dimension of the foundations. Alternatively, the effective shear modulus (G_e) of weakened soil during seismic events can be assumed as low as 20% of its initial value (G_o) (CSA 2019b; FEMA 1997). The initial modulus (G_o) varies with the soil type and characteristics, however, a representative sample is adopted from MTO (2020) and Santos and Correia (2000). Other relevant soil parameters include the friction angle of the sand (ϕ) and the cohesion coefficient of the clay (c), with sample values adopted from the Bureau of Reclamation (1998). To explore the variation in demands with column and bearing deterioration, random deterioration levels are generated corresponding to the CCI and BeCI values in Table 5.1. Finally, to include uncertainties in construction material and dimensions, the young's modulus of concrete (E_c) and the column height (h) are considered normally and uniformly distributed, respectively. The mean values of E_c and h are 26100 MPa and 6 m, respectively (Tavares et al. 2013), and the coefficient of variations (cov) of E_c and h are taken as 8% and 3%, respectively (Mirza et al. 1979; Nowak and Rakoczy 2013).

Table 5.1. Investigated properties for the parametric study

Parameter	Value (units)
$Sa(T_1)$	0.25, 0.5, 0.75, 1, 1.25, 1.5 (g)
Effective soil shear modulus (G_e)	10, 15, 20, 30, 40, 50, 60 (MPa)
Cohesion (Clay)	30, 60, 80, 100, 120 (kPa)
Friction angle (Sand)	32, 34, 36, 38, 40, 42
Foundation width-to-length ratio	0.15, 0.28, 0.45, 0.6
Foundation thickness (H)	1, 1.25, 1.5, 1.75, 2, 2.25 (m)
Foundation depth (D)	0.5, 1, 1.5, 2, 2.5 (m)
Column condition index (CCI)	40, 50, 60, 70, 80, 90, 100
Bearing condition index (BeCI)	5, 34, 65, 82, 100
Young's modulus of concrete (E_c)	Normally distributed, $\mu=26100$ MPa, cov = 8%
Pier height (h)	Uniformly distributed, 6 ± 0.25 m

5.3.2.2. Seismic Demand Generation and Record Selection

The current study generates the seismic demands using the multiple-stripe analysis technique (MSA) as it can capture the variation in the characteristics of seismic events at different IM levels (Mackie and Stojadinović, 2005). The earthquake ground motions used in the MSA are from the Pacific Earthquake Engineering Research Center (PEER) strong motion database (Chiou et al., 2008). The selection of the ground motion records is based on typical seismic hazard deaggregation for the bridge population. The records selected here are based on the typical deaggregation values in the eastern Canadian region (Halchuk et al., 2019; Noade and Becker, 2019) where the bridge is located (e.g., deaggregation values for Quebec City and Trois Rivières). The selected records were scaled for $Sa(T_1)$ of 0.25g to 1.50g at increments of 0.25g.

The optimum number of records that yields stable results is problem dependent and can vary depending on the fragility analysis methodology and the damage limits (Kiani et al. 2018). As such, there is no consensus on the optimum number of records which may vary from a minimum of 11 records (CSA 2019; ASCE 2017) up to 80

records (Nielson and Pang 2011). For the current study, a sensitivity analysis (Fig. 5.4) is conducted to determine the minimum number of records yielding a reliable mean of the seismic response, similar to Cimellaro et al. (2011). The results indicate that a minimum of 30 records is sufficient for each investigated combination of the parameters in Table 5.1.

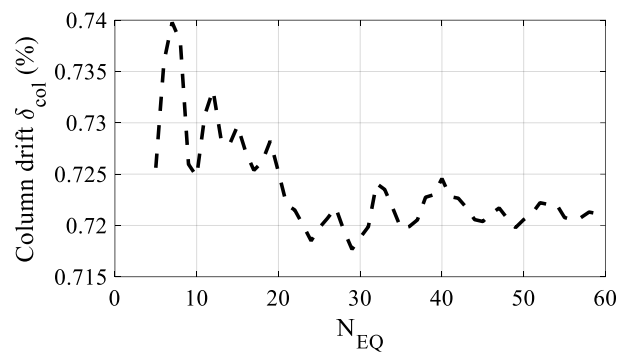


Fig. 5.4 Column drift δ_{col} (%) vs. number of earthquake records N_{EQ}

5.3.2.3. Damage Limits for Bridge Components

Three critical bridge components are of interest: columns, and either elastomeric bearings or high rocker bearings. The seismic damage is assessed based on the relative drift of the columns (δ_{col}) and the horizontal displacements of the bearings (Δ_b). Ideally, the damage limits should be based on the performance criteria defined by bridge owners. For demonstration, the damage limits of columns and elastomeric bearings are defined based on the performance criteria specified in the Canadian highway bridge design code (CHBDC) (CSA, 2019a), namely, minimal, repairable, extensive, and probable replacement. Whereas the damage limits for the high rocker bearings are based on the damage criteria specified in HAZUS-MH (FEMA 2015), which resembles that of the CHBDC (Bandini et al., 2021).

The fragility curves of bridge components are assumed to follow the lognormal

distribution (Nielson and DesRoches 2007; Mangalathu and Jeon 2019) with the medians (θ_{DL}) and dispersions (β_{DL}) reported in Table 5.2. For the columns, the median is based on full-scale experiments on a replica of the columns of the Chemin des Dalles Bridge (Rubio et al., 2019). For the elastomeric bearings, the median is based on the work of Choi et al. (2004) and Tavares et al. (2013), while the dispersion values for the columns and elastomeric bearings are adopted from Nielson (2005). Finally, the median and dispersion for the high rocker bearings are adopted from Nielson and DesRoches (2007).

Table 5.2. Fragility definitions for critical bridge components

Component response	Minimal		Repairable		Extensive		Probable Replacement	
	θ_{DL}	β_{DL}	θ_{DL}	β_{DL}	θ_{DL}	β_{DL}	θ_{DL}	β_{DL}
δ_{col} (%)	0.5	0.25	1.4	0.25	2	0.46	2.2	0.46
$\Delta_{b-elastic}$ (mm)	30	0.25	60	0.25	150	0.46	300	0.46
$\Delta_{b-rocker-long}$ (mm)	37.4	0.6	104.2	0.55	136.1	0.59	186.6	0.65
$\Delta_{b-rocker-tran}$ (mm)	6	0.25	20	0.25	40	0.47	187	0.65

5.3.3. Formulation of the Seismic Vulnerability Index (SVI)

The fragility analysis is conducted for bridges with elastomeric or high rocker bearings. For each of these two configurations, the seismic demand distributions of the critical bridge components (i.e., column and bearing) are evaluated for various combinations of the parameters in Table 5.1. Then, a capacity distribution is chosen from Table 5.2, as discussed in later sections. Based on the capacity and demand distributions, the CL_o of the critical components is evaluated for each investigated parameter combination. The values of CL_o are then related to the parameters via regression analysis. Based on the CL_o models, the SVI can be computed.

Given the fuzziness in bridge deterioration (Fig. 5.2), the CL_o of each component is also fuzzy; thus, it is expressed as a membership function. For each investigated parameter combination, the worst, best, and most probable CL_o of each bridge component are evaluated. The worst and best CL_o correspond to $\mu = 0$. Whereas the most probable CL_o is at $\mu = 1$. Using this data, regression models are then proposed to predict the worst, best, and most probable CL_o . To optimize the regression models, tree-based regression is adopted in which CL_o is related to different combinations (i.e., trees) of the parameters in Table 5.1. The tree balancing the goodness-of-fit and complexity is then chosen as the optimum one. The tree-based regression is conducted using genetic programming via the GPTIPS2 toolbox in Matlab (Searson, 2015) given its ability (1) to generate and test multiple iteration models with a range of complexity and (2) to select the most statistically significant parameters.

To estimate the SVI, the overall CL_o membership function of each bridge is first computed by aggregating the individual CL_o membership functions of the individual components (i.e., column and bearing) through a fuzzy union operation (Chakraverty et al. 2019) (e.g., Fig. 5.5a). The overall CL_o membership function $\mu_{oa}(x)$ can be expressed as

$$\mu_{oa}(x) = \max(\mu_{col}(x), \mu_b(x)) \quad (3)$$

where $\mu_{col}(x)$ and $\mu_b(x)$ are membership functions of columns and bearings, respectively. Given a chosen threshold value ($CL_{o\text{-threshold}}$), the overall membership function is divided into a safe and an unsafe portion (e.g., Fig. 5.5b). The SVI can be then computed as the percentage of the unsafe area

$$SVI = \frac{\int_{CL_{o-min}}^{CL_{o-threshold}} \mu_{oa}(x) dx}{\int_{CL_{o-min}}^{CL_{o-max}} \mu_{oa}(x) dx} * 100 \quad (4)$$

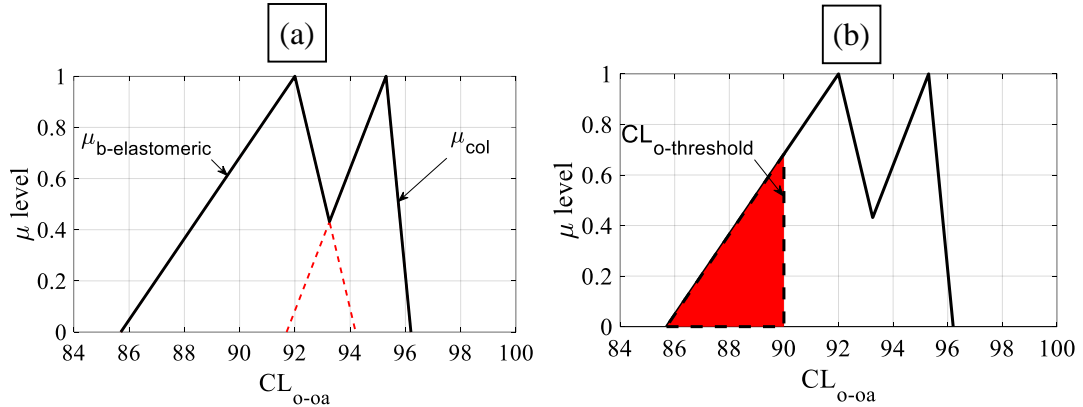


Fig. 5.5 (a) Aggregation of bridge components' CL_o membership functions and (b) overall CL_o membership function with threshold value ($CL_{o-threshold}$) = 90%

5.4. Case Study Bridge and OpenSees Model

The Chemin des Dalles Bridge is used as a case study to demonstrate the proposed framework, because the bridge is representative of MSC concrete girder bridges (Tavares et al. 2012; Bandini et al. 2022). The bridge has three 35.5 m long spans, a concrete deck with a thickness of 165 mm, and six AASHTO Type-V precast prestressed concrete girders with depth and spacing of 1.6 m and 2.2 m, respectively. The bridge is supported by two piers on shallow foundations. Each pier has three circular columns with a diameter of 900 mm and a height of 6 m, connected by a bent beam with a 1.25 m square cross-section. At the piers and the abutments, six bearings are located directly below each of the six girders. Only the abutment bearings can translate, whereas the others allow for rotation only. More details can be found elsewhere (Roy et al. 2010; Tavares et al. 2013; Siqueira et al. 2014).

The 3D OpenSees model of the Chemin des Dalles Bridge used in this work (Fig. 5.6) is a modified version of the model created by Abdelmaksoud et al. (2022). The original model has a first mode period of 0.43 sec in the transverse direction which closely matches the results reported by Tavares et al. (2013). The deck and columns are modelled using nonlinear displacement-based fibre elements. The material models for concrete and steel reinforcement are *Concrete02* (Yassin, 1994) and *Steel02* (Filippou et al. 1983), respectively. The prestressed concrete girders are modelled using elastic elements as they are typically designed to be uncracked (Roy et al. 2010). If elastomeric bearings are used, they are modelled as zero-length elements. The vertical stiffness of the bearings is modelled as a linear spring, and the rotational stiffness is computed based on the work of Kelly and Konstantinidis (2011). The shear behaviour is modelled using a bilinear model with low yield strength for the abutment bearings. If high rocker bearings are used, the stiffness of the zero-length elements is taken from the experiments conducted by Mander et al. (1996).

To incorporate the foundation behaviour, the shallow foundations are modelled as a grillage mesh of elastic elements (Biazar et al., 2022). At each node of the foundation mesh, three nonlinear springs are assigned in the three translation directions to simulate the soil. The material models for the soil are adopted from Raychowdhury and Hutchinson (2008a) and require knowledge of the soil stiffness in addition to the bearing, sliding, and passive capacities. The soil stiffness is computed per Gazetas (1991). Meanwhile, the soil capacities are computed based on Raychowdhury and Hutchinson (2008b) and using the soil properties from Table 5.1.

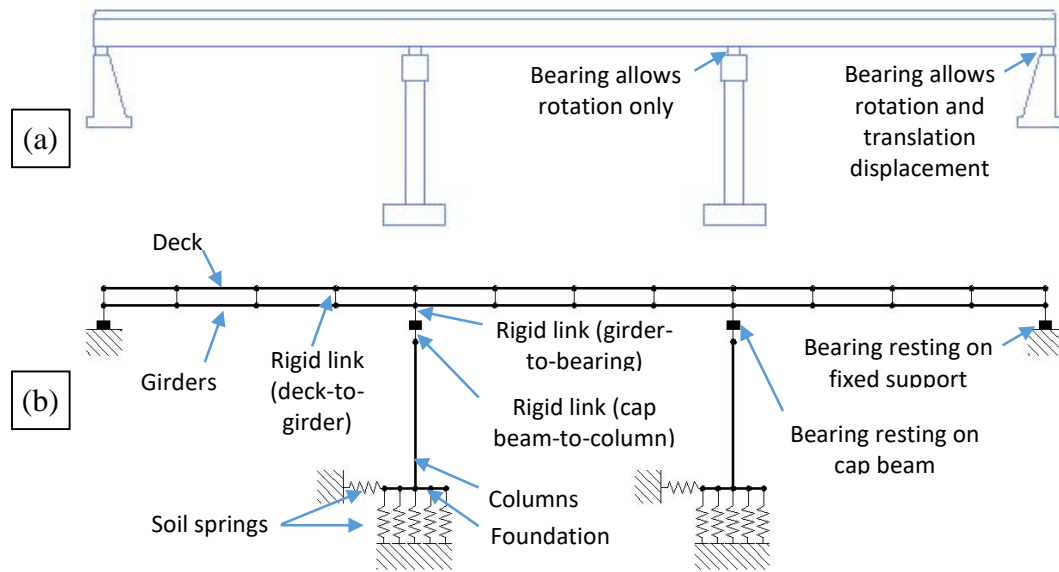


Fig. 5.6 (a) Elevation of Chemin des Dalles Bridge and (b) Elevation of OpenSees model

5.5. Application of Proposed Framework for MSC Concrete Girders Bridges

5.5.1. Condition Indices for Bearings (*BeCI*) and Columns (*CCI*)

For the MSC concrete girders bridge class, the bearing condition index (*BeCI*) can be computed using Eq. (1) with weights (W_i) = 0.05, 0.40, 0.75, and 1.00 for bearings with very severe, severe, medium, and light deterioration, respectively. The column condition index (*CCI*) can be computed using Eq. (2) with a scaling factor (C_o) = 2.3, weights (W_j) = 0.05, 0.35, 0.60, and 1.00 for the very severe, severe, medium, and light corrosion, and location factor (Lo_k) = 0.15, 0.16, and 1.00 for the column's top, middle, and bottom section. Plastic hinging is most likely to occur at the bottom of the column. Thus, if corrosion occurs at the bottom, the shear capacity and confinement of columns will be significantly reduced, leading to higher displacement demands. Hence, the columns' bottom is given the highest value for the location factor (Lo_k). Fig. 5.7 shows the correlation between the proposed *CCI* and the column drifts.

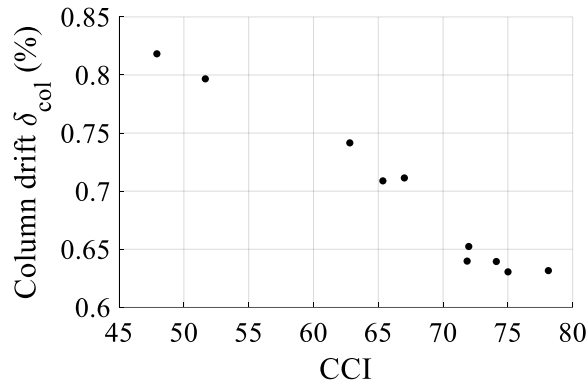


Fig. 5.7 Column drift δ_{col} (%) vs. CCI for sample simulations at $Sa(T_1) = 0.75$ g

5.5.2. Prediction Models for the Confidence Level (CL_o)

For the MSC concrete girders bridge class, the prediction models for the confidence level (CL_o) are formulated based on different capacity limits for bridges with elastomeric and high rocker bearings. While elastomeric bearings are not immune to damage, they typically have a high displacement capacity before reaching the replacement limit (i.e., 300 mm from Table 5.2), leading to a CL_o higher than 99% for all parameter combinations. As such, the replacement limit is deemed non-critical, and the CL_o model is instead developed for the repairable damage limit. In contrast, high rocker bearings have relatively lower displacement capacity prior to replacement (i.e., 187 mm from Table 5.2), leading to lower CL_o . Thus, the CL_o model for bridges with high rocker bearings is developed using the replacement limit. The CL_o for a bridge component is expressed as

$$CL_o = a_0 + a_1 * SS + a_2 * (CCI \text{ or } BeCI) + a_3 * G_e + a_4 * D \leq 100 \quad (5)$$

$$\text{where } SS = \frac{m * h^2 * Sa(T_1)}{E_c * I_{col}}$$

where a_0 to a_4 are the regression coefficients (Table 5.3), SS is dimensionless factor reflecting the major structural and seismic properties of the bridge, G_e is the effective

soil shear modulus (MPa), and D is the foundation depth (m). The factor SS is a function of the seismic mass m ; the spectral acceleration at the fundamental period $Sa(T_1)$; and the columns' height (h), young's modulus (E_c), and total inertia (I_{col}).

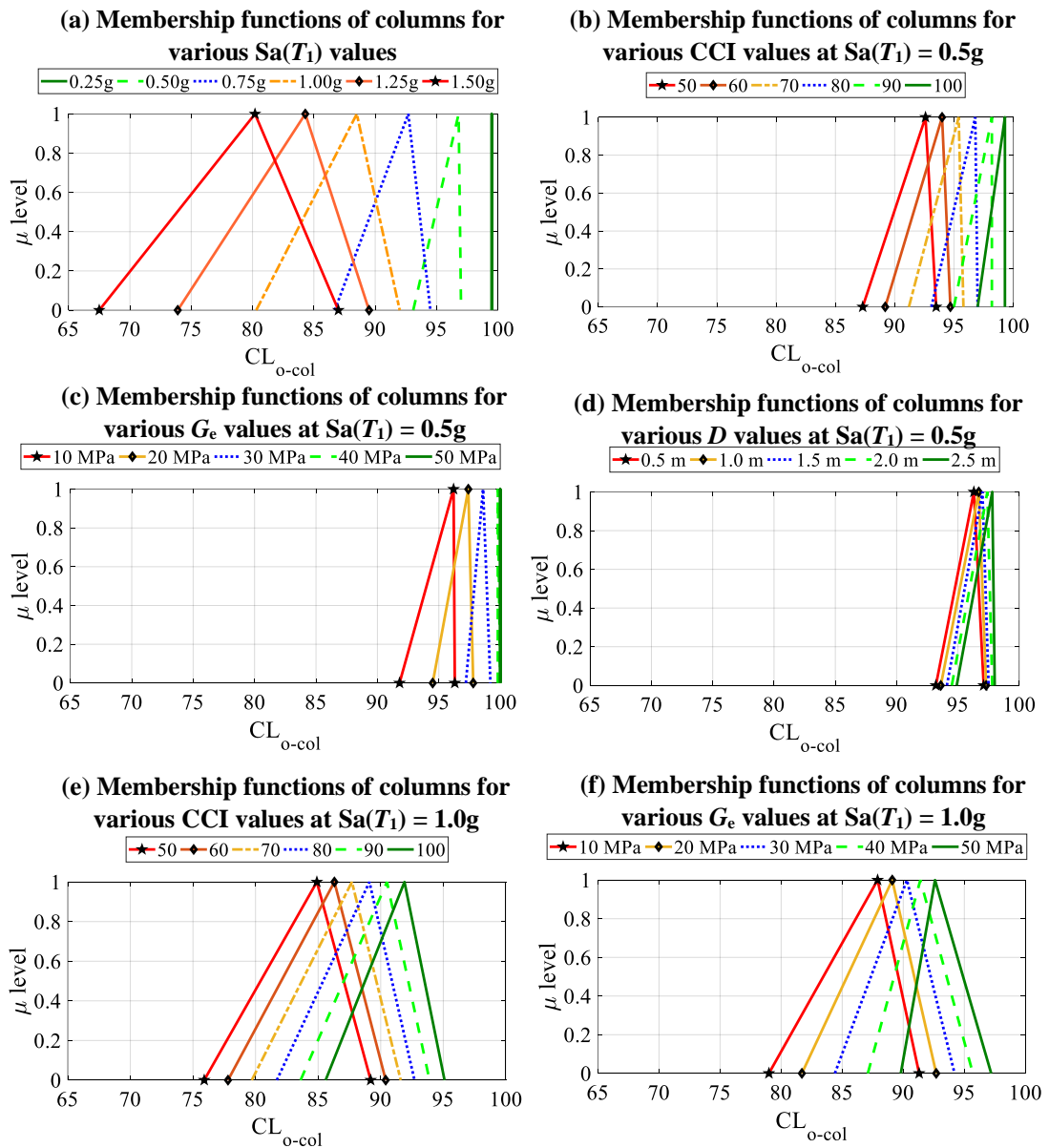
Table 5.3. Regression coefficients for the prediction models of CL_o

Bridge type	Damage limit	Component	Case	β_o	β_1	β_2	β_3	β_4
MSC concrete girder bridge on elastomeric bearings	Repairable damage	Column	B*	89.6	-89.5	0.12	0.15	0.43
			MP*	90.7	-148.7	0.14	0.12	0.72
			W*	84.7	-228.2	0.19	0.27	0.81
		Bearing	B*	106.8	-488.7	0.12	0.26	1.49
			MP*	108	-549.5	0.14	0.24	0.35
			W*	98.8	-582.5	0.15	0.31	2.90
MSC concrete girder bridge on high rocker bearings	Probable replacement	Column	B*	94.2	-46	0.055	0.08	0.22
			MP*	94.7	-73.7	0.070	0.05	0.35
			W*	91.0	-106.6	0.095	0.13	0.43
		Bearing	B*	95.1	-79.8	0.033	0.10	1.35
			MP*	92.3	-85.4	0.033	0.12	2.07
			W*	91.4	-101	0.055	0.08	2.01

* B, W, and MP correspond to best, worst, and most probable values for the CL_o

As expected, the factor SS , representing the seismic and structural properties, is the main contributor to CL_o . For example, Fig. 5.8a shows the decreasing trend in the CL_o membership functions for the original Chemin des Dalles Bridge columns when subjected to increasing spectral accelerations. Meanwhile, Fig. 5.8b reveals that ignoring column deterioration leads to overestimated confidence in the seismic performance of old bridges. The more the column deteriorates (i.e., the lower the CCI), the lower the confidence. Similarly, soil-foundation-structure interaction has a non-negligible impact (Fig. 5.8c and 5.8d). Stiffer foundations and soil (i.e., larger G_e and D) result in lower foundation translation and rotational movements, limiting the relative column drift and increasing the column's CL_o . It is noted that the higher the seismic

intensity, the higher the sensitivity of the seismic performance to the column deterioration (Fig. 5.8e) and soil-foundation-structure interaction (Fig. 5.8f). Similar trends are observed for the elastomeric bearings. For example, Fig. 5.8g and 5.8h show the variation of bearing's CL_o with the BeCI at $Sa(T_1)$ of 0.5g and 1.0g, respectively. Comparing Fig. 5.8b to 5.8g and Fig. 5.8e to 5.8h reveals that the bearings tend to be slightly more vulnerable compared to columns given the same condition index value.



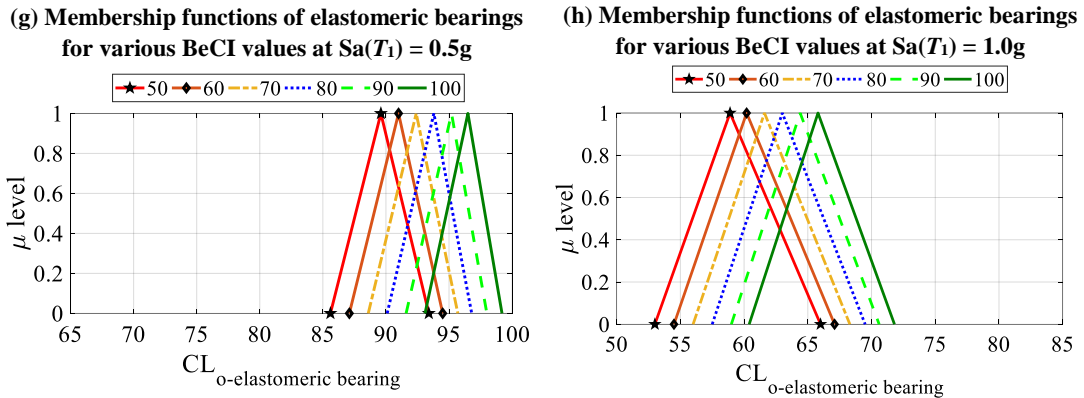


Fig. 5.8 Membership functions of CL_o for the Chemin des Dalles Bridge’s columns and elastomeric bearings

5.5.3. Proposed Seismic Screening Procedures

For the MSC concrete girders bridge class, the current study proposes a two-stage seismic screening procedure based on Eq. (3) to (5) to select and prioritize a portfolio of bridges for detailed evaluation. First, a number of bridges can be automatically excluded from further investigation if they satisfy all of the following conditions: (1) the bridge has elastomeric bearings, (2) $SS < 0.0276$, (3) $CCI > 75$, and (4) $BeCI > 40$. Because, these bridges almost always have a $CL_o > 99\%$, and thus, their vulnerability is negligible.

Secondly, the SVI is computed for the remaining bridges to determine their priority for further evaluation. For each bridge, the membership functions of columns and bearings are computed based on Eq. (5) and Table 5.3. Then, these functions are aggregated using Eq. (3) to obtain the overall CL_o membership function. Given a chosen threshold value ($CL_{o\text{-threshold}}$), the SVI can be then computed using Eq. (4). For example, consider a bridge with elastomeric bearings, $SS = 0.0564$, $G_e = 20$ MPa, $D = 1.0$ m, $CCI = 70$, and $BeCI = 70$. For this bridge, the overall CL_o membership function is plotted in Fig. 5.5a. Given a chosen threshold value ($CL_{o\text{-threshold}}$), the overall membership

function is divided into a safe and an unsafe portion (Fig. 5.5b). The SVI can be then computed as the percentage of the unsafe area (e.g., for $CL_{o\text{-threshold}} = 90\%$, $SVI = 23.7$ for the previous bridge).

The threshold value ($CL_{o\text{-threshold}}$) can be calibrated by BMSs to suit their safety requirements as well as to accommodate budget limitations on detailed seismic investigations. A high threshold allows for lower damage risks but requires a high budget. In contrast, a low threshold results in a lower budget at the expense of higher damage risks. The choice of the optimum threshold that balances the damage risks and budget limits is not the focus of this study. However, it is suggested that BMSs use life-cycle cost (LCC) analysis to calibrate their own thresholds using the steps detailed in Abdelmaksoud et al. (2021).

5.6. Conclusions

The current study proposes new risk-based procedures to rapidly screen bridges for seismic vulnerabilities warranting detailed seismic evaluation. The proposed procedures address two limitations in the currently available seismic screening approaches: (1) the dependence on qualitative, rather than quantitative, measurements of seismic performance, which induces significant uncertainty in the screening process, and (2) the negligence of the potential increase in seismic vulnerability with bridge aging and deterioration.

Unlike the typical qualitative approach of BMSs, the proposed procedures focus on quantifying the seismic damage risks for typical bridge classes based on fragility analysis. The impact of bridge deterioration is also investigated by incorporating deterioration, such as reinforcement corrosion and bearing aging, into the bridge model.

Based on a parametric study, parameterized models are formulated to predict the seismic damage risks given the bridge's condition and other relevant properties, such as seismic intensity, type of bearing, foundation stiffness, etc. Then, a risk-based seismic vulnerability index (SVI) is derived to aid bridge owners in ranking bridges in terms of priority for detailed seismic investigations.

The proposed SVI reflects the damage risks of two critical bridge components: columns and bearings. The analysis reveals that the deterioration of such components is significantly detrimental to seismic performance and cannot be ignored. To facilitate capturing the trends in SVI with deterioration, this study proposes new BMS-compatible condition indices that can be easily evaluated and updated from typical visual inspections. The proposed indices are calibrated using fuzzy logic principles to inform the seismic response of the deteriorating bridge component.

The current work focused on a single bridge class, the multi-span continuous (MSC) concrete girders bridges, and the most common indicators of seismic vulnerability, such as the seismic intensity, bearing type, and component deterioration. However, future work could investigate other special structural features that can impact the vulnerability, such as substructure redundancy and uplifting potential of drop spans. Also, the framework can be extended to include other bridge classes, such as multi-span simply supported (MSSS) bridges, or bridges with different types of girders, such as steel or box girders.

5.7. Data Availability Statement

All data, models, or code that support the findings of this study are available from the corresponding author upon reasonable request.

5.8. Acknowledgements

The authors gratefully acknowledge the support from the Ontario Graduate Scholarship provided by the Government of Ontario, and the start-up funding provided by the Faculty of Engineering at McMaster University. Any opinions, findings, and conclusions or recommendations expressed in this material are those of the authors and do not necessarily reflect the views of the sponsor.

5.9. References

- Abdelmaksoud, Ahmed M, Georgios P Balomenos, and Tracy C Becker. 2021. "Parameterized Logistic Models for Bridge Inspection and Maintenance Scheduling." *Journal of Bridge Engineering* 26 (10): 4021072.
- Abdelmaksoud, Ahmed M, Minesh K Patel, Tracy C Becker, and Georgios P Balomenos. 2022. "Parameterized Models for Prediction of Lifetime Bearing Demands." *Engineering Structures* 252: 113649.
- Alipour, Azadeh, Behrouz Shafei, and Masanobu S Shinozuka. 2013. "Capacity Loss Evaluation of Reinforced Concrete Bridges Located in Extreme Chloride-Laden Environments." *Structure and Infrastructure Engineering* 9 (1): 8–27.
- American Society of Civil Engineers (ASCE). 2017. *Minimum Design Loads and Associated Criteria for Buildings and Other Structures* : ASCE/SEI 7-16.
- Bagnariol, Dino, and Jim Au. 2000. "Seismic Assessment of Provincial Bridges: Phase 1 – Preliminary Screening." Bridge Office, Engineering Standards Branch, Ministry of Transportation of Ontario (MTO).
- Baker, Jack W. 2015. "Efficient Analytical Fragility Function Fitting Using Dynamic Structural Analysis." *Earthquake Spectra* 31 (1): 579–99.
- Bandini, Pedro Alexandre Conde, Gustavo Henrique Siqueira, Jamie Ellen Padgett, and

- Patrick Paultre. 2022. “Seismic Performance Assessment of a Retrofitted Bridge with Natural Rubber Isolators in Cold Weather Environments Using Fragility Surfaces.” *Journal of Bridge Engineering* 27 (6): 4022040.
- Bazzucchi, Fabio, Luciana Restuccia, and Giuseppe Andrea Ferro. 2018. “Considerations over the Italian Road Bridge Infrastructure Safety after the Polcevera Viaduct Collapse: Past Errors and Future Perspectives.” *Frattura e Integrita Strutturale* 12.
- Biezma, María Victoria, and Frank Schanack. 2007. “Collapse of Steel Bridges.” *Journal of Performance of Constructed Facilities* 21 (5): 398–405.
- Biondini, Fabio, Elena Camnasio, and Alessandro Palermo. 2014. “Lifetime Seismic Performance of Concrete Bridges Exposed to Corrosion.” *Structure and Infrastructure Engineering* 10 (7): 880–900.
- Bonthron, Leslie, Corey Beck, Alana Lund, Farida Mahmud, Xin Zhang, Rebeca Orellana Montano, Shirley J Dyke, Julio Ramirez, Yenan Cao, and George P Mavroeidis. 2021. “Empowering the Indiana Bridge Inventory Database Toward Rapid Seismic Vulnerability Assessment.” Joint Transportation Research Program Publication No. FHWA/IN/JTRP-2021/03. West Lafayette, IN: Purdue University.
- Brown, Colin B, and James T P Yao. 1983. “Fuzzy Sets and Structural Engineering.” *Journal of Structural Engineering* 109 (5): 1211–25.
- Bureau of Reclamation. 1998. “Earth Manual: Part 1.” Washington, US: Department of Interior.
- Chakraverty, Snehashish, Deepti Moyi Sahoo, and Nisha Rani Mahato. 2019. “Defuzzification.” In *Concepts of Soft Computing*, 117–27. Springer.

- Chiou, Brian, Robert Darragh, Nick Gregor, and Walter Silva. 2008. “NGA Project Strong-Motion Database.” *Earthquake Spectra* 24 (1): 23–44.
- Choi, Eunsoo, Reginald DesRoches, and Bryant Nielson. 2004. “Seismic Fragility of Typical Bridges in Moderate Seismic Zones.” *Engineering Structures* 26 (2): 187–99.
- Cimellaro, G P, A M Reinhorn, A D’Ambrisi, and M De Stefano. 2011. “Fragility Analysis and Seismic Record Selection.” *Journal of Structural Engineering* 137 (3): 379–90.
- Conde Bandini, Pedro Alexandre, Jamie Ellen Padgett, Patrick Paultre, and Gustavo Henrique Siqueira. 2021. “Seismic Fragility of Bridges: An Approach Coupling Multiple-Stripe Analysis and Gaussian Mixture for Multicomponent Structures.” *Earthquake Spectra*, 87552930211036160.
- Coronelli, D, and P Gambarova. 2004. “Structural Assessment of Corroded Reinforced Concrete Beams: Modeling Guidelines.” *Journal of Structural Engineering* 130 (8): 1214–24.
- CSA, (Canadian Standards Association). 2019a. *Canadian Highway Bridge Design Code. CSA S6-19*. Toronto, Canada.
- CSA, (Canadian Standards Association). 2019b. *Commentry on CSA S6-19, Canadian Highway Bridge Design Code. CSA S6-19*. Toronto, Canada.
- Deng, Pu, and Gordon P Warn. 2016. “Modeling the Compression Stiffness Degradation in Circular Elastomeric Bearings Due to Fatigue.” *Journal of Engineering Mechanics* 142 (1): 4015057.
- Dicleli, Murat, and Michel Bruneau. 1996. “Quantitative Approach to Rapid Seismic

- Evaluation of Slab-on-Girder Steel Highway Bridges.” *Journal of Structural Engineering* 122 (10): 1160–68.
- Dukes, Jazalyn, Sujith Mangalathu, Jamie E Padgett, and Reginald DesRoches. 2018. “Development of a Bridge-Specific Fragility Methodology to Improve the Seismic Resilience of Bridges.” *Earthquake and Structures* 15 (3): 253–61.
- Eads, Laura, Eduardo Miranda, Helmut Krawinkler, and Dimitrios G Lignos. 2013. “An Efficient Method for Estimating the Collapse Risk of Structures in Seismic Regions.” *Earthquake Engineering & Structural Dynamics* 42 (1): 25–41.
- Fan, Xiaohu. 2014. “Characterization of the Cyclic Behavior of Corroded Steel Bridge Bearings and Their Influence on Seismic Bridge Performance.” Doctoral Dissertation, University of Michigan, Ann Arbor, Michigan, United States.
- Fang, Cheng, Dong Liang, Yue Zheng, and Shiyuan Lu. 2022. “Seismic Performance of Bridges with Novel SMA Cable-restrained High Damping Rubber Bearings against Near-fault Ground Motions.” *Earthquake Engineering & Structural Dynamics* 51 (1): 44–65.
- FEMA (Federal Emergency Management Agency). 1997. “NEHRP Guidelines for the Seismic Rehabilitation of Buildings.” Washington, D.C.
- FEMA (Federal Emergency Management Agency). 2015. “Multi-Hazard Loss Estimation Methodology - Earthquake Model - Hazus-MH 2.1: Technical Manual.” Washington, D.C.
- Filiatrault, André, Stéphane Tremblay, and René Tinawi. 1994. “A Rapid Seismic Screening Procedure for Existing Bridges in Canada.” *Canadian Journal of Civil Engineering* 21 (4): 626–42.

- Filippou, Filip C, Egor Paul Popov, and Vitelmo Victorio Bertero. 1983. “Effects of Bond Deterioration on Hysteretic Behavior of Reinforced Concrete Joints.”
- Gazetas, G. 1991. “Foundation Engineering Handbook, Chapter 15.” New York: Fang H.
- Halchuk, Stephen, John Adams, Michal Kolaj, and Trevor Allen. 2019. “Deaggregation of NBCC 2015 Seismic Hazard for Selected Canadian Cities.” In Proceedings of the 12th Canadian Conference on Earthquake Engineering, Quebec City, QC, Canada, 17–20.
- Hammad, Ahmed W A, Jianxia Yan, and Behzad Mostofi. 2007. “Recent Development of Bridge Management Systems in Canada.” In 2007 Annual Conference and Exhibition of the Transportation Association of Canada: Transportation-An Economic Enabler (Les Transports: Un Levier Economique) Transportation Association of Canada (TAC).
- Hearn, George, Jay Puckett, Ian Friedland, Tom Everett, Kenneth Hurst, George Romack, George Christian, Richard Shepard, Todd Thompson, and Ronald Young. 2005. “Bridge Preservation and Maintenance in Europe and South Africa.”
- Kelly, James M, and Dimitrios Konstantinidis. 2011. *Mechanics of Rubber Bearings for Seismic and Vibration Isolation*. John Wiley & Sons.
- Kenedi, Walter, and Dino Bagnariol. 2007. “Seismic Index in the Bridge Management System (BMS).” Bridge Office, Ministry of Transportation of Ontario (MTO), 301 St. Paul Street St. Catharines, ON.
- Kiani, Jalal, Charles Camp, and Shahram Pezeshk. 2018. “On the Number of Required Response History Analyses.” *Bulletin of Earthquake Engineering* 16 (11): 5195–

5226.

Kiureghian, Armen Der, and Ove Ditlevsen. 2009. “Aleatory or Epistemic? Does It Matter?” *Structural Safety* 31 (2): 105–12.

Luco, Nicolas, and C Allin Cornell. 2007. “Structure-Specific Scalar Intensity Measures for near-Source and Ordinary Earthquake Ground Motions.” *Earthquake Spectra* 23 (2): 357–92.

Mackie, Kevin, and Božidar Stojadinović. 2003. *Seismic Demands for Performance-Based Design of Bridges*. Pacific Earthquake Engineering Research Center Berkeley.

MacQueen, James. 1967. “Some Methods for Classification and Analysis of Multivariate Observations.” In *Proceedings of the Fifth Berkeley Symposium on Mathematical Statistics and Probability*, 1:281–97. Oakland, CA, USA: Statistical Laboratory of the University of California, Berkeley.

Mander, John B, D K Kim, S S Chen, and G J Premus. 1996. “Response of Steel Bridge Bearings to Reversed Cyclic Loading.”

Mangalathu, Sujith, and Jong-Su Jeon. 2019. “Stripe-based Fragility Analysis of Multispan Concrete Bridge Classes Using Machine Learning Techniques.” *Earthquake Engineering & Structural Dynamics* 48 (11): 1238–55.

Markow, Michael J, and W Hyman. 2009. “NCHRP Synthesis 397: Bridge Management Systems for Transportation Agency Decision Making.” National Cooperative Highway Research Program.

McKay, Michael D, Richard J Beckman, and William J Conover. 2000. “A Comparison of Three Methods for Selecting Values of Input Variables in the Analysis of Output

- from a Computer Code.” *Technometrics* 42 (1): 55–61.
- McKenna, Frank, Michael H Scott, and Gregory L Fenves. 2010. “Nonlinear Finite-Element Analysis Software Architecture Using Object Composition.” *Journal of Computing in Civil Engineering* 24 (1): 95–107.
- Medasani, Swarup, Jaeseok Kim, and Raghu Krishnapuram. 1998. “An Overview of Membership Function Generation Techniques for Pattern Recognition.” *International Journal of Approximate Reasoning* 19 (3–4): 391–417.
- Mirza, Sher Ali, James G MacGregor, and Michael Hatzinikolas. 1979. “Statistical Descriptions of Strength of Concrete.” *Journal of the Structural Division* 105 (6): 1021–37.
- Mitchell, Denis, Sharlie Huffman, Robert Tremblay, Murat Saatcioglu, Dan Palermo, René Tinawi, and David Lau. 2013. “Damage to Bridges Due to the 27 February 2010 Chile Earthquake.” *Canadian Journal of Civil Engineering* 40 (8): 675–92.
- Moehle, Jack P, and Marc O Eberhard. 2003. “Earthquake Damage to Bridges.” In *Bridge Engineering*, 52–84. CRC Press.
- MTO (Ministry of Transportation Ontario). 2015. “Bridge Repairs.” 2015. <http://www.mto.gov.on.ca/english/highway-bridges/ontario-bridges.shtml> (Accessed October 2018).
- MTO (Ministry of Transportation Ontario). 2018. *Ontario Structure Inspection Manual (OSIM)*. [https://www.ogra.org/files/OSIM April 2008.pdf](https://www.ogra.org/files/OSIM%20April%202008.pdf).
- MTO (Ministry of Transportation Ontario). 2020. “MTO: Foundation Library.” 2020. <http://www.mto.gov.on.ca/FoundationLibrary/map.shtml?accepted=true>.
- Nielson, B G, and W C Pang. 2011. “Effect of Ground Motion Suite Size on Uncertainty

- Estimation in Seismic Bridge Fragility Modeling.” In Structures Congress 2011, 23–34.
- Nielson, Bryant G. 2005. Analytical Fragility Curves for Highway Bridges in Moderate Seismic Zones. Georgia Institute of Technology.
- Nielson, Bryant G, and Reginald DesRoches. 2007. “Analytical Seismic Fragility Curves for Typical Bridges in the Central and Southeastern United States.” *Earthquake Spectra* 23 (3): 615–33.
- Noade, Bryanna M, and Tracy C Becker. 2019. “Probabilistic Framework for Lifetime Bridge-Bearing Demands.” *Journal of Bridge Engineering* 24 (7): 4019065.
- Nowak, A S, and A M Rakoczy. 2013. “Uncertainties in the Building Process.” *Bulletin of the Polish Academy of Sciences: Technical Sciences*, no. 1.
- Omar, T, M L Nehdi, and Tarek Zayed. 2017. “Integrated Condition Rating Model for Reinforced Concrete Bridge Decks.” *Journal of Performance of Constructed Facilities* 31 (5): 4017090.
- Oyado, M., Y. Saito, A. Yasojima, T. Kanakubo, and Y. Yamamoto. 2007. “Structural Performance of Corroded RC Column under Seismic Load.” In *Proceedings of the First International Workshop on Performance, Protection, and Strengthening of Structures under Extreme Loading*. Whistler, Canada.
- Priestley, M J Nigel, Frieder Seible, and Gian Michele Calvi. 1996. *Seismic Design and Retrofit of Bridges*. John Wiley & Sons.
- Raychowdhury, Prishati, and Tara Hutchinson. 2008a. “Nonlinear Material Models for Winkler-Based Shallow Foundation Response Evaluation.” In *GeoCongress 2008: Characterization, Monitoring, and Modeling of GeoSystems*, 686–93.

- Raychowdhury, Prishati, and Tara C Hutchinson. 2008b. “ShallowFoundationGen OpenSees Documentation.” Open System for Earthquake Engineering Simulation (OpenSEES): University of California, San Diego.
- Roeder, Charles W, John F Stanton, and Andrew W Taylor. 1990. “Fatigue of Steel-Reinforced Elastomeric Bearings.” *Journal of Structural Engineering* 116 (2): 407–26.
- Roy, Nathalie, Patrick Paultre, and Jean Proulx. 2010. “Performance-Based Seismic Retrofit of a Bridge Bent: Design and Experimental Validation.” *Canadian Journal of Civil Engineering* 37 (3): 367–79.
- Rubio, Luis F Zuluaga, Yoann Le Tartesse, Christopher Calixte, Georges Chancy, Patrick Paultre, and Jean Proulx. 2019. “Cyclic Behaviour of Full Scale Reinforced Concrete Bridge Columns.” In *12th Canadian Conference on Earthquake Engineering*. Quebec City, Canada.
- Santos, J A, and A Gomes Correia. 2000. “Shear Modulus of Soils under Cyclic Loading at Small and Medium Strain Level.” In *12th World Conference on Earthquake Engineering*, 1–8.
- Sasmal, Saptarshi, and KJESWA Ramanjaneyulu. 2008. “Condition Evaluation of Existing Reinforced Concrete Bridges Using Fuzzy Based Analytic Hierarchy Approach.” *Expert Systems with Applications* 35 (3): 1430–43.
- Searson, Dominic P. 2015. “GPTIPS 2: An Open-Source Software Platform for Symbolic Data Mining.” In *Handbook of Genetic Programming Applications*, 551–73. Springer.
- Siqueira, Gustavo Henrique, Danusa Haick Tavares, and Patrick Paultre. 2014.

- “Seismic Fragility of a Highway Bridge in Quebec Retrofitted with Natural Rubber Isolators.” *Revista IBRACON de Estruturas e Materiais* 7: 534–47.
- Song, Xiayun, Haiwang Li, Xingyu Wang, and Jie Zhang. 2021. “Experimental Investigation of Ultra-Low-Cycle Fatigue Behaviors of Plate Bearings in Spatial Grid Structures.” *Engineering Structures* 231: 111764.
- Sozen, Mete A. 2003. “The Velocity of Displacement.” In *Seismic Assessment and Rehabilitation of Existing Buildings*, 11–28. Springer.
- Tavares, D H, J R Suescun, P Paultre, and J E Padgett. 2013. “Seismic Fragility of a Highway Bridge in Quebec.” *Journal of Bridge Engineering* 18 (11): 1131–39.
- Tavares, Danusa H, Jamie E Padgett, and Patrick Paultre. 2012. “Fragility Curves of Typical As-Built Highway Bridges in Eastern Canada.” *Engineering Structures* 40: 107–18.
- Tee, A B, M D Bowman, and K C Sinha. 1988. “A Fuzzy Mathematical Approach for Bridge Condition Evaluation.” *Civil Engineering Systems* 5 (1): 17–24.
- Tesfamariam, S, and S M Modirzadeh. 2009. “Risk-Based Rapid Visual Screening of Bridges.” In *TCLEE 2009: Lifeline Earthquake Engineering in a Multihazard Environment*, 1–12.
- Wagstaff, Kiri, Claire Cardie, Seth Rogers, and Stefan Schrödl. 2001. “Constrained K-Means Clustering with Background Knowledge.” In *ICML '01: Proceedings of the Eighteenth International Conference on Machine Learning.*, 1:577–84. Morgan Kaufmann Publishers Inc.
- Yassin, Mohd Hisham Mohd. 1994. “Nonlinear Analysis of Prestressed Concrete Structures under Monotonic and Cyclic Loads.” University of California, Berkeley.

Zadeh, Lotfi A. 1965. "Fuzzy Sets." *Information and Control* 8 (3): 338–53.

6. Summary, Conclusions, and Future Work

6.1. Summary and Conclusions

The primary goal of this thesis was to propose methodologies that can enhance the current practices of managing deteriorating bridges by providing better modelling and understanding of the trends in the deterioration of bridges and their components. To this end, four main objectives were defined: (1) providing an alternative to the Markov Chains method as a probabilistic tool for analyzing inspection data, (2) accounting for the subjectiveness of inspection data, (3) understanding the in-practice behavior of bridge bearings, and (4) assessing the impact of deterioration on seismic vulnerability.

6.1.1. Risk-based Management in Presence of Time-Dependent Deterioration

Logistic regression is a promising tool for probabilistic analysis of inspection data and was proposed as an alternative to the Markov Chains method. Thus, to examine the effectiveness of the logistic regression, a framework was developed for scheduling bridge inspection and maintenance based on parameterized logistic models. Maintenance and inspection limit states were defined based on inspection guidelines. Then, logistic models were formulated to predict the probability of exceeding these limits given the bridge age, maintenance history, and location. Furthermore, a framework for life cycle cost analysis was proposed to optimize the probability thresholds of the logistic models. The proposed framework better predicted the maintenance needs compared to the Markov Chains method adopted by many North American BMSs. Applying the framework on a case study bridge also showed potential savings in the number of required inspections by 30%. While the results may vary for other bridges, this highlights that the framework can improve current bridge management practices.

After validating its effectiveness as a probabilistic tool, logistic regression was integrated with the fuzzy set theory to develop a BMS-compatible framework for incorporating randomness as well as subjectiveness in inspection data. The framework does not require extensive deterioration measurements and only utilizes available data from the inspection database (i.e., age and repair history) or other databases (i.e., meteorological conditions). The same maintenance and inspection limit states were used to develop logistic deterioration models; however, subjective regression parameters were modelled as membership functions rather than discrete values. This resulted in logistic models with fuzzy coefficients, leading to a range of possible logistic models bound by worst and best-case models. Conservatively, only the worst-case models were examined. Furthermore, a modified framework for life cycle cost analysis was proposed to optimize (1) the probability thresholds of the logistic models and (2) the additional risks from the subjectiveness of inspection data. For an examined case study bridge, the methodology demonstrated potential reduction in bridge inspections by about 30% throughout the service life, compared to biennial inspection practices.

6.1.2. Loading Protocol for Life-span Assessment of Bridge Bearings

A generalized loading protocol is proposed to simulate the lifetime bearing demands for temperature, traffic, and seismic loading to facilitate comprehending the in-practice behavior of bridge bearings. The protocol was derived based on the bearing demand attributes (i.e., cycle count and amplitudes) estimated from nonlinear analysis in OpenSees. The analysis investigated a variety of standard highway bridge configurations with varying the number of spans (1, 2, or 3) and superstructure types (deck on concrete girders or steel girders). For each configuration, a range of design

parameters (e.g., deck thickness, depth-to-span ratio, pier stiffness, etc.) was studied. Also, the impact of bridge aging on bearing demands was assessed. The analysis revealed that the bearing demands and, consequently, the bearing loading protocol are highly sensitive to the bridge configuration and design parameters but not to the bridge aging. Based on regression analysis, parameterized models were developed for the bearing demands as a function of the bridge configuration and loading conditions. A case study was then presented to demonstrate the procedures for generating the loading protocol from these models.

6.1.3. Risk-based Seismic Screening for Deteriorating Bridges

New risk-based bridge screening procedures are proposed to rapidly assess the seismic vulnerabilities of bridges and set priorities for further detailed seismic evaluations. Here, the vulnerability was defined as the risk of a critical bridge component, namely the columns or bearings, incurring damage at a specified level of deterioration. The damage risk was estimated through fragility analysis conducted on a 3D OpenSees bridge model, which incorporated the following deterioration mechanisms: column reinforcement corrosion, bearing fatigue, and bearing corrosion. The analysis revealed that the deterioration of such components is significantly detrimental to seismic performance and cannot be ignored. To capture the trends in the fragility of deteriorating components, new BMS-compatible condition indices for such components were proposed. The indices were calibrated using fuzzy logic principles to facilitate their evaluation from typical visual inspections. Then, parameterized models were formulated to predict the component fragility given its deterioration level and other relevant properties, such as seismic intensity, type of bearing, foundation

stiffness, etc. Using the individual component fragilities, a risk-based seismic vulnerability index (SVI) can be computed for the whole bridge to rank its priority for detailed seismic investigations. The higher the SVI, the higher the priority for detailed seismic investigations.

6.2. Future Work

The suggestions below represent either an area that, given time, I would have liked to explore more, or novel questions that became apparent through this research.

1. While the proposed fuzzy-logistic models were directed toward capturing time-dependent deterioration of bridge conditions, they do not account for the effect of accidents or extreme events. Hence, future work could develop similar models to predict the drop in bridge conditions following such events.
2. The presented bearings demand prediction models can be used to develop experimental fatigue loading protocols for bridge bearings. These protocols can be used for testing and rating sample bridge bearings to better understand bearing fatigue life. Additionally, this could be used to study the seismic performance of fatigued bearings. This future research will aid bridge owners and bearing manufacturers predict the bearing life expectancy, allowing for better replacement scheduling and budget estimation.
3. The proposed seismic screening framework were developed for the multi-span continuous (MSC) concrete girders bridges, and focused on the most common indicators of seismic vulnerability. Future work could investigate other special structural features that can impact the seismic vulnerability, such as substructure redundancy and uplifting potential of drop spans. Also, the framework can be

extended to include other bridge classes, such as multi-span simply supported (MSSS) bridges.

4. A new concept was proposed to aid in assessing the seismic performance of deteriorating bridges given data from visual inspections. The concept is based on mapping the observed damage into possible hidden deterioration values that can be explicitly modelled, allowing for quantitative performance assessment. Future work can focus on optimizing the mapping process and extending such concept to assess the degradation of other performance aspects such the traffic load carrying capacity of the superstructure.